1985

Current, erosional and depositional patterns at a river confluence and bend in the Nottawasaga River, Angus, Ontario

Gregory Robert Brooks
Wilfrid Laurier University

CANADIAN THESES

THÈSES CANADIENNES

NOTICE

The quality of this microfiche is heavily dependent upon the quality of the original thesis submitted for microfilming. Every effort has been made to ensure the highest quality of reproduction possible.

If pages are missing, contact the university which granted the degree.

Some pages may have indistinct print especially if the original pages were typed with a poor typewriter ribbon or if the university sent us an inferior photocopy.

Previously copyrighted materials (journal articles, published tests, etc.) are not filmed.

Reproduction in full or in part of this film is governed by the Canadian Copyright Act, R.S.C. 1970, c. C-30. Please read the authorization forms which accompany this thesis.

AVIS

La qualité de cette microfiche dépend grandement de la qualité de la thèse soumise au microfilmage. Nous avons tout fait pour assurer une qualité supérieure de reproduction.

S'il manque des pages, veuillez communiquer avec l'université qui a conféré le grade.

La qualité d'impression de certaines pages peut laisser à désirer, surtout si les pages originales ont été dactylographiées à l'aide d'un ruban usé ou si l'université nous a fait parvenir une photocopie de qualité inférieure.

Les documents qui font déjà l'objet d'un droit d'auteur (articles de revue, examens publiés, etc.) ne sont pas microfilmés.

La reproduction, même partielle, de ce microfilm est soumise à la Loi canadienne sur le droit d'auteur, SRC 1970, c. C-30. Veuillez prendre connaissance des formules d'autorisation qui accompagnent cette thèse.

THIS DISSERTATION HAS BEEN MICROFILMED EXACTLY AS RECEIVED

LA THÈSE A ÉTÉ MICROFILMÉE TELLE QUE NOUS L'AVONS REÇUE

CURRENT, EROSIONAL AND DEPOSITIONAL PATTERNS
AT A RIVER CONFLUENCE AND BEND
IN THE NOTTAWASAGA RIVER, ANGUS, ONTARIO

By
Gregory Robert Brooks
B.A., University of Guelph, 1983

THESIS
Submitted to the Department of Geography
in partial fulfilment of the requirements
for the Masters of Arts degree
Wilfrid Laurier University
1985

ACKNOWLEDGEMENTS

Initially, I wish to thank my thesis committee of Dr. Houston Saunderson, Dr. Gunars Subins, and Dr. John McMurry, and also Dr. Sydney Bulman-Fleming (outside reader), and Dr. Robert Ellis (Chairman). Additional thanks is extended to Dr. Houston Saunderson who served as the major advisor for this thesis. His continuous encouragement and enthusiasm towards this reseach is much appreciated. Financial support for the research was provided by the Natural Sciences and Engineering Research Council of Canada through grant number A2481 to Dr H. Saunderson.

I would also like to express thanks to David Bennett for help with data collection, to Mike Stone for logistical support and the boat modifications, to Dr. James Blackburn and Svein Vik for designing and programming the data logger, and to Pam Schaus for consultation on the major diagrams. Gratitude is also extended to Vera Law on whom the burden of proof-reading was thrust.

ABSTRACT

At a bend and confluence of the Nottawasaga River, sixty-four measurements of flow velocities were recorded at points along vertical profiles regularly spaced across a series of cross-sections. From the summarization of the data into a 'three dimensional' diagram, the current velocity patterns in the river reach were evident.

As observed at low discharge levels, the low speeds and directional uniformity of the flow in the Nottawasaga River entering the study reach suggests that the observed asymmetrical channel was a remnant of higher discharge levels. On the other hand, in the Pine River prior to entrance into the confluence, channel morphology was being influenced by much higher flow speeds in combination with two cells of contra-rotating helicoidal flow. Active dunes and ripples were observed migrating along the asymmetrically shaped channel bottom. The erosional and depositional pattern of the tributary suggests that the Pine River mouth was slowly migrating upstream.

The fusion of the waters at the confluence resulted in very complex flow patterns. In the waters entering from the tributary, the presence of a helicoidal flow cell appeared to be causing a large bar to built along the bank immediately downstream from the Pine River mouth. Across the channel, the deflection of the Nottawasaga River flow was causing erosion of the opposite bank.

Downstream at the riffle area, flow in the Nottawasaga River accelerated as channel morphology became almost symmetrical.

Around the bend, the development of a high speed filament and helicoidal flow cell were reflected by the asymmetrical channel and the erosional and depositional pattern along the banks. A large eroded area in the bank suggested that a proximal reverse circulation observed in the flow pattern along the outside of the channel was capable of causing erosion during high discharge levels. The overall velocity pattern observed at the bend became much less intense as flow entered a deep pool that was situated in the downstream section of the study reach.

Paleocurrent measurements of ripple marks on the point bar at the bend and small 'side' bars immediately downstream, gave an indication of flow patterns occurring along the inner bank of the at high discharge levels. These measurements showed that a large reverse circulation exists along the inner bank causing scouring of the downstream end of the point bar.

Excavations into the slumped area opposite the point bar revealed numerous sedimentary structures. Amongst these structures was evidence of point bar accretion, upstream migration of the tributary, a channel cut-off, and vertical accretion deposits on the floodplain.

TABLE OF CONTENTS

LIST OF FIGURES

LIST OF TABLES

CHAPTER ONE

INTRODUCTION

Despite long term interest from geomorphologists and engineers, many aspects of river meanders remain unknown. Within the last ten years or so, research concerning flow in rivers has shifted from flume research to natural rivers. While much has been learned from flume research, flow conditions in a flume are not reproductions of natural flow conditions. In a natural river the channel width and depth are much larger than in a flume. Also channel geometry is much more complex. Concerning the flow itself, in the natural river, secondary circulation patterns and complex turbulence make the flow much more complicated.

The recent development of electromagnetic current velocity meters now allows for detailed field research that in the past could not have been practically done. Thus, studies have emerged in the literature that have analysed different facets of natural rivers and streams. Among the different aspects studied are flow patterns, bedform patterns and morphology, and sediment size distribution along the bed. The following paragraphs are a review of much of the recent literature related to flows in natural rivers.

<u>Review of Literature</u>

From laboratory and field observations it has long been known that a spiral or helicoidal flow pattern becomes generated as a river passes through a meander (e.g. Thomson, 1876). In the literature two contrasting theories concerning the spatial distribution of helicoidal flow exist: Wilson (1973) theorized that at each meander apex, a single helix exists. This helix extends downstream from the bend at which it was generated, into the successive meander. Along the outer bank of the successive meander, it becomes gradually pinched out by a locally generated contra-rotating helix that has developed in response to the opposite curvature of this bend. At the apex of this successive bend, the locally generated helix exists as a single cell. At the inflexion point of the meanders, the two helices co-exist, with the surface waters of the cells converging. This pattern is repeated from meander to meander downstream along the river.

The second theory concerning the spatial distribution of helicoidal flow is the twin spiral system of Hey and

Thorne (1975). They theorized that along a meandering river two helices will co-exist continuously from one bend to another. At the meander apices, the larger inner helix rotates in the 'expected' manner, while the outer helix rotates in the opposite direction. The divergence of the two cells at the bed of the channel was expected to cause scouring, accounting for the presence of a pool at the meander apices of rivers. At the inflexion point, the rotation of the two cells is opposite, so that the bottom currents converge causing a deposition of sediment on the bed. This deposition of sediment was thought to give rise to the shallow area of the channel, between bends, known as a riffle.

Which theory is correct has been difficult to establish as contradicting evidence can be found in the literature. Jackson (1975), Hickin (1978), and Bridge and Jarvis (1982) at meander apices for example, have all observed single cell helicoidal flow, while Bathurst et al. (1977) have observed two cells. Bathurst et al. considered that the observed outer helix had been locally generated at the river bend. Conversely, in a flume study, Toebes and Sooky (1967) also observed two cell helicoidal flow, but they found that the outer cell was an extension of the helix that had been generated at the upstream meander. It must be noted that the size of the outer cell in relation to the cross-sectional area of the stream was very small. At inflexion points of rivers, Jackson (1975), Hickin (1978), Thorne and Hey (1979), and Bridge and Jarvis (1982) all report observing two cell helical flow. Thorne and Hey, and Bridge and Jarvis, both attribute the convergence of the bottom currents to the development of a mid-channel ridge. Interestingly, Hickin (1978) does mention that two - or multiple - cell circulation can develop in shallow, wide channels where local variations in shear stress occur around submerged bars.

Many other important attributes concerning natural rivers have been observed throughout the literature. Hickin (1978) analysed mean flow characteristics through a continuous series of meanders of the Squamish River and identified likely hydraulic controls of lateral channel migration. By analysing regularly spaced cross-sectional profiles, he examined such parameters as downstream and cross-stream velocities, secondary circulation strength and direction, mean boundary shear stress and flow resistance. In this study Hickin observed that in sharply curved meanders the high velocity filament of flow was located towards the center of the channel rather than proximal to the outer bank where it is normally expected. This occurrence is thought to limit the outward migration of a meander, a control that, from river modelling was previously unknown.

Dietrich et. al. (1979) analysed bedload transport and dune orientation around a meander of Muddy Creek, in Wyoming. They found that the area of maximum bedload transport corresponded to the calculated pattern of maximum boundary shear stress. The particle size distribution of the bed could also be correlated to the boundary shear stress distribution, with larger size fractions being located in the areas of high shear stress, and the smaller size fractions being located in the areas of low shear stress. Dune orientation was not dependent on the secondary circulation but on the location of the area of high boundary shear stress. The area of high boundary shear stress caused the section of the dune it was flowing over to move more rapidly than the extremities. Since the area of maximum boundary shear stress shifts from the inside bank at the upstream section of the meander, to eventually the outside bank, different sections of a dune will move more rapidly according to the location of the dune with respect to location of maximum boundary shear stress. The net result is that the orientation of the dune becomes distorted as the dune migrates around the meander.

Jackson (1975, 1976) and Bridge and Jarvis (1976, 1977, 1982), conducted detailed studies on flow patterns, bedforms and bed sediments. Jackson (1975) observed velocity patterns, sediment size and bedform distributions in four meanders of the Wabash River, Illinois, with different discharge levels. He documented how the pattern of flow around the bend became modified in response to large changes in discharge. Sediment size and bedform distribution were also found to be sensitive to the flow conditions. Taking a more detailed look at bedforms, Jackson (1976) looked at the morphology, hydraulic and morphologic relationships, hydrodynamic regime and stratification of a number of different types of bedforms. His study added insight as to whether bedforms like scroll bars, sand waves, and transverse bars are larger scale versions of dunes. Based on hydraulic characteristics Jackson concluded they were different. He also found that by separating lagged bedforms from unlagged, the stability fields for small-scale ripples, dunes, and the lower plane bed can be identified on depth, velocity and sediment size charts as Southard (1971) had done with flume data.

Bridge and Jarvis in a series of papers examined in detail many facets of a bend along the River South Esk, Scotland. In Bridge and Jarvis (1976) various characteristics of flow hydraulics and sedimentation along a meander were tested against theoretical and laboratory equations and models. Flow resistance was found to increase with larger sized bedforms due to form drag, the spiral flow pattern was observed to develop quicker in the meander with lower discharges, and the slope of the water surface around the bend was found to be irregular. Bedforms were discussed in relationship to flow resistance and sediment size. From the same data, the 1977 paper measured vertical velocity profiles and resistance coefficients for bedforms ranging from lower stage plane bed, ripples to dunes. Bridge and Jarvis (1982) again examined river flow and sediment movement in relation to hydraulic models. Flow was studied by measuring velocity distribution, secondary circulation, and water surface variations. Bedform sediment transport rates were also measured. Bedform data was plotted on depth, velocity and sediment size diagrams. Additionally, data on dunes was plotted on diagrams of water depth to dune height, and water depth to dune length. The depth, velocity and sediment size diagrams appeared to show good correlation to laboratory data despite the much greater depths of the natural river. However, the depth to dune length, and depth to dune height graphs showed a lot of scatter. Unlike Dietrich et. al. (1979), the location of the highest area of sediment transport did not correspond to the area of highest bed shear stress. Bridge and Jarvis explained the discrepancy by pointing out that the rate of sediment transport varied with sediment grain size and not just with bed shear. Thus the highest area of bed shear stress may be occurring over a coarse textured area where little transport of sediment was occurring. In all three papers, the different features of the bend were compared to models and/or laboratory studies. No attempt was made to synthesize the observations of the different bend components, for example, spatial distribution of bed sediments to the current velocity pattern.

These papers clearly show that study of natural rivers and streams is feasible. Yet, in each of those papers, the river cross-sections were analysed two-dimensionally without the three-dimensional aspect of flow being truly reconstructed. Although Jackson (1975) did illustrate the near-bottom velocities in comparison to the surface velocities (in his Figs. 3, 4, 5 and 6).

Objectives of Study

The objectives of this study were to obtain a better understanding of the flow and sedimentary processes occurring in and along a river confluence and bend. The study involved conducting very detailed measurements of flow velocities during low discharge levels for the purpose of constructing a 'three-dimensional' depiction of flow. From this diagram, characteristics and patterns within the flow will become apparent, providing information on the observed morphology of the river reach. During the undertaking of the field research for this thesis, it was realized that the paleocurrent direction of ripple marks found on the exposed bars along the river banks could be used to produce an estimate of the pattern of flow occurring at higher discharges. This estimate was used to supplement the flow diagram to get a better understanding of processes which were not apparent from the analysis of the low discharge flow pattern, but which have influenced the observed morphology of the river along the study reach at higher stages. The origin of exposed sediments along a section of the left bank was also interpreted.

Study Site

The study site of this thesis was located in the drainage basin of the Nottawasaga River. The Nottawasaga River drainage basin is located in Southern Ontario just to the west of Lake Simcoe, draining into the southeastern corner of Georgian Bay (Fig. 1). The actual study site was located just to the northeast of the town of Angus, Ontario (Fig. 2). The site can be located on the NTS map 31 D/5 entitled 'Barrie' at grid reference 898092. This location is on the Camp Borden Sand Plains, just upstream of the Minesing Swamp (Chapman and Putnam, 1966). In this area, the banks of the river were four meters high. The floodplain of the river was indistinguishable from the flat topography of the sand plain. The bed of the river consisted of generally sand sized material.

The river reach that constituted the study area of the thesis consisted of a single asymmetrical meander that included, at the upstream end, the junction of a major tributary, the Pine River (Fig. 3). The river banks of the study site were designated left and right with respect to the flow direction of the Nottawasaga River.

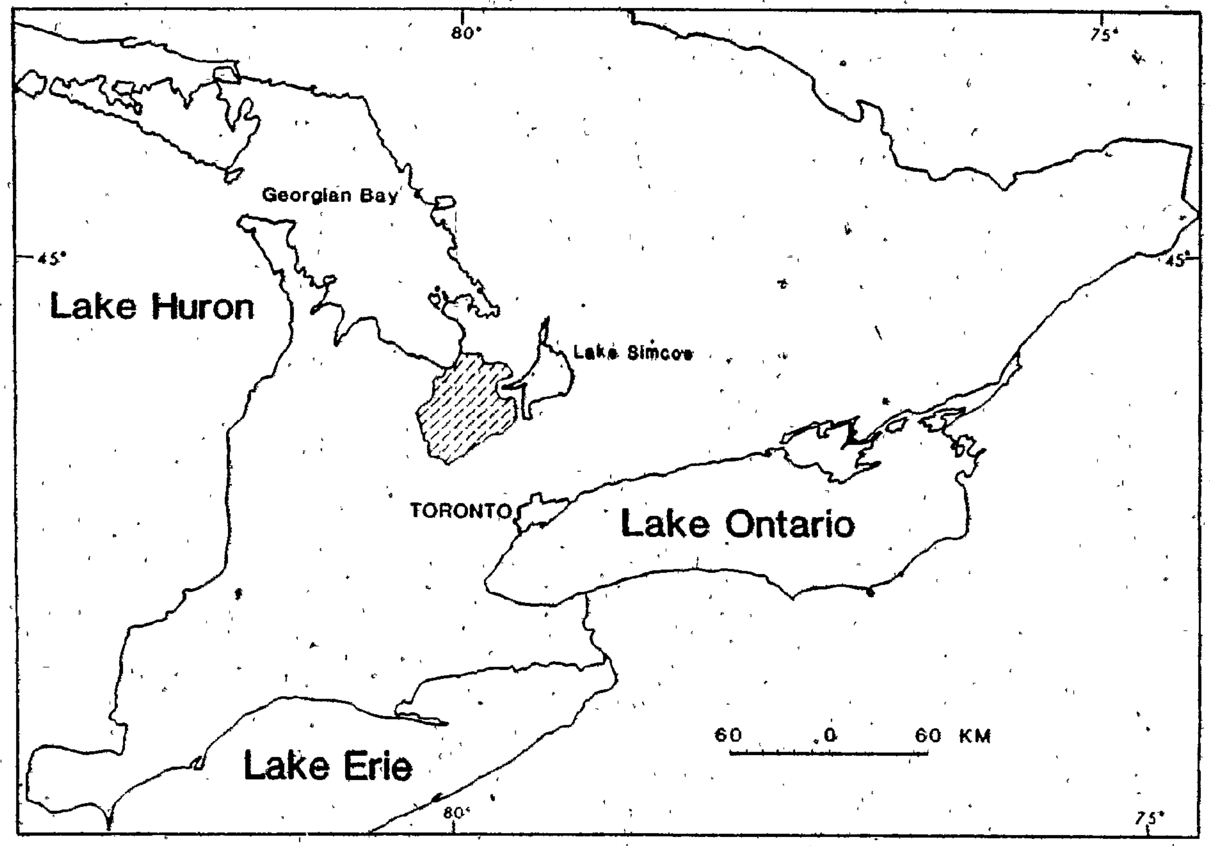

Fig. 1 Map of Southern Ontario showing the location of Nottawasaga River Drainage Basin.

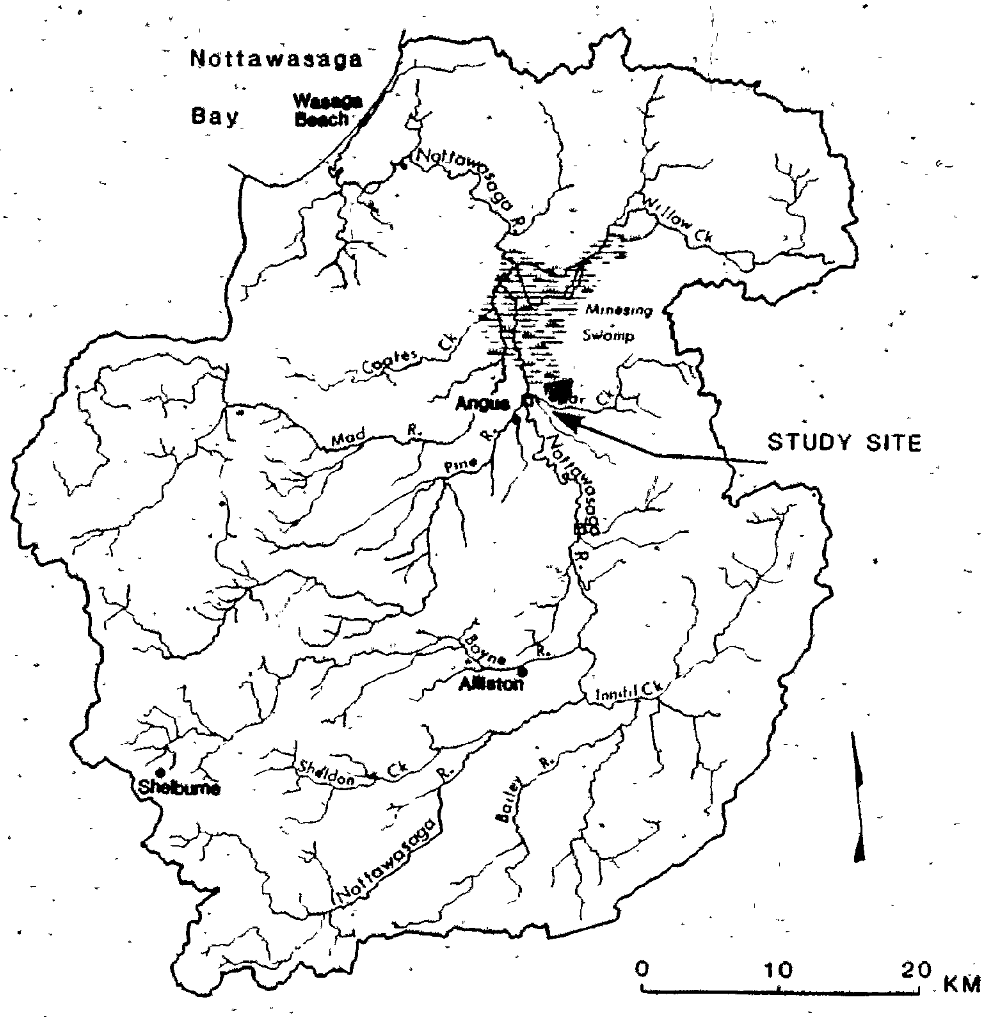

SOURCE: Nottawasaga Valley Conservation Authority

Fig. 2 Map of Nottawasaga Drainage Basin showing the main river and major tributaries. The study reach was located near Angus, Ontario.

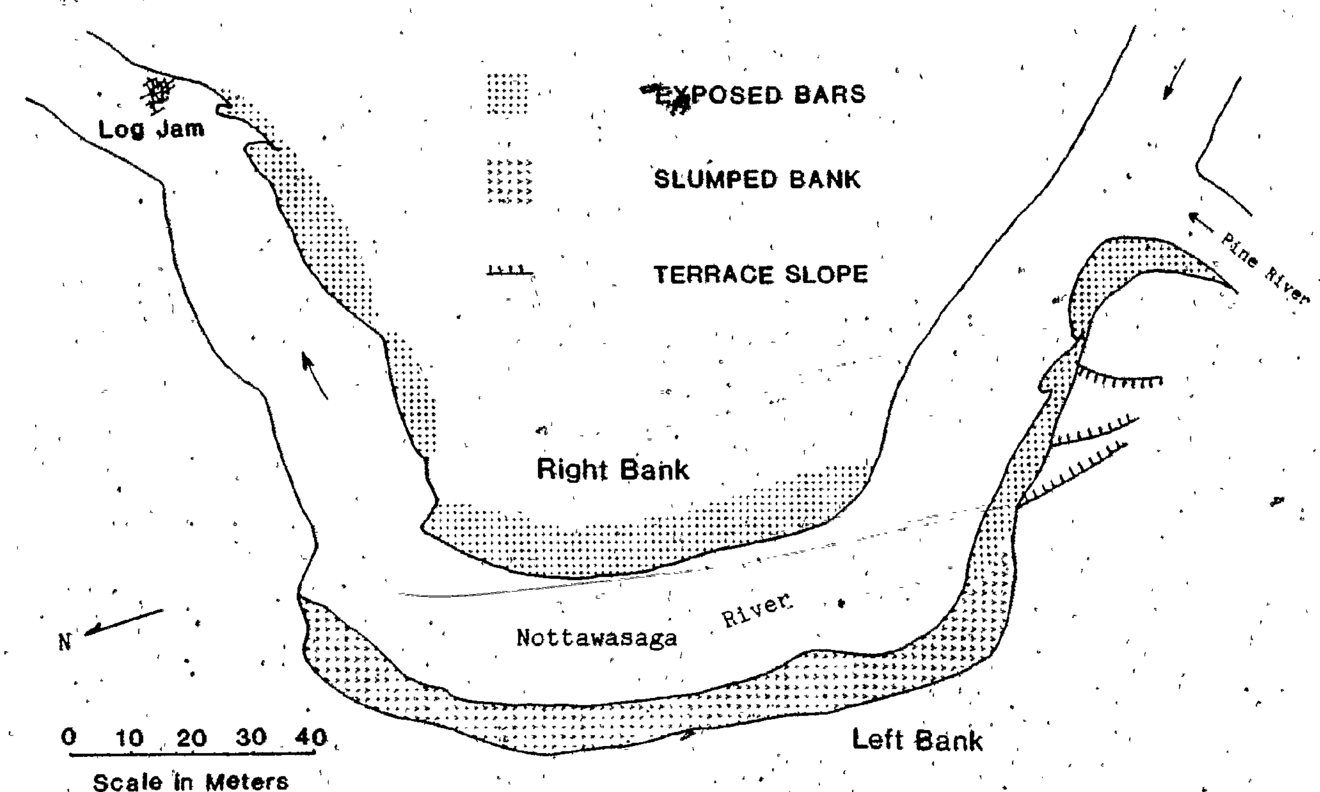

Fig. 3 Map of the study site.

Along the right side of the meander (Fig. 3), the river bank opposite to the Pine River was very steep and covered with vegetation in the form of grass and saplings. Downstream of the steep slope, the bank became more gently sloped and changed into a large point bar. The point bar terminated abruptly in a scarp at its downstream end. The remainder of the right bank consisted of two small side bars. Downstream of the second side bar, just outside the study area was a small log-jam.

At the upstream end of the study area along the left bank (Fig. 3), a large bar had formed immediately downstream of the mouth of the Pine River. Just downstream of this confluence, was a major depression in the river bank. This depression led back to the Pine River, suggesting its probable origin was similar to that of a meander cut-off. This cut-off was composed of a 'channel' and a bench that was located along its north side. At the river bank, the height of the cut-off above the low water level of the Nottawasaga river was approximately half a metre. This height increased gradually with a greater distance from the river bank. At higher stages of discharge, the cut-off would be occupied by water, only to be abandoned as flow waned.

Downstream of the depression to approximately opposite the terminus of the point bar, the left bank was composed of areas of freshly exposed slopes and slumped material, and similar areas that had been stabilized by herbaceous vegetation. Within this area of the bank were two slight depressions into the floodplain surface. The remainder of the left bank was very steep and more vegetated, not unlike the section of the right bank opposite the Pine River.

CHAPTER TWO

SURFICAL GEOLOGY OF THE NOTTAWASAGA DRAINAGE BASIN

The Nottawasaga drainage basin covers an area of 2,931 sq. km. or 1,145 sq. miles (Chapman and Putnam, 1966). The contained river and streams drain a landscape primarily created by a variety of glacial, glacio-fluvial, and glacio-lacustrine processes during the Pleistocene Epoch. The surfical Pleistocene geology of the Nottawasaga drainage basin is primarily associated with the Wisconsinan glaciation, and the glacial and post-glacial stages of Lake Huron/Georgian Bay. This account generally follows the sequence of events as presented by Deane (1950) for the Wisconsinan glaciation/Algonquin Great Lake stages, and that of Lewis (1969) for the Nipissing/Post-Nipissing stages. Reference is also made throughout the account to the development of specific physiographic regions within the drainage basin.

Pleistocene Geology

Pre/Early Wisconsinan. It is believed that an ice lobe moving out of the Georgian Bay basin formed a series of terminal and recessional moraines that today are known as the Simcoe Uplands, the Oro kame moraine and the Edenvale till moraine (Fig. 4). Since the movement of the northern lobe of the main Wisconsinan ice sheet in the area was in a general northeast to southwest direction, which is roughly parallel to the orientation of these features, it has been hypothesised that they were created by an

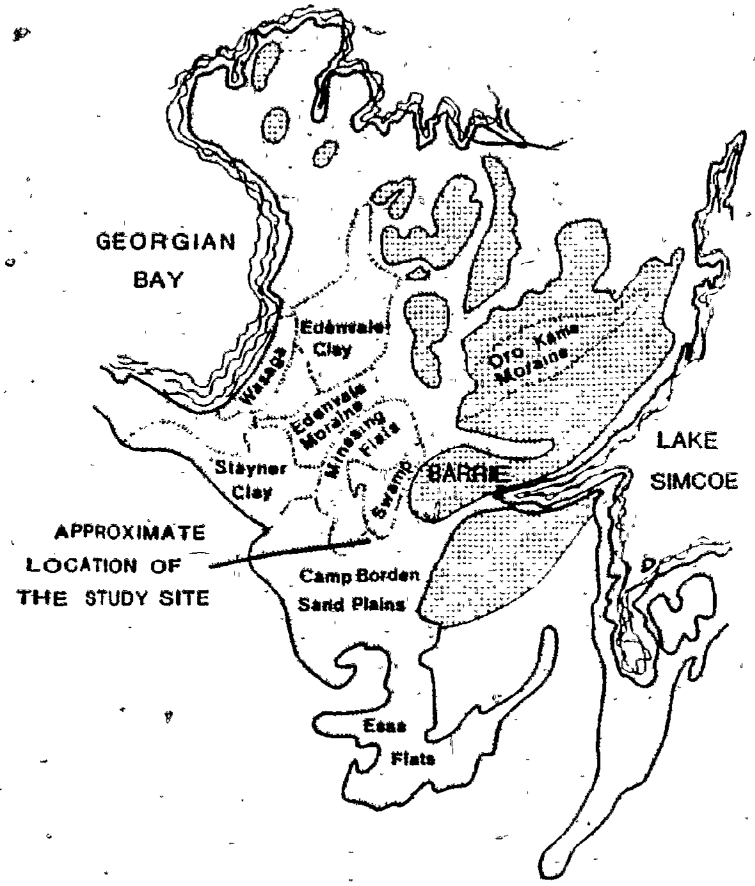

Simcoe Uplands

Simcoe Lowlands

SOURCE: Modified from Chapman Putnam, (1966)

Fig. 4 Map of Simcoe Uplands and Lowlands. The physiographic divisions within each area are also shown.

earlier ice movement of Early or pre-Wisconsinan origin (Taylor, 1908; Chapman and Putnam, 1966). These features were then modified during the later glacial stage. In the case of the Simcoe Uplands, modification resulted in shearing and deposition of till on the ridge surfaces, the ridge slopes were steepened, and the valleys broadened (Taylor, 1908; Deane, 1950). Discontinuously along the edge of the ridges, kame moraines were formed from glacial meltwaters. Today the Simcoe Uplands can be seen as a series of broad, curved, steep-sided ridges separated by wide, flat valleys (Chapman and Putnam, 1966). As the Oro and Edenvale moraines have been eroded by the ice sheets they became rather subtle features in the present day landscape. An alternative explanation of the origin of the Oro moraine is that it formed between two lobes of the main Wisconsinan ice sheet (Chapman and Putnam, 1966).

<u>Maximum Wisconsinan Advance</u>. During the maximum advance of the Wisconsinan glaciation, the Nottawasaga drainage basin was entirely covered by ice. During this glacial stage, the Northern Lobe of ice which occupied the drainage basin formed terminal and kame moraines upon and against the Niagara escarpment (Fig. 5). This resulted in pre-glacial valleys cut into the escarpment being filled with drift, much of which would be later eroded by streams and deposited in Lake Algonquin once the ice had retreated (Deane, 1950). The advance(s) of the Northern Lobe of ice formed the glacial features (till plains, drumlins, moraines) found within the drainage basin, aside from these features

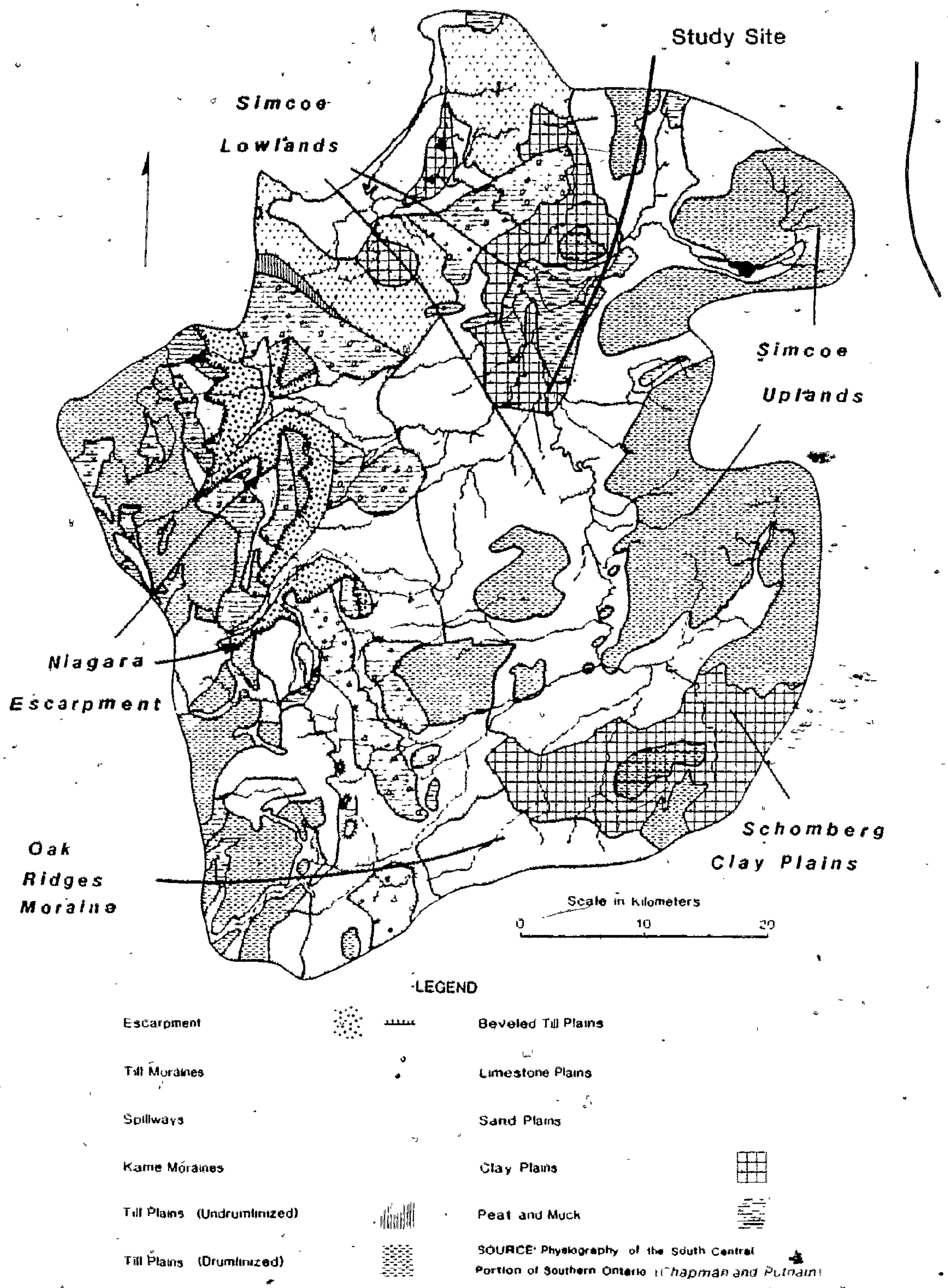

Fig. 5 Map showing the physiography of the Nottawasaga Drainage Basin. Boundary of map is an approximation of the drainage basin margin.

already identified as having a possible alternative origin.

The merging of the Northern Lobe and the Southern Lobe (originating out of the Lake Ontario basin) resulted in the forming of the extensive Oak Ridges kame moraine. A portion of this moraine lies within the southern section of the drainage basin.

Lake Schomberg. Slight retreat of the Northern Lobe from its maximum position resulted in a narrow marginal lake being formed between the ice front and the Oak Ridges moraine. This lake, known as Lake Schomberg, was probably short-lived, since no recognizable shoreline features have been found (Deane, 1950). Evidence of its existence can be found in the form of varved clays, which make up the clay plain in the southern section of the drainage basin (Fig. 5). This clay plain has been referred to as the Schomberg Clay Plain (Chapman and Putnam, 1966). Lake Schomberg was contemporaneous with the early Lake Algonquin, which occupied the southern end of the Lake Huron basin (Chapman and Putnam, 1966).

The Schomberg Clay Plain has an undulating topography because the underlying glacial drift is in the form of drumlins, till ridges and hills of ground moraine (Deane, 1950). Some of these glacial features are prominent enough that drift protrudes above the varved clay layers.

Kirkfield Outlet. The existence of Lake Schomberg was terminated by the rapid retreat of the Northern Lobe out of the

Nottawasaga, Lake Simcoe, and southern Georgian Bay basins. This retreat, in combination with the depression of the land surface, resulted in the expansion of the waters of glacial Lake Algonquin. In the area of the Nottawasaga drainage basin, this resulted in the submergence of the area known as the Simcoe Lowlands (Fig. 4). The Simcoe Lowlands include a large portion of the central Nottawasaga drainage basin, as well as the Lake Simcoe basin (Chapman and Putnam, 1966).

The initial water level of Lake Algonquin in the area is thought to have been higher than the later level which formed a very prominent 'main' Lake Algonquin shoreline (Chapman and Putnam, 1966). Possible evidence of this early lake level has been found in the form of (beach?) ridges in the Simcoe basin (Deane, 1950). This initial lake level would have existed briefly, as the rapidly retreating ice uncovered the Kirkfield (Leverett and Taylor, 1915) or Fenelon Falls outlet. This outlet, located on the eastern side of Lake Simcoe, allowed the lowering of the lake level as water was discharged through Kirkfield, Fenelon Falls, and the Kawartha Lakes chain, into glacial Lake Iroquois. Discharge through the Kirkfield outlet led to such extensive lowering of Lake Algonquin that southern outlets located at Port Huron and Chicago were entirely cut off from outflow of water (Leverett and Taylor, 1915). Possible shoreline evidence of this early stage of Lake Algonquin has been found in the form of 'impounded' beach spits at Sucker Creek, near Meaford, Ontario (Stanley, 1938).

Lake Algonquin. During the Valders glacial substage of approximately 11,200-11,000 years b.p. (Hough, 1963; Karrow et al., 1975), the Kirkfield outlet was again covered by the Northern Lobe. This caused the raising of the water level of Lake Algonquin so that the Port Huron and possibly the Chicago outlets became active once more. The extent of this re-advance of the Northern Lobe in the general Lake Simcoe area is not known, because no terminal moraine was built. This lack of terminal moraine suggests that the re-advance was brief (Karrow et al., 1975); however, the Dummer moraine ~~east of Lake~~ Simcoe (Chapman and Putnam, 1966) is thought to be a recessional moraine of this advance (Deane, 1950).

The Kirkfield outlet was again re-opened with the subsequent retreat of the Northern Lobe. In the time period that had elapsed during the re-advance and retreat of the ice, isostatic rebound had raised the outlet to such an extent that the lake level no longer dropped to its earlier level when discharge was cut off to the southern outlets. This segment of Lake Algonquin history has been referred to as the 'two-outlet' stage in reference to drainage out of the Kirkfield and Port Huron outlets, although it also seems that discharge may have occurred out of the Chicago outlet as well (Leverett and Taylor, 1915; Hough, 1963).

During this two-outlet stage, the water level of Lake Algonquin was at what is recognized as the 'main' lake stage. During the main Lake Algonquin stage the water level remained at a relatively stable height of 605 feet a.s.l. (Goldthwait, 1910), while a very prominent shoreline of bluffs, boulder beaches and spits was formed. These features were observed in the eastern section of the Nottawasaga drainage basin along the slopes of the Simcoe Uplands that were exposed to wave action (Fig. 4). The Lake Algonquin shoreline, as well as succeeding shorelines, would be gradually uplifted above its original height through isostatic rebound. The rate of rebound in the Georgian Bay area as a whole increased in a northeastern direction from a 'hinge' line located at approximately Grand Bend, Ontario (Goldthwait, 1910). The net result of this uplift is that the Lake Algonquin beaches can be found at a much higher altitude than that at which they formed. Thus in the Nottawasaga drainage basin, these beaches can be found located relatively far inland of the present Georgian Bay shoreline.

The level of Lake Algonquin remained relatively stable until approximately 10,400 years b.p. (Hough, 1963; Karrow et al., 1975). Further retreat of the ice northwards began to expose a series of new lower outlets in the Lake Nipissing area causing the water level of Lake Algonquin to slowly recede. Short term halts in the recession of the lake resulted in the formation of much less prominent beaches, below the main Lake Algonquin beach. These lower beaches have been divided into two groups: the Upper and Lower Algonquin beaches (Stanley 1936, 1937).

The Upper Algonquin beaches consist of the Ardea, Upper Orillia, and the Lower Orillia beaches (Deane, 1950), and are located in close proximity to the main Algonquin beach. The Upper Orillia beach is thought to correspond to the final closing of the Kirkfield outlet, with the discharge of Lake Algonquin being entirely out of the Port Huron outlet. The Lower Orillia beach may possibly correlate with the closing of the Port Huron outlet and the opening of an outlet to the north. This would have allowed discharge to begin through the present day Mattawa-Ottawa river valleys into the Champlain sea (Deane, 1950).

The Lower Algonquin beaches consist of the Wyebridge, Penetang, Cedar Point, and Payette beaches found on the present day Simcoe Lowlands in the Nottawasaga drainage basin (Stanley 1936, 1937), as well as the Sheguiandah, Korah and the Stanley-Hough beaches located below the present day shoreline of Lake Huron (Hough, 1963; Prest, 1970). As mentioned, these beaches are thought to be related to successively lower outlets being uncovered by the receding ice in the North Bay area. The net result of these successive lower outlets being uncovered was that glacial Lake Algonquin became gradually reduced in size to such an extent that separate lakes, Lake Stanley and Lake Hough, occupied the Huron and Georgian Bay basins (Prest, 1970).

During the Payette stage, the Minesing basin, located in the Simcoe Lowlands, was occupied by a lake separate from Lake Algonquin. This lake, referred to as Lake Minesing, can be identified by a series of poorly developed shorelines below the Wyebridge beach of Lake Algonquin (Fitzgerald, 1982). The decline of the Payette stage, with the continued recession of the Lake Algonquin waters, allowed the early Nottawasaga river to cut a steep valley through the Edenvale moraine a valley that is still occupied by the river today (Fitzgerald, 1982).

The present landscape of the section of the Simcoe Lowlands that were covered by the waters of the various stages of Lake Algonquin have been formed primarily by deltaic and lacustrine sedimentation (Figs. 3 and 4). Generally, in the deeper waters, clay and silt deposition formed varved clay deposits. In shallower nearshore waters, sand and silts were deposited in delta deposits by rivers flowing into the lake from the terminal and kame moraines along the Niagara escarpment. Recession of the lake in some areas resulted in the migration of these sedimentary environments so that the sandy surface deposits overlie varved clays (Deane, 1950). The flat central/southern section of the Simcoe Lowlands consisting of the Essa Flats and the Camp Borden Sand Plains are such areas. In the northern section of the drainage basin the Stayner and the Edenvale clay plains are areas where the deep water deposits have not been affected to any great extent by nearshore sedimentary processes.

<u>Nipissing Great Lakes</u>. With continued retreat of the ice sheet northward, gradual uplift of the North Bay area outlet resulted in the transgression of the waters in the Lake Huron and Georgian Bay basins. The transgression would eventually cease with the water level rising to 596 feet a.s.l. which closely approached the level of the main Lake Algonquin beach (Stanley, 1936). This

new high water level referred to as the Nipissing Great Lakes, was sufficient to allow the reopening of the long closed Port Huron and Chicago outlets (Hough, 1963). The isostatic rebound that caused the uplift of the North Bay outlet was an extension of earlier uplift that had tilted the earlier Lake Algonquin shorelines. Continuation of this uplift would eventually result in the permanent closing of the North Bay outlet, and the tilting of the Nipissing shoreline (Goldthwait, 1910). The timescale for the Nipissing Great Lakes is considered to be approximately 5,500 to 3,700 years b.p., with the closing of the North Bay outlet occurring approximately 4,700 years b.p. (Lewis, 1969).

In the Simcoe Lowlands previous uplift of the area prevented inundation of much of the area covered by the earlier waters of Lake Algonquin. Thus, most of the lacustrine sediment and portions of the lower Algonquin beaches have remained preserved. A major source of destruction of these features has, however, occurred through headland erosion along the Nipissing shoreline bluffs by storm waves (Stanley, 1937). Despite the lack of penetration into the present day Nottawasaga drainage basin by the Nipissing shoreline, some significant features can be attributed to it at the lower end of the basin.

In the area of present day Wasaga beach, a beach barrier was constructed by the lake, behind which a lagoon was created. Within the still water environment of this lagoon, layers of peat, marl and storm-deposited sand were formed (Martini, 1974). This lagoon environment was formed on top of an earlier 'impounded' Payette stage beach (Stanley, 1936). Present day Marl Lake is a relic of the lagoon environment (Martini, 1974).

The rise of the Nipissing Great Lakes were also sufficent to allow the reformation of a lake within the Minesing basin. This lake, referred to as 'Lake Edenvale', was smaller than the earlier Lake Minesing (Fitzgerald, 1982). Despite the later recession of the lake, the Minesing basin remains incompletely drained as the area is occupied by an extensive wetland area known as the Minesing Swamp.

Post-Nipissing Great Lakes. Downcutting of the Port Huron outlet resulted in the lowering of the Nipissing Great Lakes to a level known as the Algoma Great Lakes (Hough, 1963). The water level attributed to the Algoma Great Lakes persisted from approximately 3,200 to 2,500 years b.p. (Lewis, 1969). With increased downcutting again at the Port Huron outlet, the lake level slowly dropped to the present day level of Lake Huron, where it has remained at a relatively stable level. At some time during this recession the use of the Chicago outlet was terminated.

The influence of the Post-Nipissing recession can be seen at Wasaga beach. Sands exposed by the drop in water to the Algoma level were reworked by aeolian processes forming transverse dunes over much of the Nipissing barrier/lagoon complex. The receding waters also constructed a ridge and swale topography of raised beaches and small parallel dunes just inland of the present day Georgian Bay shoreline (Martini, 1974). This topography of dunes and raised beaches was responsible for the deflection of the Nottawasaga river in the area.

Recent History

Recent history in the Nottawasaga drainage basin has seen the displacement of the native Indians in the area by the arrival of the European settlers in the early 19th century (Hunter, 1908). The initial arrival of the settlers brought about limited clearing of the native forests for agricultural purposes. This small-scale cutting was followed by widespread exploitation of the forests by lumber companies by the middle of the century (Porter, 1973; Pollin, 1974). During this period, the Nottawasaga river and its tributaries were utilized as sources of power for the saw and grist mills that supported the logging and agricultural industries in the area (Paterson, 1961). By the mid 1870's the logging boom had ended, and over-exploitation of the forests had resulted in thousands of stumps remaining of once great forests. The impact of this over-exploitation on the landscape was widespread sheet and gully erosion of the soils by water (Harris et al., 1975), as well as erosion and drifting of soil by winds (Craig, 1977). So extensive was aeolian erosion in the Camp Borden area that sand dunes were formed in the previously flat sand plain. This widespread erosion must have certainly resulted in an increased sediment load of the river. The actual impact of this does not appear to be documented and remains speculative.

The Nottawasaga River

The Nottawasaga river flows along a ninety mile course from the southwestern corner of the drainage basin, eventually flowing into Georgian Bay (Chapman and Putnam, 1966). The river remains free-flowing, unobstructed by flood control devices and dams, unlike some of its tributaries e.g. Bear Creek. In its floodplain the river freely meanders creating numerous meander scars that are easily visible in aerial photographs. Ox-bow lakes can also be found, but do not appear to be too common a feature in this drainage basin.

The monthly pattern of discharge (Fig. 6a) and frequency of discharge level (Fig. 6b) show generally low discharge levels through the year, with a marked increase occurring in March and April. This increase can be attributed to the spring melting of snow. Depending on the amount of snow and rate of melt, extremely high short-term discharge levels can occur, which far exceed the monthly average (Fig. 6c). The pattern of discharge level allows the river to be classified as having a CFb regime (Beckinsale, 1969).

Throughout this paper reference will be made to discharge levels in qualitative terms. The usage of the term 'high discharge level' refers to levels associated with spring runoff, as shown in Fig. 6a. Such levels of discharge were far higher than any observed during the course of this study. Low

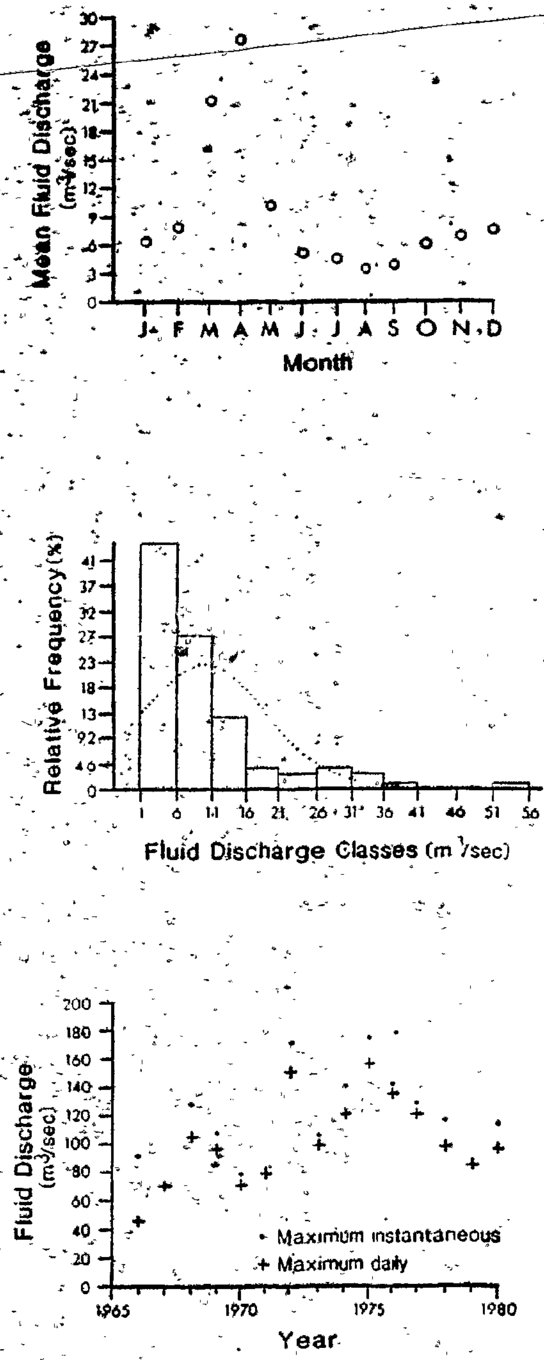

Fig. 6 Graphic summarization of hydraulic data of Nottawasaga River. Data was collected from a gauging station near Baxter, Ontario. (Source of data: Water Survey of Canada)

discharges' or 'low dicharge levels' refers to the characteristic discharges occurring during the months of June and July as defined by Fig. 6a. It was water levels in this range of discharge that were observed during this river study.

A marked contrast is prevalent between the banks of the river upstream and downstream of the Minesing swamp. Upstream of the swamp, the banks of the Nottawasaga river during early summer are partially comprised of barren point and side bars which can be attributed to the deposition of eroded sediment during high discharge levels. Such sediments are derived from the erosion of the sand and varved clay deposits of the Essa Flats and the Camp Borden Sand Plains, by the meandering of the river. This was evident from the formation of actively eroding bluffs in these areas. The suspended load portion of the sediment load gives the river a murkiness and brown colour. Downstream of the swamp, the banks of the river are heavily vegetated containing few extensive areas of freshly deposited sediment. This suggests that sediment being transported by the river was being deposited into Minesing swamp, possibly because of a decrease in river competence. Little sediment was being deposited on the banks of the river due to the decreased sediment load caused by the upstream presence of the swamp.

Summary

The Nottawasaga drainage basin is located in an area of Southern Ontario that has a complex Pleistocene history. The area has been formed by advances in the Wisconsinan ice sheets and by the various stages of glacial Lake Algonquin and the Post-glacial lakes. More recently, the impact of man clearing the forests has resulted in the modification of some areas by fluvial and aeolian erosion. The Nottawasaga river remains today free-flowing, unobstructed by major flood control devices of man.

CHAPTER THREE

FIELD EQUIPMENT AND PROCEDURES

Field Equipment

Current Meter. The measurements of the current velocities in the Nottawasaga River were obtained with a Marsh-McBirney Model 512M electro-magnetic current meter. This current meter utilizes two perpendicular coils, formed in a square cross, to measure the flow velocity. Each coil produces a magnetic field around itself, which generates an electric current proportional to the velocity of the current passing across it. A flow in one direction across a coil produces a positive output value, flow in the opposite direction produces a negative value. Since a coil is sensitive to water passing directly across it, the angle of the flow affects the amount of electric current generated. For example, a flow with a given velocity will produce more electric current by moving perpendicular to a coil, than by flowing at an angle to it. As two coils are utilized by the meter, the outputs from both coils can be used to resolve the flow velocity into two components. By designating one of the coils 'X', the other 'Y', a convenient coordinate system is produced which can allow the coil outputs to be easily resolved mathematically or on a graph to yield flow vectors. The sign of the 'X' and 'Y' coordinates defines the quadrant that the vector resultant falls in, therefore indicating flow direction. The flow direction was measured from the '-Y' axis (zero degrees) in a clockwise manner.

The accuracy of the current meter is +/- .015 cm/s. A potential limitation to the current meter may be caused by flow moving at an angle through the plane formed by the two coils. Such a flow would have a 'Z' coordinate which was not being measured by the meter, thus the speed of the current could be larger than that which was calculated by the meter. At an extreme, a flow moving perpendicular to the plane of the two coils would be measured as zero.

The outputs from the current meter were stored directly into the memory of a Radio Shack TRS-80 model 100 micro-computer. This micro-computer was a major component of a custom-built data-logger (see Blackburn et al., 1984). For each depth location along a vertical profile, sixty-four measurements of the current velocity were recorded each at an interval of one second. In these profiles the current meter was oriented in the water so that the coils were aligned in a horizontal plane. In order to relate the direction of the flow to true north, the azimuth of the '+X' axis on the meter which was parallel to the lubber line of the boat, was measured for each vertical profile. Using this azimuth, it was later possible to mathematically rotate the axes; so that the '-Y' axis (zero degrees in direction on the current meter) and hence, the measured vectors became oriented relative to true north. The equation utilized for this calculation was:

$$CD = AB + 90. + VEC - MD \quad (1)$$

CD - corrected direction of flow to true north.
AB - azimuth of the '+X' axis on the current meter (which corresponded to the lubber of the boat).
90. - angle between '-Y' axis and '+X' axis of current meter.
VEC - measured direction of flow.
MD. - magnetic declination (approximately 9 degrees).

The vector mean and vector magnitude of the measurements at each depth of each profile were calculated using software in resident RAM of the micro-computer according to theory outlined by Curray (1956). The 'X' and 'Y' coordinates of the vector mean were plotted on isometric graph paper, producing a 'three-dimensional' reproduction of the flow for each profile. The graphs could then be placed on a map of the river reach parallel to one another with the '-Y' axis aligned to true north. The flow vectors on the graphs would fall in their correct orientation relative to true north and the banks of the river. In order to produce a practical and legible diagram, it was necessary to trace the graphs onto enlargements of their respective cross-sections. This had to be done carefully as both the orientations of the graphs and the cross-sections needed to be preserved. Reductions of the individual cross-sections were then obtained, and by correctly orienting the reductions around a reduced map of the study reach, a flow diagram was produced.

Plots of the individual measurements of flow speed and direction, near the water surface and channel bed, were constructed for a single profile from some of the selected cross-sections over the study reach. This was done to show how representative of the flow the vector mean was, as well as possibly indicating if the measurements were being affected by turbulence around the current meter. These samples were done over the thalweg, since it was believed that greatest amount of turbulence would exist over the deeper portions of the cross-sections (Yalin, 1977). Exceptions to this were in cross-section 'C' where profile four was used because of an irregular vector distribution, and in cross-section 'E' due to the fact that flow was fastest in the mid-channel area.

Boat. In the river, current velocity measurements were obtained with the data-logger and the current meter being operated from a boat. The boat contained special bow modifications which allowed the meter to be easily maneuvered in the water. These modifications included a square aluminum pole which served to hold the meter in the water. Being held by a pivoting sleeve that was mounted between two slotted plates (Fig. 7), the pole could be easily positioned vertically for velocity measurements, and horizontally for boat movement and equipment setup. This sleeve could be locked into place in any desired position through vertical to horizontal positions by wing nuts. The pole could be lowered to, and raised from the river bed by the retraction of a cable attached to a base plate mounted on the bottom of the pole, through the use of a winch mounted on the bow of the boat. The azimuth of the current meter was measured from a platform on the sleeve, which held a Brunton compass parallel to the "+x" coil on

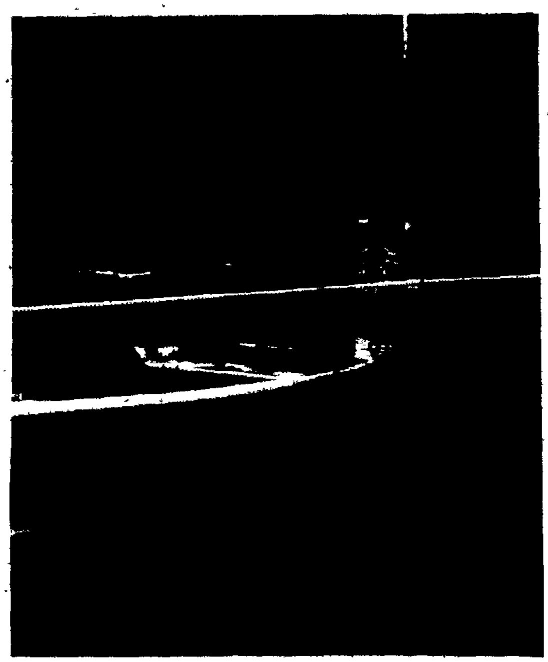

Fig. 7 Photograph showing modifications made to the bow of the boat.

the current meter. The baseplate on the bottom of the pole was spiked, so it could be thrust into the river bed aiding in the stablization of the boat. Extra stabilization of the boat was obtained by tethering the boat to eye splices on a rope that had been suspended and tightened between two 'eyed' pegs (see Fig. 8). Lateral drift of the boat was minimized by the anchoring of the stern of the boat. When the pole was placed in the bottom of the river, graduations along the side of the pole indicated the depth of the water.

The current meter was held in a constant position relative to the boat by a fixture that was mounted to a second sleeve, which rode up and down the aluminum pole. This sleeve could be maneuvered vertically in the water along the pole by a second winch on the bow of the boat. The sleeve allowed the meter to be placed within ten cm. of the river bed. Overall, the modifications to the boat allowed current measurements to be taken along a vertical profile with little destabilizing of the boat.

Depth Indicator. Echo soundings of river reach and cross-sections were obtained from a Raytheon MODEL DE-719B Survey Fathometer. This device produced the depth of the river on a chart output, with an accuracy of approximately ten percent of the reported depth. Because these soundings were done after the cross-sectional measurements, problems arose in acquiring proper reference of the boat to the shore and in keeping the boat in line with the earlier cross-sections, as the depths were obtained

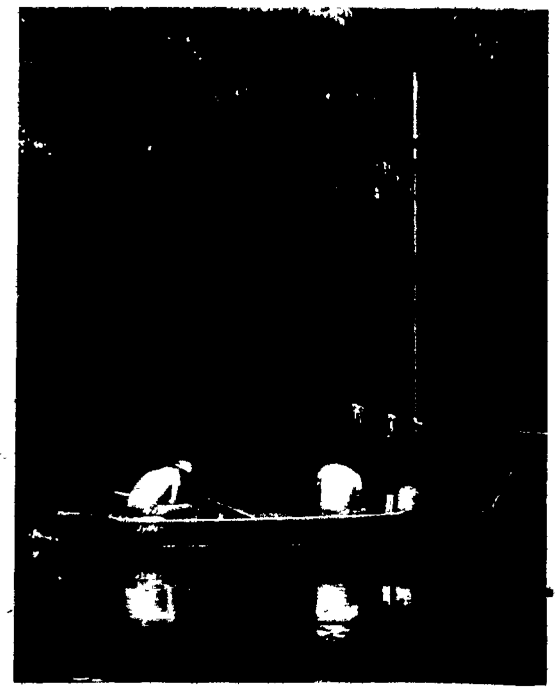

Fig. 8 The boat in operation taking flow velocity measurements.

without the aid of the rope suspended across the river. This meant that the produced outputs only served to give an indication of the bed topography. The soundings of the approximate thalweg of the meander, plus an additional section of river downstream of the study area were obtained by allowing the boat to move in a controlled drift. Although the position of the boat with respect to reference points on the shoreline were marked on the depth output chart, this too served only as an rough indicator of the downstream topography of the reach.

Suspended Load Sampler. Suspended load samples of the river were also taken from the boat, using an Isco Sequential Sampler Model 2100. The concentration of the sediment (milligrams/litre) was later calculated for surface and bottom samples taken in the Nottawasaga and Pine Rivers above the confluence.

Field Procedures

River Measurements. The flow of the river was measured at different depths from six vertical profiles spaced approximately 3.1 meters apart, for most of the fourteen cross-sections (see Figs. 10 or 11). For wider areas of the river up to two additional profiles approximately 2.6 metres apart were added to a cross-section. The profiles were designated numerically by increments of one, beginning at the right bank (see Fig. 11, cross-section 'M') For the cross-section at the Pine River mouth, the numbering started at the southern end of the cross-section 'B'. The cross-sections were spaced irregularly so as to provide the most detail along the bend section of the river reach. The depth interval at which the measurements were recorded initially ranged from ten, twenty and thirty centimeters (cm.) for the early cross-sections before a set format of twenty cm. intervals beginning from five cm. from the water surface was eventually established. This interval of twenty cm. was believed to provide sufficent detail of the flow, while allowing one or two cross-sections, depending on their depth, to be completed in a day's work.

Sedimentology Procedures. Sedimentology data of the exposed bar and slumped areas of the river banks was obtained by a series of excavations. Within each excavation, the exposed sedimentary structures were identified. Along the slumped section of the left bank, the sediments were sampled, sketched and classifed into facies. The grain size of these sampled sediments were later analysed in the laboratory. The cumulative percentage for each size fraction was calculated and plotted on probability paper.

Paleocurrent measurements were obtained on climbing ripple deposits found on and within the exposed bars, and in the facies of the left bank. The paleocurrent directions of the climbing ripples were calculated by similar methods outlined in Saunderson (1975). This involved making a vertical cut across the ripple marks to acquire the general direction of the flow, from the dip of the ripple cross-laminae. A horizontal plane of approximately one square meter was cut across the ripple marks, revealing the internal pattern of the cross-laminations of the exposed ripple troughs. The true direction of flow was obtained by measuring the azimuth of a line normal to the tangent of maximum curvature of the cross-laminations that best represented a single trough (Fig. 9). As in Saunderson's study, the ripple cross-laminations were generally in-phase, thus only one measurement per trough was recorded. A sample of fifty paleocurrent measurements was taken from each sampling location or sampling bed (where different beds were sampled at the same location).

A visual representation of the measurements for each sample was created by grouping the data into intervals of ten degrees, and plotting the resulting groups on a circular histogram. The paleocurrent data was farther summarized by methods outlined by Curray (1956). This produced calculations of the vector mean and the vector magnitude for each set of fifty azimuths recorded from a sample location or bed. It was concluded that each sample set had not originated by random sampling of a circular uniform distribution, by establishing its significance from the Rayleigh test of significance. The vector mean of each sample from an exposed bar was drawn on a diagram of the river to show the spatial pattern of the paleocurrent directions.

The paleocurrent measurements were useful in determining the flow direction at that area of the river channel at the time of deposition. The data collected from the exposed bars in the river was used for estimating the high water flow patterns in

Fig. 9 Photograph showing current ripple marks. Paleocurrent direction is roughly from the bottom to top of the photograph.

sections of the river. In the case of the exposed sediments of the left bank, paleocurrent data aided in the interpretation of some of the observed facies.

CHAPTER FOUR

RIVER CHARACTERISTICS

The field measurements of the river flow were carried out from the middle of June to early July of 1984. During this time period, discharge in the river fluctuated slightly in response to periods of dryness and precipitation, but the average discharge for June and July remained relatively constant. The general surface flow pattern that was observed over the course of the study did not appear to vary significantly from these slight changes in discharge. It was assumed that the internal flow patterns of the river also did not vary significantly as discharge fluctuated. This assumption must be made in order to compare the flow patterns of the cross-sections measured along the study reach but taken at different days and at slightly varied discharges.

For discussion purposes, the study reach has been divided into six sections. In each of these sections, the measured cross-channel geometry, flow speed and flow direction are analysed in an attempt to explain the observed channel morphology and sedimentary processes.

Nottawasaga River Upstream of Confluence. The channel of the Nottawasaga River was relatively straight as it entered the study reach. In this section of the river, the observed channel morphology appeared to be a remnant of higher discharge levels. This was evident as the asymmetry of the channel (Fig. 10) seemed

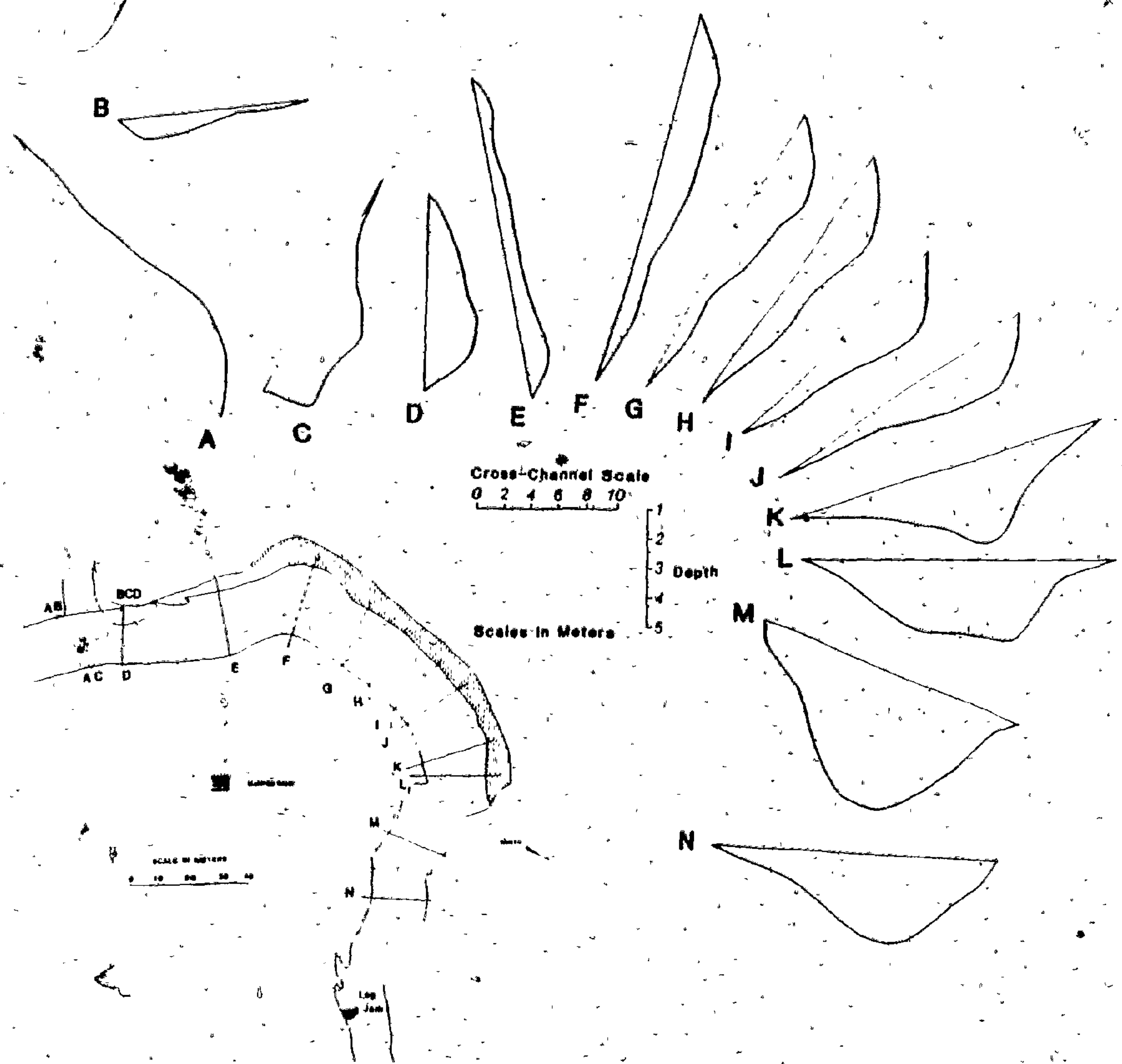

Fig. 10 Diagram showing channel geometry for each of the fourteen cross-sections. Map of the study reach illustrates the location of each cross-section along the river. The alignment of the individual cross-sections correspond to their respective orientations on the on the reference map.

indicative of being formed by helicoidal flow, but the uniformity of the flow vectors in cross-section 'A' showed none was present (fig. 11). Despite the asymmetry, neither the shallow portion of the channel along the left bank, nor the bank itself, appeared to resemble active bars. Also, given the general uniformity of flow speed (16-19 cm/s) through much of the cross-section (fig. 11), in combination with the observation of inactive current ripples along the visible portions of the bed, no significant modification was occurring to the bed, and hence to the channel morphology. Suspended load samples of the water taken across the channel contained an average amount of 25.9 mg/l.

When discharge levels rise in a river, Jackson (Fig. 6, 1975) has shown that the downstream extent of a helix generated at a bend increases. As the observed cross-channel morphology corresponded to the expected asymmetry of the upstream meander, it may have been formed during high discharge levels by helicoidal flow inherited from this meander. Field measurements of the flow taken at high discharges would be needed to confirm this hypothesis. Presumably during these periods of high discharge, active current ripples would be migrating along the channel.

A plot of flow speed and direction vs. time revealed that flow direction and speed over the thalweg were very regular (Fig. 12). The little degree of fluctuation in both at the water surface and bed indicated that a very low degree of turbulence occurred in these slow moving waters. The fluctuation in flow

Fig. 11 Enclosed in back pocket of thesis.

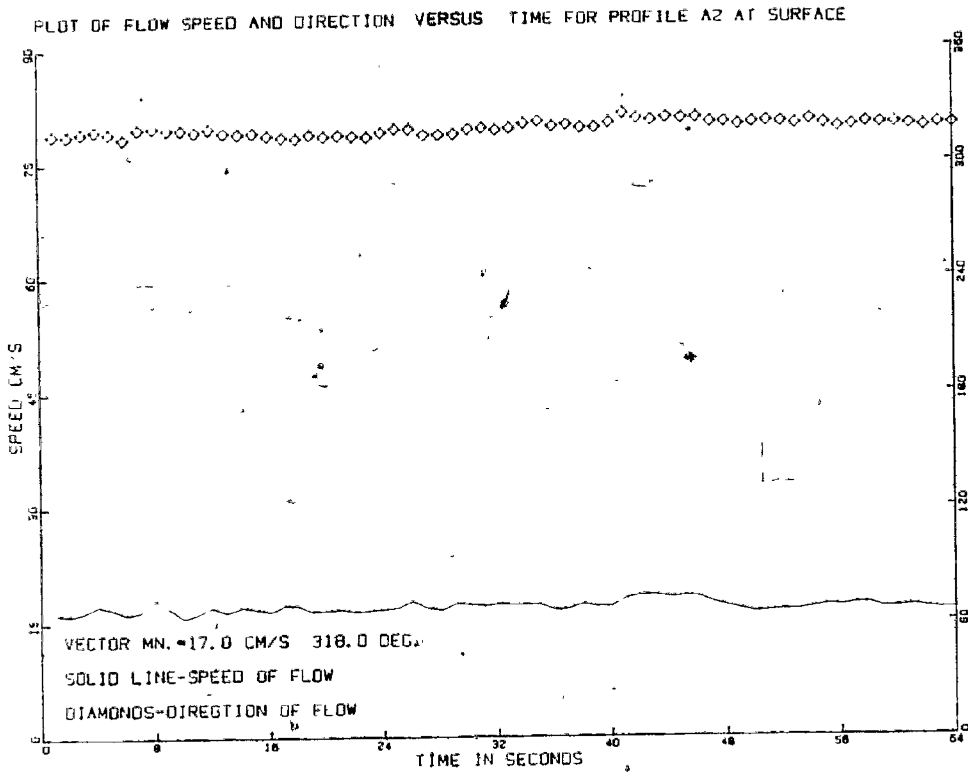

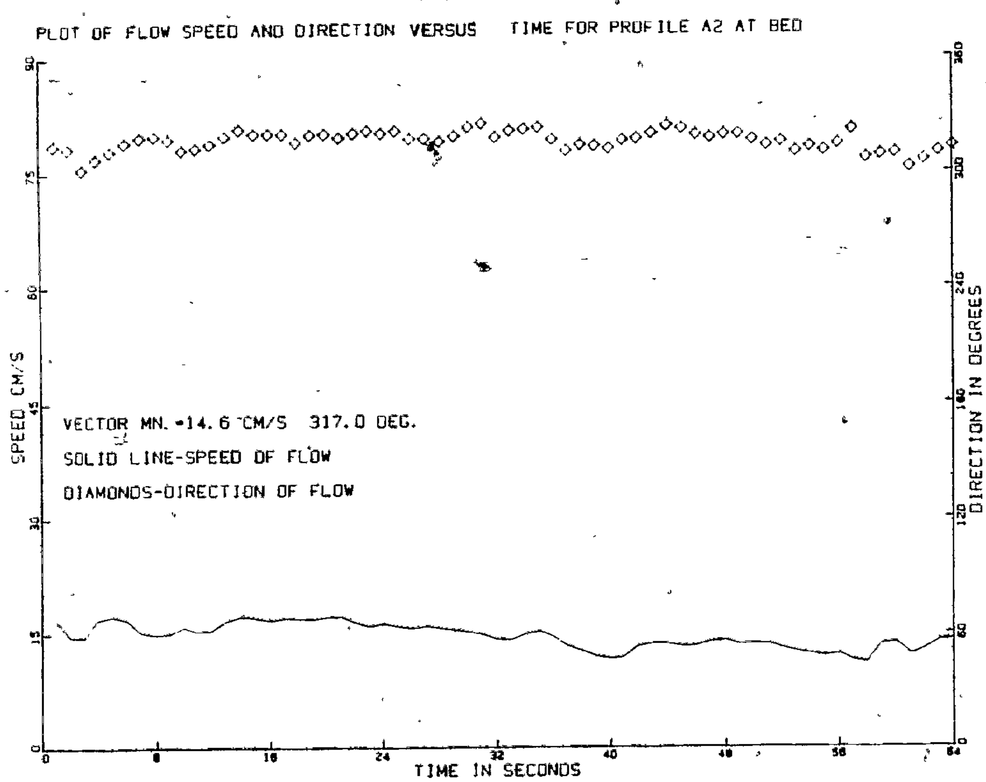

Fig. 12 Plots of speed and direction for each individual measurement of flow obtained at the bed and water surface of profile two, cross-section A. See Fig. 11 for the location of the profile.

speed and direction in this section of the study reach was the lowest observed in any of the cross-sections sampled.

<u>Pine River Upstream of Confluence</u>. In the Pine River, flow passed through a meander as it entered the Nottawasaga River. Here flow conditions were such that active sedimentary processes could be observed. Cross-channel geometry, with the thalweg located along the southern bank (proximal to profile one) and a point bar gently sloping from the opposite bank, was asymmetrical. Flow speeds were very rapid over the thalweg area of the channel, while being considerably slower over the submerged bar (cross-section 'B' in fig. 11). The highest magnitudes measured were towards mid-channel, in profile two. Here speeds averaged 54 cm/s, which was slightly higher than the average of 47 cm/s measured in profile one along the outer bank.

In these fast waters of the Pine River, a plot of the flow speed and direction vs. time revealed that the flow direction was relatively constant, but there was a degree of fluctuation in the flow speed, especially at the bed (Fig. 13). Fluctuations in the flow speed were expected, however; the very abrupt changes in the speed at the bed may have partially been a result of water turbulence. In turbulent waters, as discussed in chapter three, current eddies could potentially pass at an angle to the horizontal plane formed by the current meter sensors, thus affecting the measured speed. Successive eddies moving in different vertical directions towards the current meter would be recorded as abrupt fluctuations in the measured flow speed even

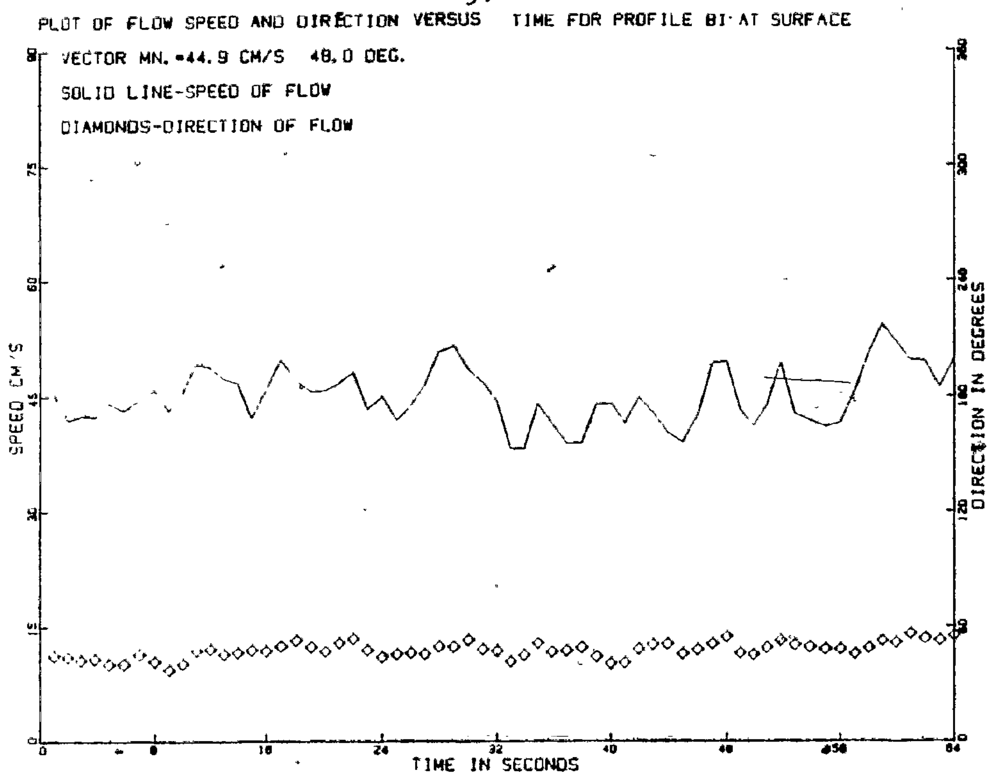

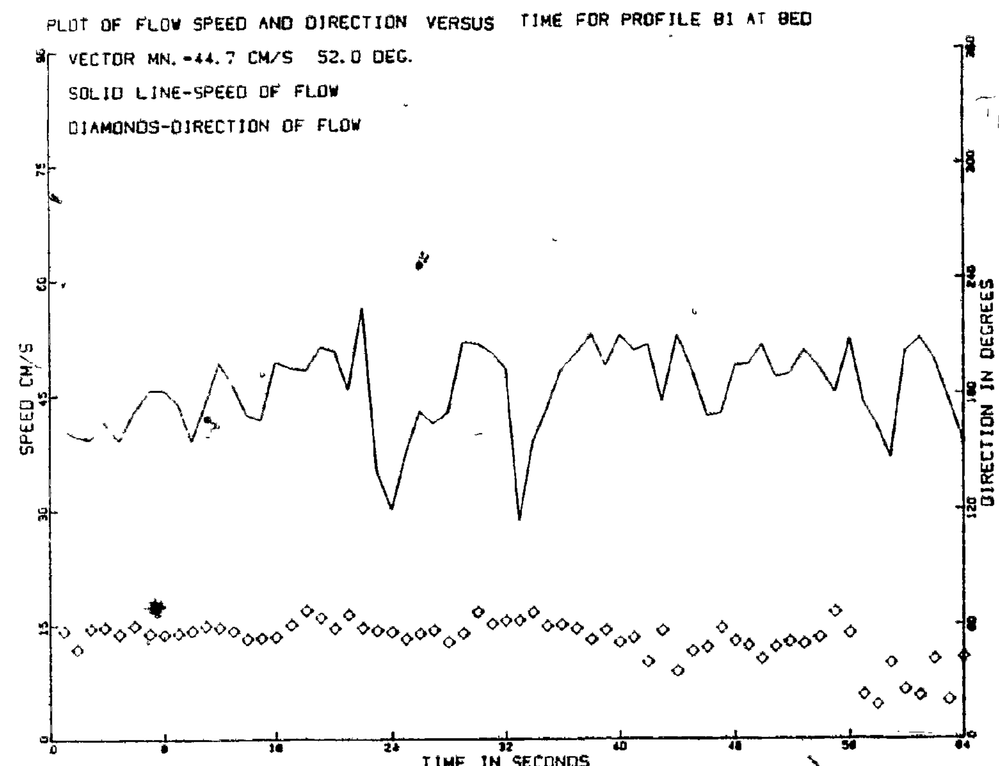

Fig. 13 Plots of speed and direction for each individual measurement of flow obtained at the bed and water surface of profile one, cross-section B. See fig. 11 for the location of the profile.

if all the eddies had roughly similar velocities. Rapid fluctuations in the flow speed, but steady flow direction similar to those observed along the bed in Fig. 13, may be a possible indicator of turbulence. If this is indeed the case, then flow would appear to have been more turbulent near the bed in the Pine River than at the water surface.

Reflective of the high flow speeds in the Pine River, bedload was obviously quite high as active dunes and ripples migrated along the bed of the stream. The dunes located in the thalweg were not readily visible on the bed due to water turbidity, but wading confirmed their presence. The dunes were estimated to be approximately 20-25 cm. high and 50-60 cm. long. Boils could be seen on the water surface to the lee of the dune crests. The current ripples were associated with the shallower portions of flow along the inner bank over the submerged section of the bar. A suspended load sample yielded a measurement of 51.5 mg/l, which seemed high as the waters of Pine River were noticeably less turbid than the Nottawasaga River. This difference in water turbidity allowed the flow from the Pine River to be readily differentiated from that of the Nottawasaga River at the confluence. Despite the mixing of the waters of the two rivers downstream of the confluence, the clearer waters of the Pine River could still be distinguished along-side the left bank at least as far as cross-section 'I'.

In cross-section 'B' two oppositely rotating helices were observed. These helices were distinguishable in cross-section

'B' through the surface convergence and bottom divergence of vectors between profiles one and two (Fig. 11). The rotation of the inner helix (that observed in profiles two and three) seems to correspond to the expected circulation pattern generated at a meander. The bottom vectors of this inner helix appeared to be transporting sediment towards the convex bank, hence the existence of a point bar along the tributary mouth. Thus the presence of this helicoidal flow cell in combination with the flow speed distribution would appear to be influencing the cross-channel morphology under the observed flow conditions. It is not known if the outer helix (that observed in profile one) was an extension of the circulation pattern formed at the upstream meander in the tributary, or locally generated in this particular section of the meander. Hey and Thorne (1975) discuss how two contra-rotating helices, where the surface vectors converge, can have a significant influence upon bed scour, sediment transport and shear stress, and hence, channel geometry. Given the high flow velocities within the tributary being readily able to transport sand-sized sediment, the possible effect of this convergence is difficult to assess.

The general asymmetry of the cross-channel geometry in the Pine River mouth can be attributed to the velocity pattern from flow passing around a meander. It is not known if active scouring of the bank proximal to the thalweg and accretion of the point bar were occurring at the time of observation. Thus it is possible sediment could have just been transported through the meander. Yet, the presence of the helicoidal flow, and high flow speeds against the outer bank, suggest active erosion and deposition of sediment was occurring. If so, then the Pine River channel was slowly migrating in an upstream direction relative to the Nottawasaga River.

River Confluence. At the confluence, the fusion of the two rivers resulted in a complex pattern of flow and sedimentary processes. The general shape of the channel (cross-section 'C') reflected the asymmetry inherited from the Nottawasaga River, but the slope along the right bank had become much steeper. The interaction between the flows of the two rivers resulted in waters of the Nottawasaga being deflected towards the right bank by the entrance of Pine River. This seemed to result in the constriction of the Nottawasaga as indicated by the speeds along the right bank in profiles one and two of cross-section 'C' being generally larger at 22-27 cm/s than those in the channel just upstream of the confluence. In these waters, the flow pattern remained in a relatively constant direction showing little evidence of secondary circulation (profiles one and two of cross-section 'C'). It was not known if active erosion was occurring along the right bank under the observed flow conditions.

The interaction of flows also results in the downstream deflection of the Pine River waters. The flow from the tributary, being in the range of 30-40 cm/s was much faster than that along the right bank. It can be readily distinguished as a high speed filament of flow in cross-section 'C' (profiles three and four, Fig. 11). Interestingly, the flow speeds measured in profile four decreased with increasing height above the bed. Flow speeds over the submerged section the bar in profile five were much slower than those in profiles three and four, and were thought to be associated with a reverse circulation.

The plot of flow speed and direction in Fig. 14 of profile C4 indicates that flow from the tributary at both the bed and the water surface had been quite turbulent in the confluence. This observed turbulence would be expected as flow from the tributary decelerated and mixed as it entered the confluence. At the bed, flow direction was relatively constant but rapid fluctuations in speed were occurring. The very erratic reading of both flow direction and speed at the surface, suggests a very high degree of turbulence, with the vector mean probably representing a net direction and speed. Given the high speeds of flow recorded just upstream in the tributary, flow speed at the water surface in profile four appears to be considerably reduced, despite the range of measured values.

A major influence on the morphology of the confluence occurred as the thalweg of Pine River extended into the Nottawasaga channel, which R. Nolk (personal communication) has reported deepens into a scour pool between cross-sections 'B' and 'C'. The upstream slope of this scour pool was initially very steep, but had become less inclined at cross-section 'C'. A second steep slope projects outward from roughly the corner of

PLOT OF FLOW SPEED AND DIRECTION VERSUS TIME FOR PROFILE C4 AT SURFACE

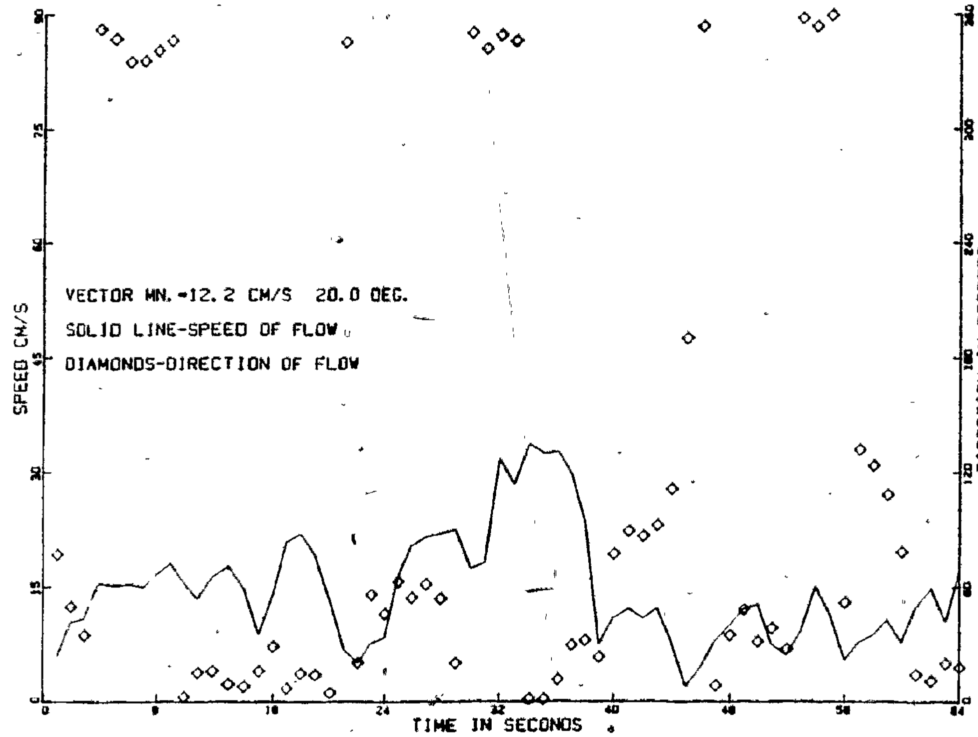

PLOT OF FLOW SPEED AND DIRECTION VERSUS TIME FOR PROFILE C4 AT BED

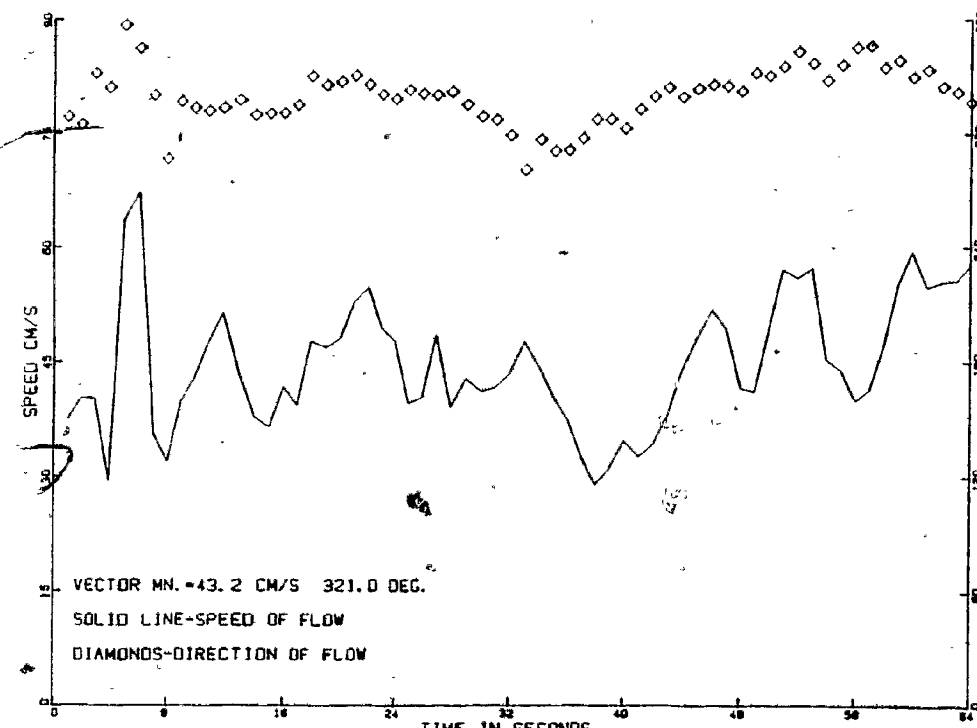

Fig. 14 Plots of speed and direction for each individual measurement of flow obtained at the bed and water surface of profile four, cross-section C. See fig. 11 for the location of the profile.

the left bank proximal to the thalweg of the Pine River channel, giving the scour pool a 'V' shape opening into the confluence. The scour pool became curved as the flow of the Pine River was deflected downstream by the water in the main channel. The deepest portion of cross-section 'C' was in fact, the scour pool (Fig. 10). The shallow area along the left bank was a submerged portion of the large bar located at the mouth of Pine River.

In the rapidly flowing waters entering from the tributary, helicoidal flow existed as evident by the variation between the surface and bottom vectors in profiles three and four. The orientation of this vector pattern was analogous to the pattern of the inner helix located just upstream in the tributary, and hence was thought to be an extension of it. As Fig. 14 indicates a high degree of turbulence in profile C4, this observed vector pattern would represent a net direction of the flow. At any given instance in time, this net direction pattern may become distorted by the water turbulence, with the amount of distortion increasing with greater distance from the bed. The combination of this helicoidal flow, which may become intensified at the confluence (Mosley, 1976), in addition to the turbulence generated from the deceleration of the tributary waters, are thought to have formed the scour pool. The fusion of waters from the two rivers resulted in the downstream deflection of the tributary flow, which also caused a corresponding curvature to the scour pool. In a flume study, Mosley (1976) observed a 'V' shaped scour pool similarly located in the confluence to one observed in this study. The depth of the scour pool was found to decrease with an increased difference in discharge, as well as an increase in the angle between the two rivers. A key difference occurred in the flow pattern over the scour pool, as he observed two helices having a similar rotation to those located just upstream in the tributary. In hindsight, an additional cross-section radiating from the large bar, located between cross-sections 'B' and 'C', would have contributed immensely to this discussion on the confluence.

Due to the presence of helicoidal flow, the waters from the tributary throughout much of the confluence appeared to be functioning as flow would be expected to while passing around a meander. The orientation to the bottom vector of the helix indicates sediment would have been transported from the scour pool to the exposed bar along the left bank, which is analogous to point bar sedimentation. The submerged portion of the bar reflected this process as it was gently sloped into the confluence, and current ripples migrated along the bar face. While low flow sedimentation on its upstream portion may resemble that of a point bar, the bar did not, as it was flat and low-lying. In the area of the reverse circulation, ripple migration occurred up the bar face. If the upstream bank of the 'channel' can be accepted as the flow boundary between the two rivers, then the 'channel' morphology of the scour pool resembled the asymmetrical form at an active meander. Conditions leading to this analogy, however, deteriorated rapidly downstream as the flow velocities and the helicoidal flow pattern of the tributary flow diminished through turbulence and mixing with waters of the Nottawasaga. Particularly noticeable was the declining steepness of the upstream slope of the scour pool. In the vicinity of cross-section 'D', the flow functioned much less like that of a meander as the vector pattern along the bed became aligned downstream, and the scour pool was absent. Downstream of cross-section 'D' the large exposed bar dropped off sharply into the shallow channel.

The sensitivity of the exposed bar to small changes in discharge was quite apparent by the modifications that occurred throughout the summer. The general trend to these modifications was that the bar seemed to grow during the lower periods of discharge, and diminished during higher discharges. This trend may result from variations in the deflection of the tributary flow with increases and decreases in discharge, as a quasi-equilibrium between bar morphology and flow was being established. Increases in discharge would be expected to result in an increased deflection of flow, hence scouring and reduction of the bar. Conversely, lowering of discharge would result in the growth of the bar through sedimentation associated with the flow helix and the reverse circulation.

How the flow pattern, confluence channel morphology, and the exposed bar would react to the very high discharges associated with the spring runoff is not known. The lack of paleocurrent measurements from the bar along the left bank prevented any interpolation of flow patterns that occurred when the bar was submerged. Yet as Mosley (1976) reports, the greatest impact a tributary will have at a river confluence occurs as the discharges between the two rivers approach unity. The lowest amount of discharge variance between the Pine and Nottawasaga Rivers occurs during low discharge levels (D. Bennett, personal communication), thus the tributary would be expected to have its largest affect on the morphology of the confluence during this flow period.

Riffle. Generally over the riffle, flow speeds increased, yet the overall flow directional pattern became much less complicated, approaching uniformity in cross-section 'E'. Flow velocities in cross-section 'D' compared to 'C', became spatially more uniform as the separate streams from the two rivers became almost indistinguishable from each other in the flow diagram. Constriction of the channel by the large bar produced an increase in flow speeds, which ranged from 40-47 cm/s mid-channel to 30-40 cm/s along the banks. From cross-section 'D' to the riffle, the flow continued to accelerate, probably due to an overall reduction in the cross-sectional area as the channel shallowed and widened. A high speed filament of flow formed mid-channel over the shallowest portion of the riffle (cross-section 'E'). Here flow speeds reach 50-65 cm/s, the highest measured in the study reach. Flow speeds along the banks were slightly lower than those of mid-channel, but still ranged from 30-40cm/s along the water surface. In these fast waters, sediment that had been transported from the confluence appeared to be carried through the riffle area.

Near the bed and water surface, flow direction in a plot of profile three of cross-section 'E' was quite steady (Fig. 15). The speed of the flow at the water surface fluctuated moderately, yet at the bed considerable variation occurred. Given the very high flow speeds that occurred in this section, these fluctuations at the bed may well have been a result of turbulence arising from the bed. This was not so obvious from the graph considering the rapid variations in flow speed attributed to turbulence that had been observed at the confluence and along the bed of the Pine River.

Over the riffle, cross-channel morphology became very close to symmetrical. The thalweg did not follow the high speed filament of flow across the channel, rather it diminished along the right bank while reforming along the left bank. This switching or thalweg cross-over, can be attributed to a centrifugal force acting on the flow in response to an increasing, but opposite curvature of the downstream meander. This location of thalweg cross-over has been termed 'delayed inflexion', and has been shown statistically to be the expected location of cross-over (Carson and Lapointe, 1983). The 'cross-over' also resulted in a shallowing of the bed occurring mid-channel at the riffle (fig. 10). As the vector pattern in cross-section 'E' was uniform in direction, the formation of this cross-channel morphology is not clear. A similar cross-channel

PLOT OF FLOW SPEED AND DIRECTION VERSUS TIME FOR PROFILE E3 AT SURFACE

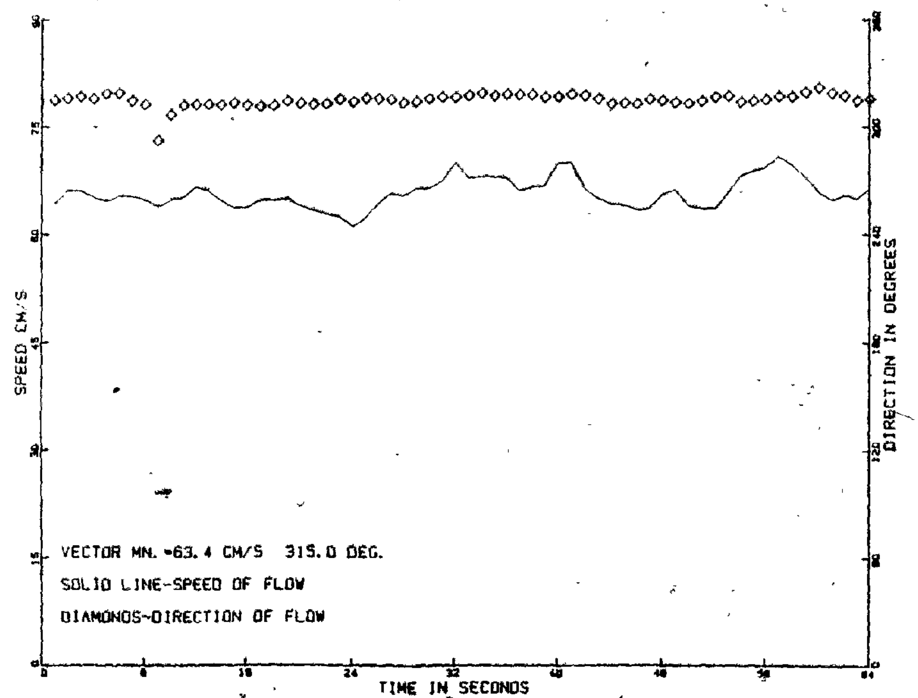

PLOT OF FLOW SPEED AND DIRECTION VERSUS TIME FOR PROFILE E3 AT BED

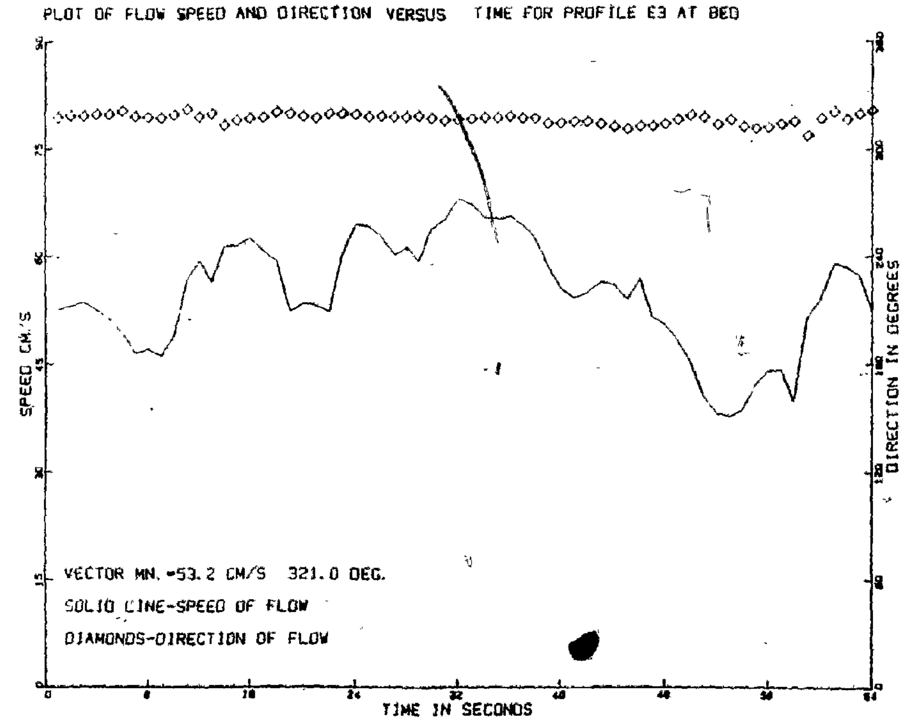

Fig. 15 Plots of speed and direction for each individual measurement of flow obtained at the bed and water surface of profile three, cross-section E. See fig. 11 for the location of the profile.

geometry at a bend entrance has been attributed to the existence of two contra-rotating helicoidal flow cells located on either side of the channel (Bridge and Jarvis, 1982). If the observed channel morphology of the riffle in this study has a similar origin, then the two helices must have existed at higher discharge levels.

Downstream depth soundings of the channel revealed a short steep slope (possibly avalanche slope) just upstream of cross-section 'F'. The slope appeared to extend across much of the channel as boils could be observed laterally along the water surface. This slope may have represented the downstream margin of the riffle (Leopold and Wolman, 1960).

Riffle areas have been found to have wider and shallower channels and higher flow velocities than bend sections of rivers (Richards 1976a, 1976b, 1978; Milne, 1982). The trend continued in this study reach. The riffle area represented the section of the river in which the thalweg switches from the outer bank of the upstream meander to the outer bank of the succeeding oppositely curved meander. It also appeared that although sediment was being actively transported through the riffle, the observed morphology may have been a remnant of higher discharge levels.

Bend. Around the bend, the expected velocity pattern and sedimentary processes were present. Entering the bend, the high speed filament that had been mid-channel over the riffle, shifted towards the left bank as the thalweg began to reform (cross-section 'F', fig. 11). In conjunction with this shift, flow speed of the filament became reduced slightly to 40-45 cm/s. The positioning of the thalweg along-side the left bank gave the channel an asymmetrical morphology. Corresponding to the shallowing of the channel into the slope of the point bar, speeds along the right bank became markedly reduced. This cross-channel asymmetry and general distribution of flow speeds continued downstream through cross-sections 'F' to 'J'. Plots of flow speed and direction vs. time as sampled over the thalweg in cross-sections 'G' and 'J' (Figs. 16 and 17), were relatively constant, indicating a low degree of turbulence.

By cross-sections 'K' and 'L', reverse circulations had developed along the banks as the thalweg and the high speed filament shifted from along-side the left bank to mid-channel. This shift resulted in a shallowing of the channel proximal to the left bank. In these reverse circulations, flow speeds ranged from 5-10 cm/s over the shallow portions of the channel. The boundary of the reverse circulation along the left bank was particularly distinguishable by a line of vortices visible at the water surface. The speeds in the flow filament above the thalweg were generally similar to those located upstream, where it had been located along-side the left bank.

The formation of these reverse circulations appeared to be related to the channel curvature in this section of the bend. Hickin (1978) hypothesized that for meanders with a radius of curvature to channel width (Rm/W) ratio lower than 3.0, the high

PLOT OF FLOW SPEED AND DIRECTION VERSUS TIME FOR PROFILE G4 AT SURFACE

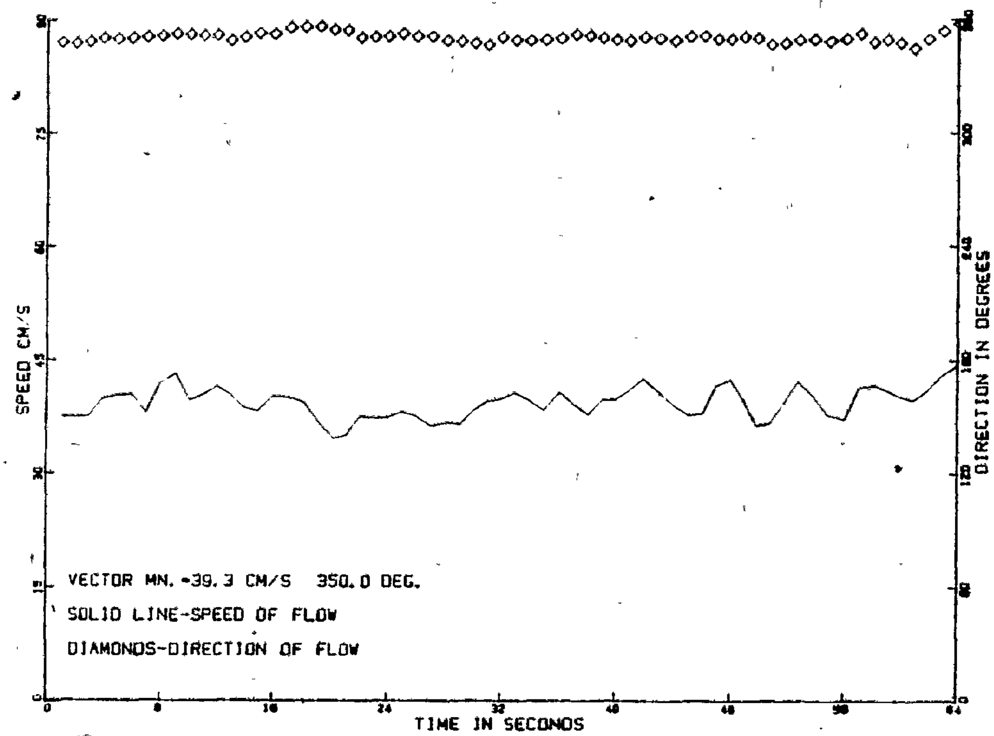

PLOT OF FLOW SPEED AND DIRECTION VERSUS TIME FOR PROFILE G4 AT BED

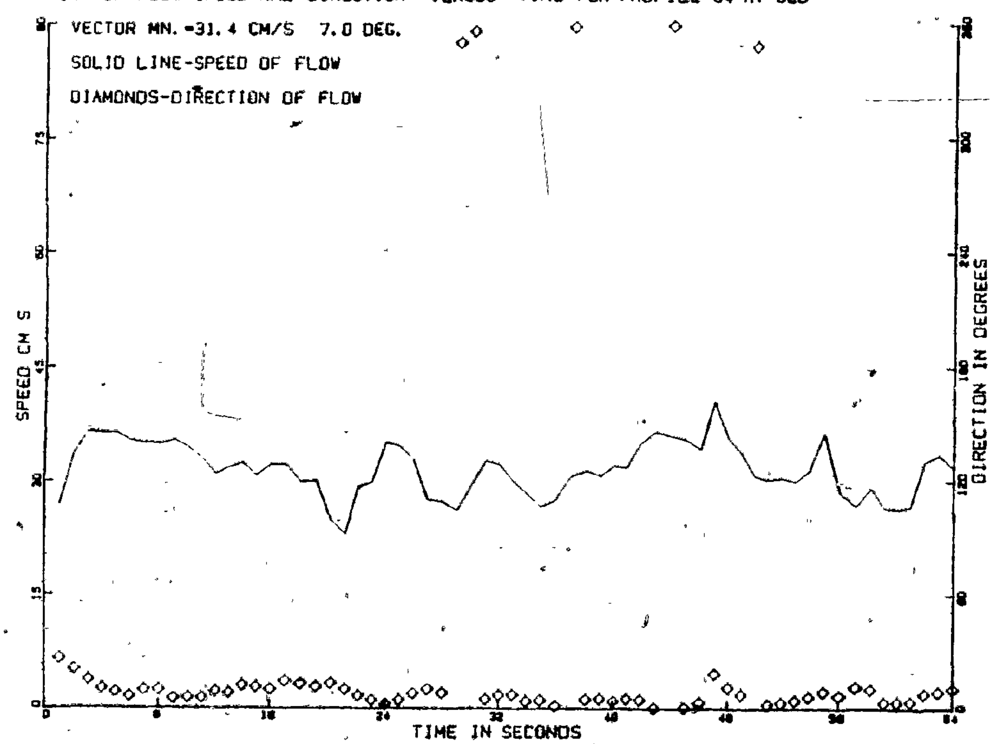

Fig. 16 Plots of speed and direction for each individual measurement of flow obtained at the bed and water surface of profile four, cross-section G. See fig. 11 for the location of the profile.

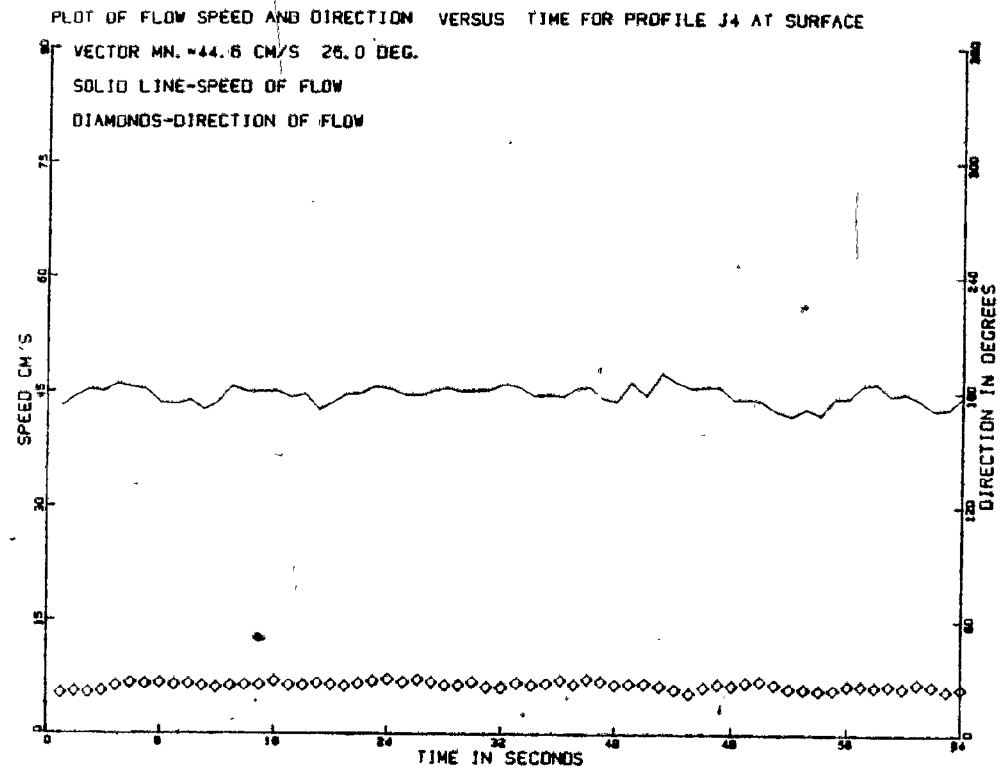

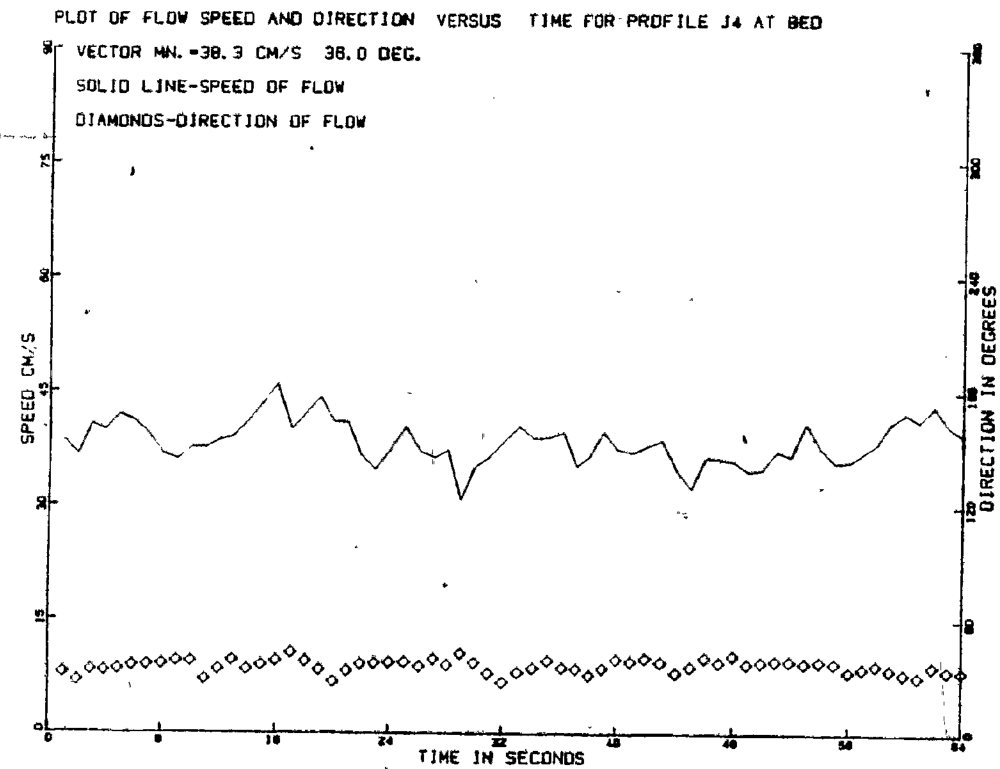

Fig. 17 Plots of speed and direction for each individual measurement of flow obtained at the bed and water surface of profile four, cross-section J. See fig. 11 for the location of the profile.

speed filament of flow shifts from along-side the concave bank towards mid-channel. A reverse circulation may then form proximal to the concave bank, insulating it from the high speed filament and reducing erosion, resulting in the decrease, halting or possibly reversal of channel migration. Bagnold (1960) reports that reverse circulations will develop along the convex bank of meanders with a Rm/W ratio ranging from two to three. The relevant section of the meander in the study reach was estimated to have a Rm/W ratio of roughly 1.6, fitting both Hickin's and Bagnold's models. In this study, however, unlike that observed by Hickin, the shift of the high speed filament towards mid-channel has also been accompanied by the shift of the thalweg.

The portion of the left bank in which the reverse circulation was situated, appeared almost as a 'notch' that had been excavated into the bank. This was especially apparent by the downstream face of the 'notch' being sharply angled towards the flow in the channel. As evident by the presence of the slumped bank, this area was an erosive feature. The excavation is thought to have been formed by the reverse circulation eroding the bank when the river waters would come in contact with the slumped bank during high discharge levels. Although the freshness of the bank face throughout the summer suggests that some erosion probably does occur at low discharge levels through minor failure of the sediment. In support of the notion that a reverse circulation along the outer bank of river can cause substantial erosion, follow-up observations of the study site made during late April of 1985 showed extensive erosion had occurred in this area of the bank. This erosion is particularly significant because in this section of the reach the thalweg was not located along the outside of the channel.

In contrast, the reverse circulation along the right bank appears to be an area of deposition during low discharges as a small bar was constructed on the point bar. Where the point bar ended just downstream from cross-section 'L', the thalweg widened considerably forming a large pool.

Probably in response to the increasing channel curvature as the flow entered the meander, a helicoidal flow began to form towards the left bank over the thalweg (cross-section 'F'). This helix grew gradually in intensity as far as cross-section 'L', as flow passed around the meander. The surface vectors of the helix were oriented towards the left bank, while the bottom vectors were oriented towards the point bar that had been formed along the right bank. The greatest variation between surface and bottom vectors along each cross-section through the bend, occurred over the thalweg. The helicoidal flow increased in intensity with greater curvature to the bend, similar to what was observed in meanders by Jackson (1975). The exceptions to this general directional pattern occurred in profiles six of cross-sections 'G' (upper three vectors) and 'I', where the vector distributions suggested that the intermittent occurrence of very small and weak helices rotating opposite to the main helix had formed along-side the left bank.

The development of a second helix along the left bank through cross-sections 'G' to 'I' of albeit weak intensity and intermittent downstream extent, is significant as the uniformity of flow direction over the riffle clearly indicate that it has been generated in the bend and not inherited from upstream. The existence of this helix has also been observed in flumes as reported by Einstein and Harder (1954) and Shen and Komura (1968). Callander (1978) related the outer helix development to a lower fluid speed occurring near the surface along the concave bank, and mentions that they may develop 'some distance into the meander'. The location of a super-elevated water surface just off the concave bank (see Bridge and Jarvis, Fig. 12, 1982) may provide an energy gradient by which this outer helix could be generated. The super-elevated water surface would have been formed as centrifugal forces generated from flow passing around the bend, push the water towards the outer bank.

Hey and Thorne (1975) point out that outer helices may potentially influence velocity and shear stress distributions, thus erosion and deposition patterns, with the net effect of altering channel geometry. Such a process may potentially affect meanders where the outer helix comprises a significant proportion of the channel area e.g. cross-section 'B' of this study. In the bend area, where the outer helices has been clearly generated within the meander, the small size in relation to the cross-sectional area of the channel suggests a very limited role was played in the influence of channel geometry.

The amount of sediment being transported in the bend was not known because of the lack of a bedload sampler. As well, it was not known whether sediment was being transported through the bend into the pool as the depth of the thalweg and the turbity of the water prevented observation of the bed. Unfortunately the depth sounder did not alleviate this situation as resolution of the device was not sufficient to detect small bedforms such as current ripples. Where the bed was visible along the right bank, inactive ripples were observed on the point bar. A clue that sediment was being transported through the thalweg of the meander was that active current ripples could be observed migrating just below the water surface along the left bank. Also, a small bar was slowly formed as sediment was deposited in the reverse circulation that occurred along the point bar in cross-sections 'K' and 'L'.

The development of the general erosional and depositional pattern and resulting asymmetrical channel morphology that occurs at a meander whereby sediment is eroded from the concave bank and deposited upon a convex bank, has been attributed to a velocity pattern in which the the high speed filament is located along the outer bank and helicoidal flow is present (Leopold and Wolman, 1960). The presence of this flow pattern from cross-sections 'F' through 'J' was reflected by the extensive area of slumping along the left bank, and the development of a large point bar on the opposite right bank. This erosional and depostional pattern continues through cross-sections 'K' to 'L' despite the fact that the thalweg was no longer located along-side the left bank. In this section of the bend erosion of the outer bank was being caused by a reverse circulation. The continuation of the depositional pattern that was building the point bar can be attributed to the strength of the water speed and the helicoidal flow through the bend to passed cross-section 'L'. Thus, the role of the helicoidal flow in the maintaining of the depositional processes through the bend is quite apparent despite the fact that the mechanisms for the outer bank erosion change. The positioning of the erosional and depositional pattern appears to be resulting in the outward migration of the meander, causing an increase in bend curvature (this can be seen in a sequence of aerial photographs (fig. 18)). The termination of the point bar and the slumping along the left bank at the upstream margin of the deep pool where flow velocities and helix intensity diminish, reinforce the role of the flow pattern in the maintainance of the channel morphology.

Pool.

Channel depth at the thalweg, which since the riffle had been gradually increasing downstream through the bend, reached a maximum of 4.45 metres at cross-section 'M'. Here the thalweg widened and deepened forming a pool. The depth of the channel between cross-sections 'M' and 'N' began to gradually increase as flow left the study reach.

The presence of the pool had an impact on the flow as the

1927

1946

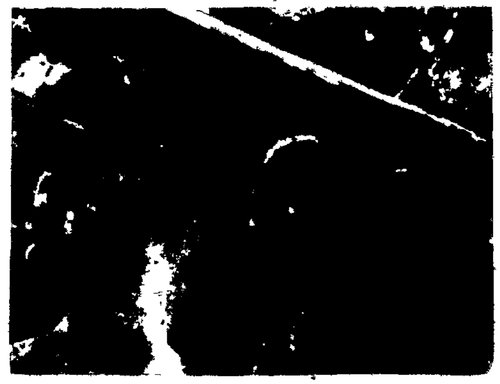

1953

1971

1978

Fig. 18 Aerial photographs of study reach in 1927, 1946, 1953, 1971 and 1978. (Source of photographs: 1927, 1946 National Air Photo Library (Ottawa); 1953, 1971, 1978 Ontario Ministry of Natural Resources (Toronto)).

magnitudes of the high speed filament became substantially reduced to 10-15 cm/s. The distribution of speeds across the channel also became more uniform, although a concentration of the higher magnitudes in cross-section 'M' were located towards the left bank. In profile four at the water surface and over the bed, flow speed and direction showed slightly more fluctuation than had been observed upstream around the bend, yet they still had a relatively low degree of fluctuation (Fig. 19).

The directional irregularity of some vectors, in cross-section 'M', made the flow pattern in the pool area of the reach more difficult to interpret. Despite this, helicoidal flow still appeared to exist through the pool, but at a reduced intensity. The orientation of the vectors in profiles five, six, and seven, suggests that flow was being deflected away from the left bank. Although not measured in any cross-section, an additional reverse circulation was observed to the lee of the point bar terminus.

By cross-section 'N', speeds were slightly increased to 15-20 cm/s and were generally more uniformly distributed across the channel. In this area of the pool there was no apparent high speed filament. A reverse circulation was located along the left bank, in which flow speeds were a very weak 1-3 cm/s. The reversal in variance of the bottom vectors at profile six with that of the other profiles suggests that a second helix has developed near the bed. The presence of a the second helix observed near the left bank with opposite rotation to the

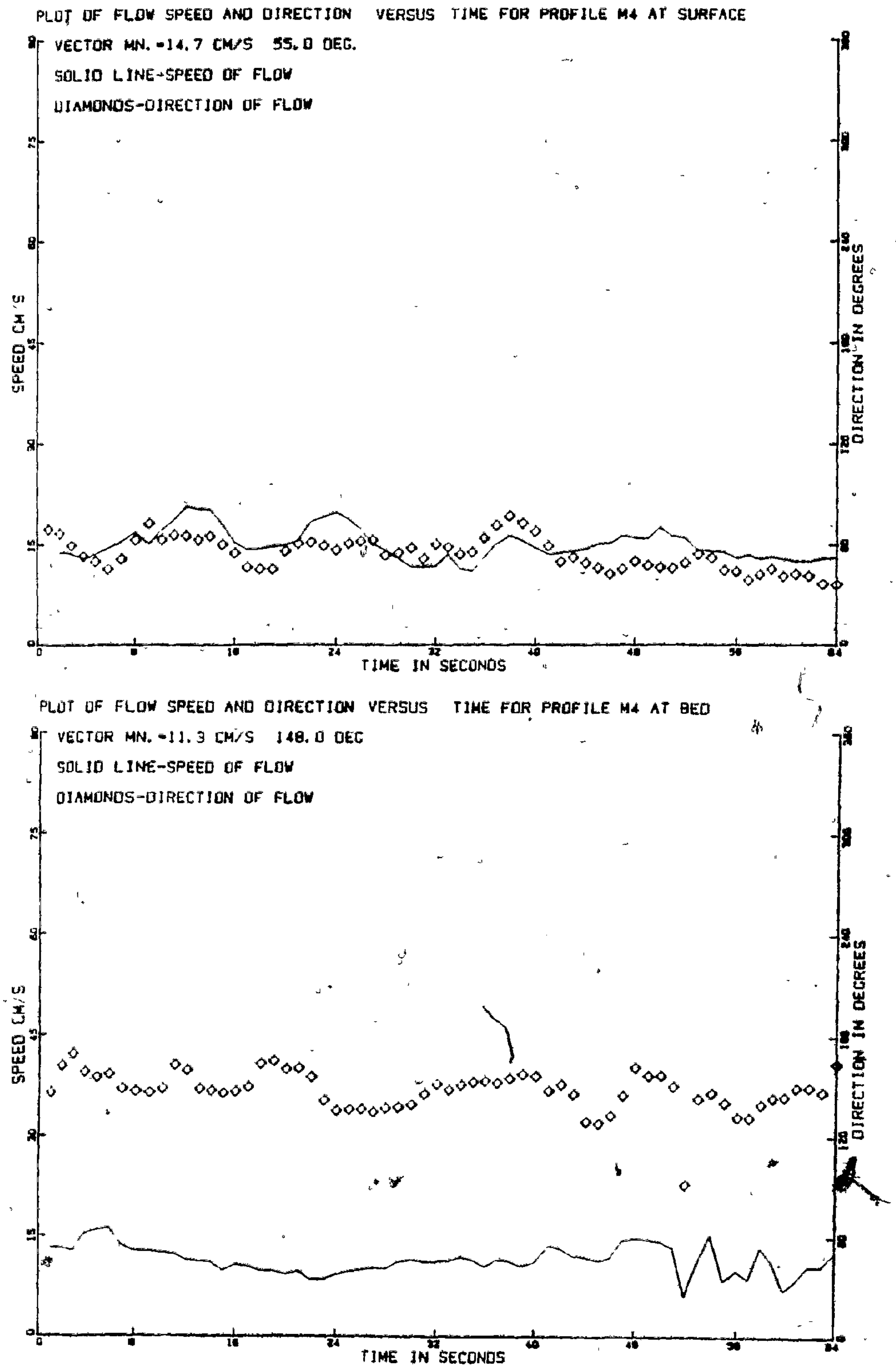

Fig. 19 Plots of speed and direction for each individual measurement of flow obtained at the bed and water surface of profile four, cross-section M. See fig. 11 for the location of the profile.

remaining flow, may be the beginning of the circulation pattern generated in response to the developing curvature of the downstream meander. Whether this second helix extended downstream into the next bend was not known as the flow passes out of the study reach.

The two reverse circulations of flow observed within the pool were both thought to originate from irregularities in the river banks (bank roughness) causing the flow to expand rapidly. With the reverse circulation along the left bank, this irregularity along the bank probably occurred due to the termination of the point bar. The reverse circulation that occurs at the base of profile six in cross-section 'M' may have been associated with a bedform or submerged log.

The formation of a pool at a river bend was not an unexpected phenomenon, yet the anomalous depth of the pool in relation to previous depth encountered throughout the study reach was surprising. Depth sounding of the next two successive bends, one of which was of greater curvature and the other of lesser curvature, revealed pools were also present but were not nearly so deep. Some deflection of the flow from the left bank is apparent in the flow diagram as has been noted, but the measured flow speeds immediately above the bed in cross-section 'M' (5-11 cm/s) were lower than than those of cross-section 'A' (10-15 cm/s) where inactive ripples had been observed, suggesting that the channel bottom was not being scoured during low discharge levels. As the observed flow speeds were not sufficient to create the pool, circumstantially this makes it a product of higher discharges. Such a premise seems in line with scour and fill characteristics observed along other rivers, in which pools were scoured during high flows and filled during low flows (e.g. Lane and Borland, 1954; Carey and Keller, 1957; Leopold and Wolman, 1960). The exact mechanism responsible for the formation of the pool was not apparent from the measured low discharge flow pattern, nor is it known if the pool is a permanent or temporary feature of the bend. A possible mechanism might be an increasing amount of deflection of the flow occurring off the left bank along-side the pool at high discharge levels, which causes scouring of the bed. The fact that the thalweg is located mid-channel here and the reverse circulation that was eroding the left bank does not extend this far downstream, may explain why the left bank has been relatively stable (as is evident by the vegetative community growing on it). An alternative explanation to the formation of the pool would be by bed scouring through form drag associated with a temporary log jam that had recently existed in the meander at approximately cross-sections 'K' through 'L'.

Once the pool had formed it would have a 'feedback' effect upon the flow as the increase in channel area would cause a reduction in flow speed, thereby reducing the erosive power of the water. The presence of the pool as mentioned, resulted in an overall decrease in flow speed and in the intensity of the helix, and occurred in a section of the reach where the depositional and erosional pattern in operation around much of the bend became significantly modified. This was evident as the point bar ended abruptly and the erosion ceased along the left bank where the deepening of the pool began. The breakdown of the sedimentation pattern occurring at low discharge levels just upstream in the bend, appears to have resulted from the decrease in flow speeds as helicoidal flow still exists over the pool.

CHAPTER FIVE

BANK SEDIMENTOLOGY

Along the banks of the Nottawasaga River were a series of bars and accretion deposits. The sedimentology of the exposed bars along the right bank was analysed to provide details of the flow pattern occurring at higher discharge levels. These bars included the large point bar and two smaller 'side' bars (Fig. 20). Also examined were the bank deposits and the series of bars along the left bank in the upstream section of the study reach. Immediately downstream of these deposits, progressive erosion along the left bank opposite the point bar was causing the exposure of a variety of sedimentary structures not attributed to present-day deposition. The general characteristics of these structures were investigated to establish the origin of these sediments.

RIGHT BANK.

Point Bar. A considerable portion of the outer margin of the point bar was initially observed to be barren (Figs. 10 or 11). The remaining area of the bar was inhabited by a thick covering of herbaceous and woody vegetation, including large trees. Much of the barren area of the bar became slowly inhabited by a thin herbaceous vegetation community over the course of the summer. This area of the bar appeared to be entirely covered with current ripples, although they were partially obscured due to drying of the bar surface by the sun, and by human footprints. These

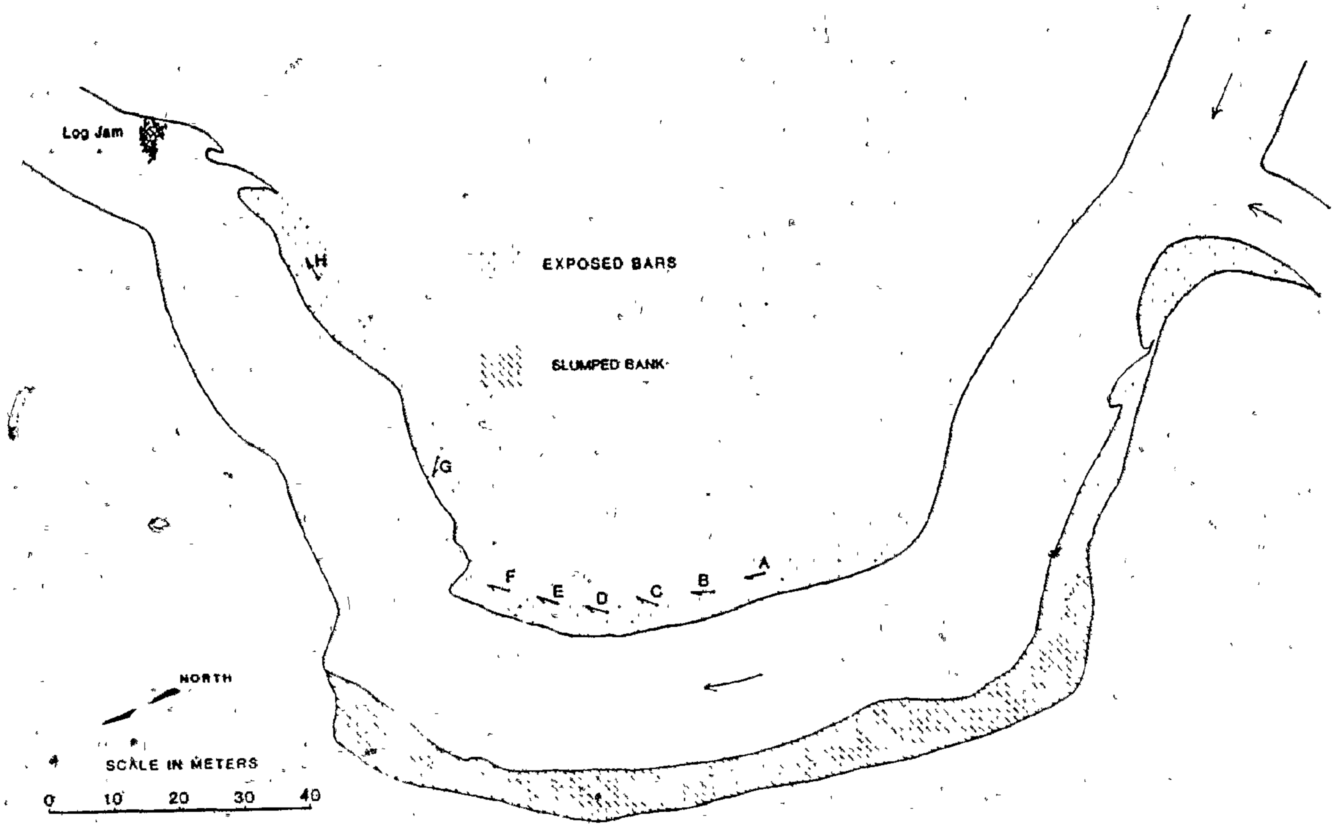

Fig. 20 Resultant paleocurrent direction of ripple mark samples on the exposed bars along the right bank. Flow of the river is from right to left.

ripples were thought to have been deposited during the high discharge levels that would have been associated with the spring runoff. This exposed area of the point bar consisted of sediment which appeared to be medium-fine sands. The exception to this was proximal to the low water surface where the sediment was markedly finer (very fine sands/silts?).

The paleocurrent directions of current ripples obtained from six locations on the point bar gave an indication of the current pattern when the bar was submerged during very high discharge levels. These paleocurrent directions are illustrated in Fig. 20 and listed in Table One. Along the point bar, flow appeared to roughly follow the curvature of the bar, moving in a constant downstream direction. The paleocurrent directions were not absolutely parallel to the bar curvature, as they are biased slightly away from the channel (Fig. 20). This characteristic was probably the result of cross-channel currents associated with the helicoidal flow, which would be more intense during high discharges (Jackson, 1975; Bridge and Jarvis 1976, 1982). As the beginning of the point bar corresponded roughly to the initial development of the helicoidal flow around the meander at low discharges (cross-section 'F'), this would suggest that at high discharges the helix probably becomes generated at a similar location in the bend. No paleocurrent evidence of the small reverse circulation observed along the right bank in cross-sections 'K' and 'L', was found on the point bar.

TABLE ONE

SAMPLE	SAMPLE SIZE	VECTOR MEAN (AZIMUTH)	VECTOR MAGNITUDE (%) OF VECTOR MEAN
A	50	4.3	95.5
B	50	16.4	95.1
C	50	40.6	90.8
D	50	32.4	94.9
E	50	34.6	90.7
F	50	38.0	91.1
G	50	301.4	95.0
H	50	79.1	94.7

(See appendix for circular histograms of sample distributions).

This may indicate that the deposit constructed by this flow becomes eroded away during high discharges, or alternatively that the reverse circulation may only occur at low discharge levels as Jackson (1975) observed, or it possibly could be a recent development to the flow pattern.

Excavations at the paleocurrent sampling sites and at the terminus of the point bar (trench A in Fig. 21) revealed the ripple troughs were Type A climbing ripples (Jopling and Walker, 1968; Allen, 1973). The climbing ripples were separated into beds by thin layers of dark brown 'muddy' sediment. Within these muddy layers, sporadic stalks and roots of herbaceous vegetation were found. The thin muddy layers were thought to represent vegetative growth that had occurred when the bar was exposed during the summer months. This vegetative growth would later be buried when sediment was deposited on the bar during the high discharge levels associated with the spring runoff. Viewed cross-sectionally from the trench at the terminus of the point bar, both the climbing ripple beds and the 'muddy' layers dipped roughly parallel to the dip of the point bar. This indicated that the point bar was migrating through lateral accretion. Bed thickness at the point bar terminus was observed to be quite variable, as the top two climbing ripple beds at the terminus were approximately fifteen and forty centimetres thick. It is not known if a single bed of climbing ripples and muddy layer stratigraphically represented an annual accretion of the point bar. Possible scouring of the bar surface during high discharge

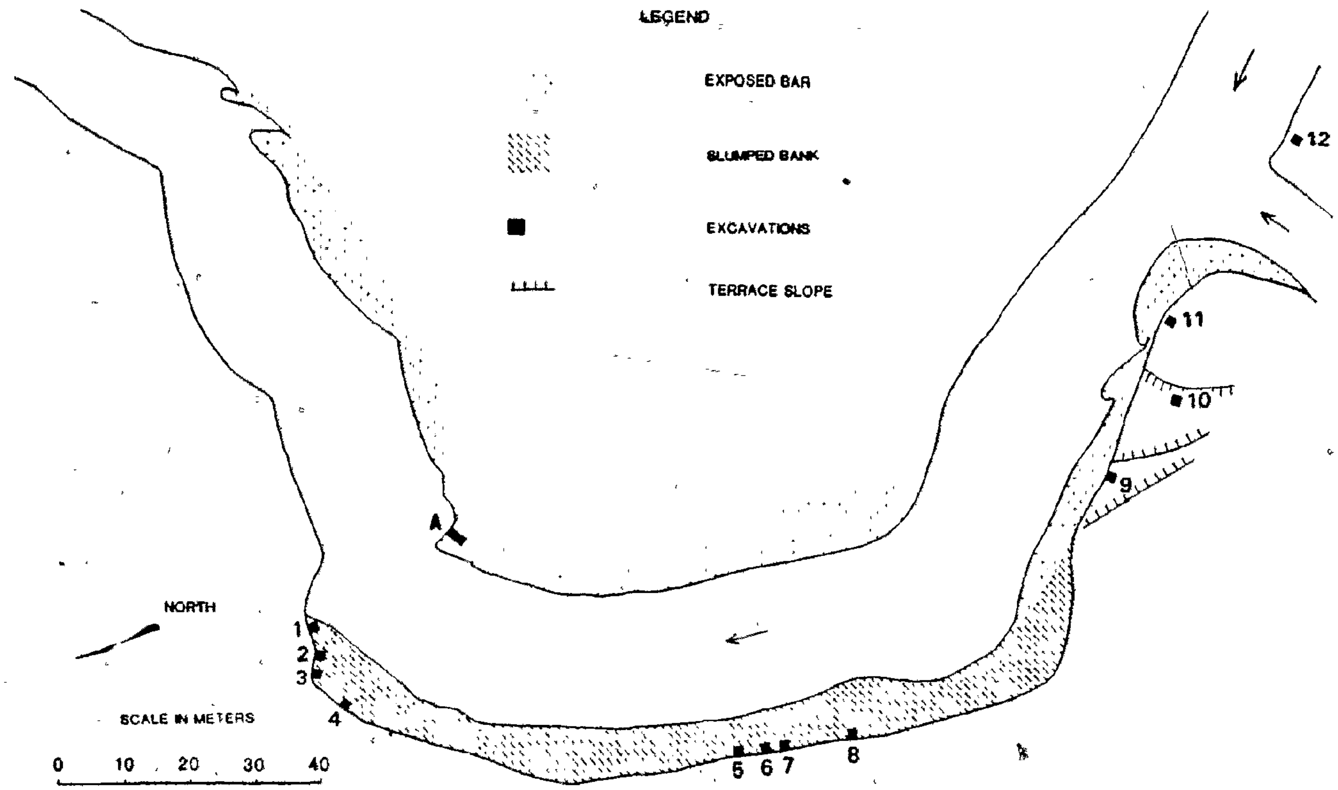

Fig. 21 Map of the study reach showing the location and designation of excavations along the river banks.

levels may well result in the partial or total removal of a muddy layer causing formation of a very thick climbing ripple bed. This very thick bed could then be falsely interpreted as representing accretion of a single season. As noted above, considerable variation between climbing ripple beds did exist.

At the terminus of the point bar, trenching revealed a deposit of cross-laminations approximately fifteen centimetres thick, that extended down the scarp slope. This deposit had obviously formed from the avalanching of sediment down the scarp slope. The presence of an erosion surface between the climbing ripple beds and the cross-lamination deposit indicated scouring had occurred transversely across the point bar terminus prior to the deposition of the cross-laminations. Excavation approximately 3.5 metres into the point bar terminus failed to expose any other occurrence of such cross-lamination deposits. The significance of this observation will become apparent in the in the section on the side bars.

Side bars. Along the right bank, two exposed side bars were located downstream of the point bar. The first side bar immediately downstream of the point bar was similar to the point bar in terms of the dip of the bank, sediment texture, as well as being entirely covered with current ripples. Paleocurrent direction of these ripples was obtained from a single sampling site and produced a vector mean (see Table One) in a roughly upstream direction (sample G, Fig. 20). Such a direction indicates that the current ripples sampled were deposited in a reverse circulation that would have existed during high discharge levels immediately downstream of the point bar. The development of the flow separation may be related to the curvature of the meander, and may have been an expansion of the small reverse circulation observed to the lee of the point bar terminus. Paleocurrent evidence of reverse circulations along point bars generated at high discharge levels has been documented in the literature by Davies (1966), Taylor Crook and Woodyer (1971), Niller and Stravrakis (1982). In all of these cases the reverse circulation actually occurred on the point bar and not behind an abrupt termination to the lee of it.

The existence of this reverse circulation of flow may have also been responsible for the erosion surface at the point bar terminus observed between the cross-lamination deposit and the climbing ripple beds, resulting in the formation of the steep slope that was observed there. The steepness of the bank and depth of the channel to the lee of the point bar terminus may also be indicative of scouring by the reverse circulation (Fig. 10, cross-section 'M'). Scouring at the upstream end of a reverse circulation has been reported by Davies (1966). He mentions an erosive contact between current ripples and an underlying silty clay plug occurring on a point bar of the Mississippi River.

If scouring of the point bar was occurring, then the deposit of cross-laminations found at the terminus may only form during the waning stages of a high water flow when the strength of the reverse circulation was reduced, otherwise they would have been eroded and hence destroyed. The lack of such cross-lamination deposits internally in the point bar may well suggest that the terminus was slowly retreating through scouring. Had the cross-lamination deposit been present it would have indicated a reactivation surface (Collinson, 1970), and therefore advancement of the terminus. The aerial photographs confirm that erosion has occurred in this area of the point bar over a considerable period (Fig. 18). Comparison of the symmetrical point bar illustrated in the 1927 photographs to any of the later photographs shows that bank erosion at the terminus has gradually been occurring. Erosion through reverse circulation in this area of the bend is significant, because in instances of flow separation on the downstream section of a point bar this is expected to be the area of maximum deposition along the inner bank of a meander (Leeder and Bridges, 1975). This is not meant to imply that no deposition was occurring in the area of the reverse circulation, as the presence of the climbing ripples on the first side bar obviously show that it has taken place. Corresponding to this area of maximum deposition, Leeder and Bridges also report that maximum erosion would be expected to occur along the opposite area of the concave bank. In this study, the area of maximum deposition along the convex bank was thought to be represented by the sedimentation on the point bar, upstream of the reverse circulation. Along the concave bank, the slumped area opposite to the point bar clearly represented the area of maximum erosion.

2 OF/DE 2

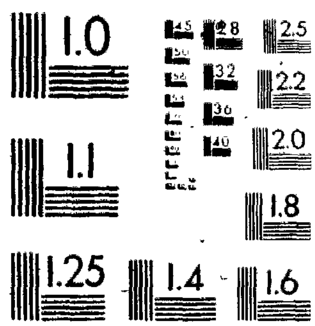

Erosion was occurring along the concave bank downstream of this slumped area, but at a much lower rate.

Inspection of aerial photographs of the Nottawasaga river upstream of the study site as far as Alliston revealed that the exposed portions of numerous other meanders had similar abrupt endings to the point bars. This suggests that the observed erosional and depositional pattern occuring at high discharges and was not necessarily a phenomenon restricted to the meander in the study area. But additional field evidence from a meander upstream of the study site near Baxter Ontario indicated that the presence of an abrupt termination of a point bar does not necessarily result in this pattern.

At the Baxter site, a point bar was observed along a meander that was much tighter than had been observed at Angus. The point bar itself was much smaller in length, width, and in the area of freshly deposited sediment (as represented on the bar as a barren area). At the time of observation, the portion of the bar that terminated abruptly, was nearly submerged. But this feature appeared to represent more a bedform deposited upon the bar, than of actually being a termination of the point bar. Any flow separation associated with this feature would probably occur in a similar manner to that observed with current ripples or dunes. Paleocurrent measurements of ripple troughs on the exposed portion of the point bar, revealed that the flow, at the time of deposition, had roughly followed the curvature of the bar. No abrupt ending to the point bar analogous to what had been observed at the Angus study reach was present. Thus, at the site near Baxter different sedimentary processes seemed to be operating, as erosion appeared to be occurring only along the left bank, with deposition being restricted to the right bank. These observations suggest that additional analysis of a number of point bars with similar morphological characteristics should be undertaken before any models regarding depositional and erosional patterns be generalized on the Nottawasaga River.

The second side bar downstream of the point bar was very different in morphology from the other previously discussed bars. This second bar appeared to be an extension of the bank, rather than a deposit on it. The bar had distinctly lower relief than either the proximal bank, point or side bars, as it protruded just above the observed water surface. The grain size over this side bar appeared to be similar to that observed on the other bars. A major portion of the exposed area of the bar was occupied by a sand wave of roughly ten centimeters thickness. Current ripples were observed on the back of the sand wave and produced a paleocurrent direction (see Table One) which indicated that they had migrated in a downstream direction (sample H, Fig. 20). Trenching of this sand wave exposed cross-beds that also dipped in a downstream direction. These cross-beds had evidently formed from the avalanching of sediment down the leeside slope of the sand wave that had been transported up the stoss slope as current ripples. This sedimentary process was thought to be active during high discharge levels associated with the spring runoff.

At high dicharges, the reverse circulation downstream of the point bar terminus became reattached to the bank between the two side bars causing sediment to again be transported in a downstream direction. This was clearly shown by the paleocurrent direction of the second side bar, indicated by ripples on the sand wave, and of the downstream migration of the sand wave itself. The existence of the second side bar seemed unusual because it was located on what was the concave bank leading into the next meander. Concave bank deposits have been documented by Woodyer (1975), Hickin (1978, 1979), Page and Nanson (1982) and Nanson and Page (1983). In all of these cases, the deposit was associated with deposition in an area of flow separation caused by the over-steepening of a meander. Indeed, such a deposit with similar characteristics was observed along the Nottawasaga river, on the concave bank of a tight meander, downstream of a previously mentioned meander near Baxter. But the downstream paleocurrent direction of the side bar clearly indicated that in this instance the same process was not occurring. It may be suggested that this side bar was analogous to the large bar located immediately downstream of the confluence, as the large bar was also located on the concave bank slightly upstream of a meander. But the presence of the large bar was believed to be related to the flow pattern inherited from the Pine River as it entered into the main channel at the confluence. Perhaps of significance to the existence of this side bar was the presence of a log jam located immediately downstream. Alhough technically located outside the study reach, it was observed that lateral accretion did occur downstream of the log jam, despite the fact that the area was located along the concave bank of a meander (i.e. of the succeeding meander to the study area). Hickin (1984) discusses the role of log jams and the flow separation zones behind them, in the formation of concave benches. Such a phenomenon appears to have been occurring here behind the log jam.

The log jam is probably younger than thirteen years old, as it was present in the 1978 aerial photographs, but not those of 1971. In view of the fact that the second side bar doesn't appear in the 1978 photos, this suggests that the deposition along the downstream end of the right bank of the study area has been a recent process. This process may well be the beginning of a new trend in the channel migration, as the aerial photographs indicate that little apparent change has been occurring in this area of the meander. The side bar upstream of this log jam appears to be part of the river's response to the presence of the log jam. Continued monitoring of this area of the bank and other log jams on the river would undoubtedly provide a better indication to both the processes and trends in operation here.

LEFT BANK.

Bar and Bank Deposits at Upstream Section.

Along the left bank was a large bar at the mouth of the Pine River, and a series of narrower bars were located downstream. At low discharge levels, these bars had relatively low relief, protruding just above the water surface. Comparatively larger portions of these bars become submerged during the intermittent rises in discharge associated with heavy periods of summer rainfall than occurred along the lowlying side bar along the right bank.

The largest and most prominent bar along the left bank was the one located immediately at and downstream of the mouth of the tributary. As discussed in Chapter Four, helicoidal flow at the confluence has a major influence on the sedimentation processes that have constructed this bar. This bar was separated by a log from a smaller bar located immediately downstream. The large bar consisted primarily of sediment which appeared to be medium-fine sand in texture; however, towards the downstream end the sediment became noticeably finer. The bar was also covered in current ripples. Unfortunately, the direction of ripple migration remains unknown, as the saturation of the sand prevented paleocurrent analysis, and the identity of the lee and stoss sides of the ripples could not be conclusively established. A box core revealed that internally the bar consisted of similar grade sediment as the bar surface. Layers of humic matter divided the core into beds of variable thickness. Within the top bed very faint Type A climbing ripples could be distinguished. Along the submerged margins of the bar, current ripples actively migrated.

The smaller bars of the left bank were covered with fine sediment similar in texture to the sediment found along the outer margins of the point and side bars on the right bank. The sediment appeared to be in the very fine sand/silt size range. The saturation of the sediment prevented any paleocurrent measurements. Unlike the large bar located upstream, the form of these bars did not appear to be modified significantly by increases in discharge. The response of these bars to a major increase in discharge that would be associated with the spring runoff is not known.

Along the left bank, one trench was excavated into the area of bank located between the tributary mouth and the cut-off. This trench, designated trench eleven in Fig. 21, revealed thick rhythmic beds of structureless sand, and thin multiple layers of dark and light brown coloured sand, for most of the section. Bed thickness ranged from five to fifteen cm. for the structureless sand, and to five through ten cm. for the dark and light brown beds. The thickness of an individual bed was not constant, varying in thickness by similar amounts. The contact between the beds was poorly defined. The beds were arranged roughly parallel to the dip of the bank, which indicates that the bank was accreting laterally. In both types of beds the sediment appeared to be fine sand, with the darker layers thought to have been caused by a large portion of organic matter. Within some of the beds, faint Type A climbing ripples were observed, oriented in an approximate downstream direction. This estimation of paleocurrent direction indicates that at the time of deposition, the sediment was being transported in roughly the downstream direction. Allen (1963) classifies heterogeneous inclined beds of this nature as epsilon cross-bedding.

In a trench, designated as trench twelve (Fig. 21), excavated on the left bank just upstream of the tributary, similar bedding to that observed in trench eleven was exposed. In this trench, however, the bedding consisted of sand containing structures of faint Type A climbing ripples, alternating with dark brown coloured sand. The dark brown colour of this sand was again attributed to a high organic matter content. Roots were located sporadically throughout these beds. Numerous strands of nylon fishing line were also observed in the bedding as was a beer bottle. These latter items suggested that the beds had been deposited relatively recently.

In both trenches a thick basal layer of Type A climbing ripples was exposed near the water table. This unit did not appear to conform with the rhythmic beds described above. Paleocurrent directions of the ripple marks produced vector means of 325.6 and 309.4, with vector magnitudes (%) of 97.6 and 91.6, for trenches eleven and twelve, respectively. These paleocurrent directions indicate that the sediment had been transported in a downstream direction at the time of deposition (Fig. 20).

Two additional trenches, nine and ten, were excavated into the left bank. Trench ten was located in the lowest area in the cut-off, while trench nine was located on the cut-off terrace. In both of these trenches, horizontal bedding was exposed. The bedding exposed in trench nine consisted of beds of structureless sediment alternating with beds of dark brown sediment. Again, the dark brown beds appear to have derived their colour from containing a high percentage of organic matter. The sediment in both beds appeared to be fine sand. Similar to the beds of trench eleven, the thickness of these beds was variable, ranging from five to ten centimeters. Also contact between the beds was poorly defined. No sedimentary structures were observed within any of the beds, therefore no indication of paleocurrent direction was obtained.

The sediments observed in trench ten were saturated with water, which gives an indication of the elevation of this area relative to the water surface in the river. In this trench, two beds were exposed; the top bed consisted of a dark brownish grey layer, while the underlying layer was dark grey in colour and contained a large amount of organic matter. Both layers consisted of sediment in the very fine sand size range. These horizontal beds in trenches nine and ten indicate that vertical accretion was occurring on the various levels of the depression.

The presence of the epsilon cross-bedding along the left bank indicate that lateral accretion of the channel was occurring. This accretion of the left bank was readily apparent from the aerial photographs (Fig. 18). In the 1946 and 1953 photographs, the bar immediately downstream of the tributary appears as a spit-like form that protruded into the main river channel. By 1971, sedimentation had occurred behind this protrusion forming a large bar that resembles the form of the bar observed in this study. The 1978 photographs revealed that this bar had become heavily vegetated, suggesting that stabilization of the feature had occurred. The thick units of climbing ripples observed in the bottoms of trenches eleven and twelve may well be bar sediments that became buried beneath the laterally accreting banks. Corresponding to the accretion of this bank has been the gradual erosion of the steep bank along the opposite side of the river. The erosion was evident by the developing inward curvature to this section of bank. The thickness of the vegetation on the bank suggested that erosion has been slow, or that the bank has recently been stable. Mosley (1976) has observed similar depositional and erosional characteristics in an experimental study of channel confluences. In flume runs where a tributary entered a straight main channel, a bar resembling that observed in this study, formed on the bank immediately downstream of the tributary mouth. Also analogous to this study, was the erosion which caused the development of an inward curvature along the bank opposite to the tributary and bar.

Slumped Area of Left Bank.

Along the slumped bank, a large area of extensive slumping between trenches four and five (see Fig. 21) prevented complete observation of the bank sedimentology. Thus, the bank sedimentology will be discussed as two sections: section A consisting of trenches one, two, three, and four, and section B consisting of trenches five, six, seven, and eight. The upstream end of Section B was separated from the cut-off depression by a second area of extensive slumping in the bank. Diagrams of the bank exposures contained in the sections A and B, are illustrated in Figs. 22 and 24. The location of the trenches in the concave bank are illustrated in Fig. 21. In each of these two sections, five sedimentary facies were identified by common origin, structure, and particle size distribution of the sediments.

SECTION A.

Facies 1A. Facies 1A was a surface facies, identified as a soil profile, despite the lack of apparent horizon development. The facies was not continuous along the bank, as it had been truncated by facies 2A (Fig. 22). Generally, facies 1A was structureless, and had been heavily penetrated by living roots. Also contained in the facies were large pieces of modern organic matter that had clearly been buried (e.g. a sawed log was observed in trench one). The presence of buried organic matter, such as the sawed log, and the lack of apparent soil horizon

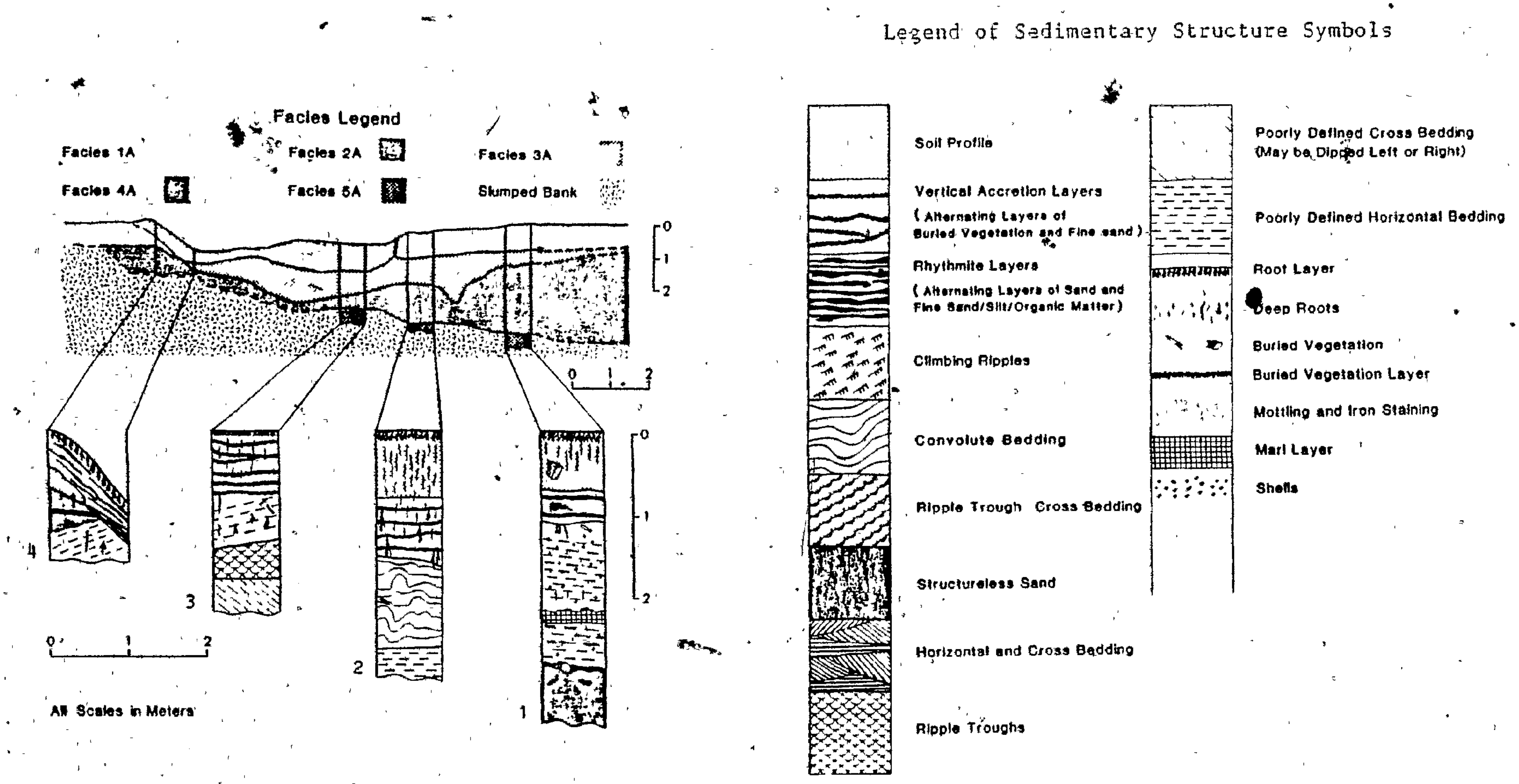

Fig. 22 Diagram showing the sedimentary facies observed in section A along the left bank. Trenches are designated one to four from right to left.

development, suggest that the facies is relatively young in age. Sedimentary structures may well have been present, but have become masked by pedological development.

Facies 2A. Facies 2A was interpreted as a vertical accretion deposit formed during intermittent overbank discharges, as a result of the ponding of water on the floodplain surface. Evidence for this interpretation was provided by the relatively large amount of the silt/clay size fraction present in the sediment, which may possibly represent the suspended and wash-load of the river (Fig. 23). Such deposition must have occurred in relatively stagnant or confined conditions, since such fine sediment could not have settled in turbulent waters. These conditions may occur during overbank flow conditions as floodwater could pond on low areas of the floodplain. This mechanism would seem to be all the more plausible as the facies was located in a slight depression on the floodplain (Fig. 22). As the facies generally consisted of alternating layers of buried humus and structureless sediment (Fig. 22), the layers of sediment would represent the actual accretion, while the humic layers are thought to represent growth of herbaceous vegetation on the sediment. It is not known if each sediment and overlying humic layer denote an individual occurrence of an overbank flow.

The facies was deposited upon an erosion surface. This erosion surface could have also been formed during overbank discharge levels; water spilling over the bank may erode as it flows to a lower level of the floodplain. Such features are

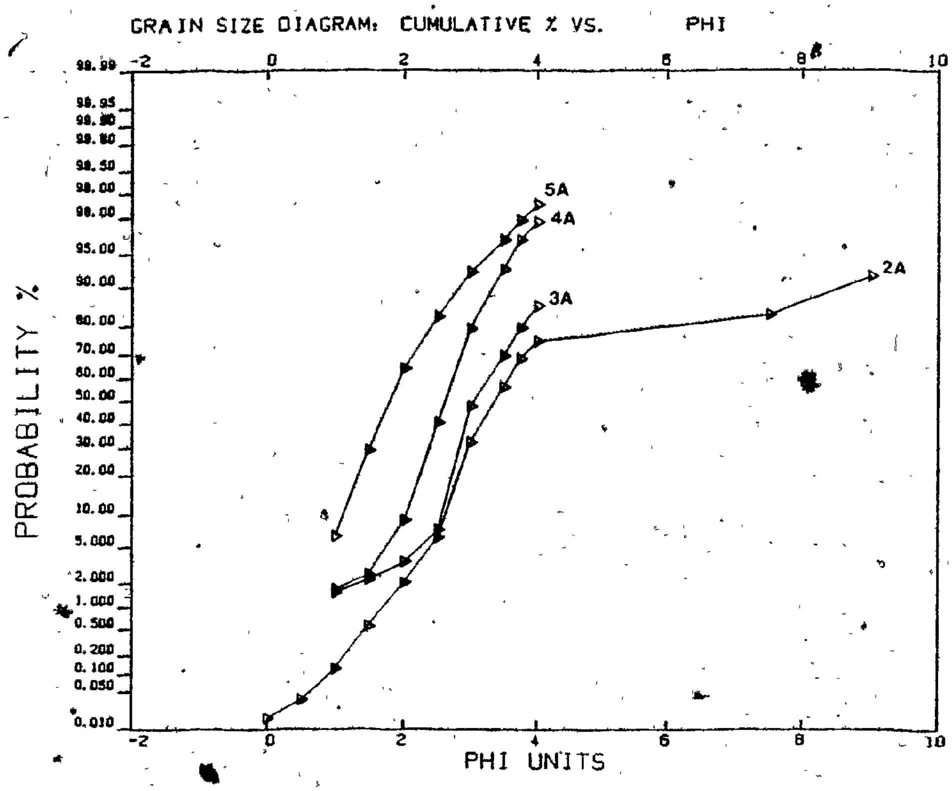

Fig. 23 Grain size diagram of sediment samples obtained from facies 2A, 3A, 4A and 5A. These facies were observed in section A of the left bank.

known as crevasse splays, but are usually associated with rivers that have levees. Yet, while no apparent levees were observed on the study site, it is possible a slight grade sufficient to allow erosion to occur may have existed between the river bank and the floodplain. This gradient appears to no longer exist as sediment was being deposited in the depression with no evidence of erosion occurring.

Facies 3A. Facies 3A was thought to be a cut-off deposit, formed from a diversion of river flow. This premise is supported by the fact that the erosion surface between facies 3A and the underlying facies 4A in trenches three and four, although irregular, has the basic outline of a channel.

As illustrated in Fig. 22, facies 3A consisted of a variety of sedimentary structures. No sedimentary structures indicative of paleocurrent direction were observed anywhere in the facies. As sedimentary structures indicative of lateral migration were not observed, it appears that cut-off was short lived, resulting from a temporary avulsion, or partial diversion of the river. The lack of vegetation layers between the poorly defined dipping beds in trench three also suggests rapid sedimentation in this area of the facies. Along the margins of the facies where vegetation/sediment rhythmites do occur, sedimentation appears to have been intermittent. Variations in sedimentary processes within the cut-off would have been responsible for the changes in sedimentary structures of the facies, observed in the four sampling trenches.

Facies 4A. Facies 4A was interpreted as being a lateral accretion deposit formed by the migration of a point bar. Evidence of the this hypothesis was the presence of epsilon cross-bedding, visible by the slightly dip to the rhythmites in trench one, and the fact that it continued downstream along the concave bank leading into an active point bar. The slightly dipped beds of ripple troughs observed in trench three (paleocurrent vector mean = 346.6 degrees, vector magnitude = 94.4%), appear nearly analogous to the climbing ripples beds that form the point bar along the right bank. The only major difference being the climbing ripple deposits was the differentiation between the individual beds. The erosion surface between facies 4A and 5A, also support this hypothesis. An anomaly to the migrating bar hypothesis would appear to be the presence of the convolute laminations of trench two.

Convolute laminations are thought to be formed through post-depositional processes in which the sediment, through a range of possible mechanisms, becomes distorted. While the actual circumstances of the formation of the convolute laminations of trench two are not known, some convolute laminations have been attributed to current ripples being deformed by the plastic flow of sediment in which they were deposited (Ten Haaf, 1956; Sanders, 1960). Thus, the convolute laminations in trench two may have been deposited as current ripples on a point bar, but the post-depositional environment was such as to allow distortion of the sediments to occur. If this is indeed the case, then the convolute lamination ceases to be an anomaly, and the migrating point bar hypothesis fits the sediments of facies 4A.

Of particular interest in trench one, was the existence of a layer of marl within facies 4A. The presence of the marl indicated that within the sequence of point bar accretion the depositional environment temporarily changed to one of very low energy. From a map in Fitzgerald (1982), it appears that the study site was submerged beneath Lake Edenvale during the Nipissing Great Lakes (see chapter two). The submergence of the study site by Lake Edenvale, probably would have significantly reduced the flow velocities of the river, creating the low energy depositional environment that allowed the marl to form. Terlecky (1974) discusses that marl may be formed either biochemically or physiochemically. In which manner the marl observed in facies 4A formed was not pursued, although fossilized mollusk shells were observed in the marl. The presence of the rhythmites overlying the marl indicates a resumption of the point bar accretion caused by an increase in the depositional environment. This increase probably occurred with the recession of Lake Edenvale.

Facies 5A.

Facies 5A is thought to represent an exposure of the sedimentation associated with the recession of glacial Lake Algonquin (see chapter two). Although not observed at the study site, this interpretation is based on the fact that upstream of the study site approximately five km., similarly textured sediments were observed overlying varved clays.

Facies 5A is the underlying facies of the entire section of sediment illustrated in Fig. 22. The facies was observed in a wide range of sedimentary structures ranging from structureless sediment, poorly defined horizontal to cross-beds. As is evident in Fig. 23, this facies was the coarsest of the five facies.

SECTION B.

Facies 1B. Facies 1B was analogous to the soil profile that was designated as facies 1A in section A. Facies 1B was not continuous along section B, as it had been truncated by facies 2B (Fig. 24) A description of the soil profile will not be repeated in this section of the chapter.

Facies 2B. Facies 2B was intrepreted as a vertical accretion deposit of similar origin to facies 2A. The two facies were structurally analogous, as both consisted of primarily alternating layers of buried organic matter and structureless sediment (Fig. 24). Grain size distributions of the facies were also similar (Figs. 23 and 25). Facies 2B was also located in a depression on the floodplain, and had been deposited upon an erosion surface. The extensive light grey area extending from the left bank section B in the 1927 aerial photograph (Fig. 18) may be one of these deposits.

Laterally, the upstream margin of the facies 2B was located approximately at trench six, while the downstream margin was not found, as the facies extended into the extensively slumped area

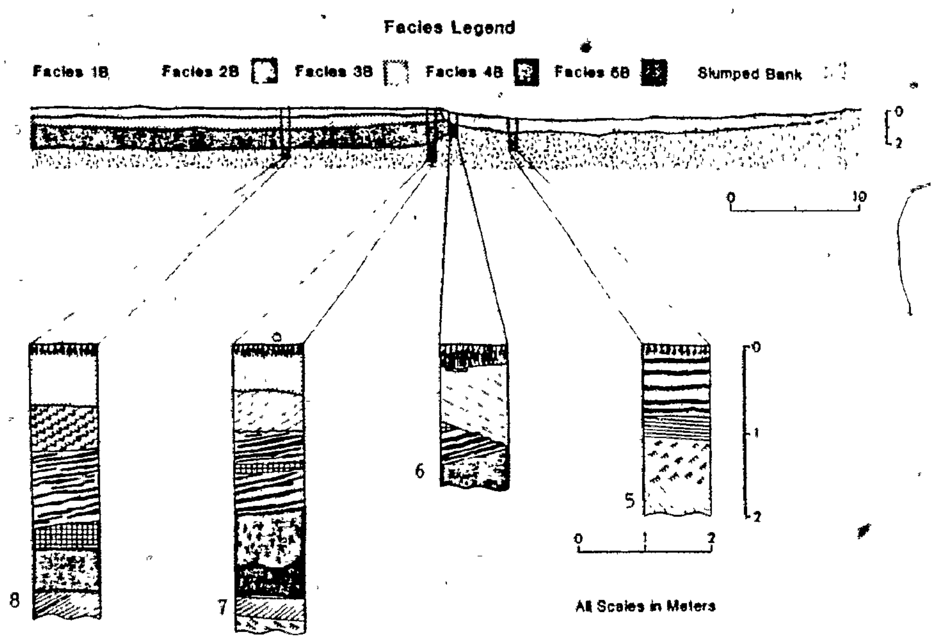

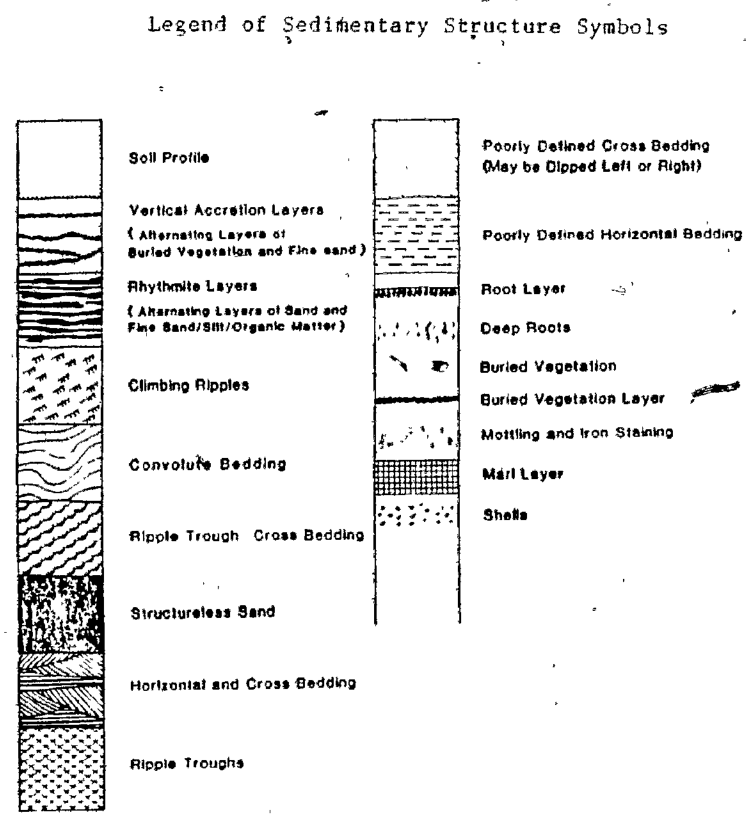

Fig. 24 Diagram showing the sedimentary facies observed in section B along the left bank. Trenches are designated five to eight from right to left.

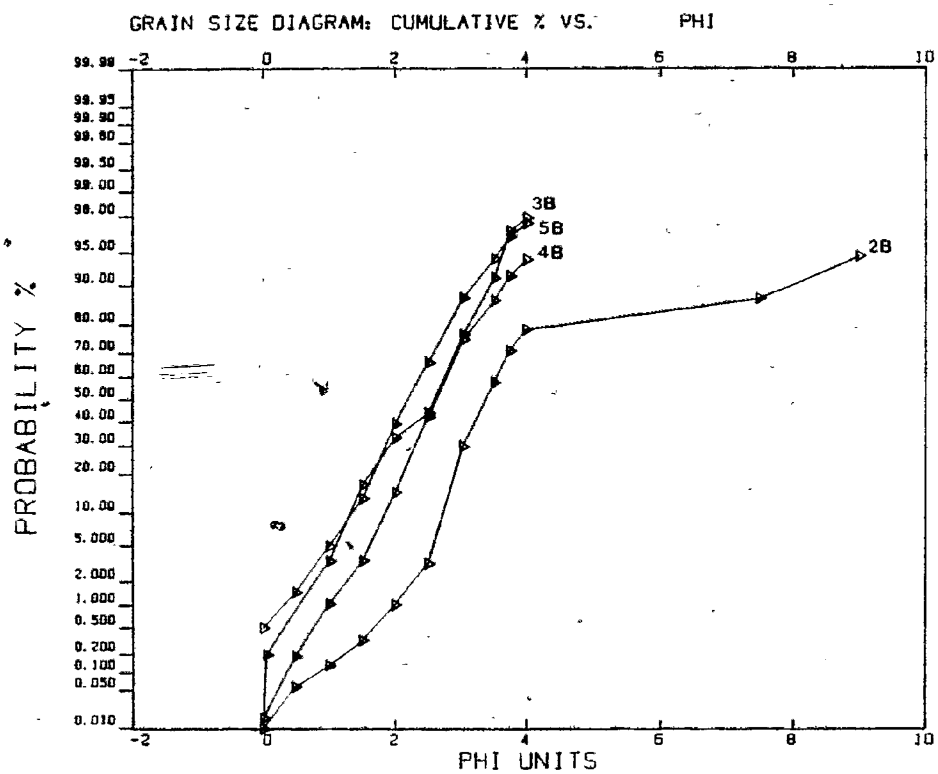

Fig. 25 Grain size diagram of sediment samples obtained from facies 2B, 3B, 4B and 5B. These facies were observed in section B of the left bank.

of the bank. The facies had a relatively constant thickness of approximately one metre.

Facies 3B. The exact origin of facies 3B was not known. Structurally, the facies appears as large-scale homogeneous laminations dipping in an upstream direction (Fig. 24). Close inspection of these cross-laminations revealed that they were not actually laminations, but rather inclined ripple troughs. The vector mean and vector magnitude of the ripple troughs was calculated to be 92.9 degrees and 98.1%. This vector mean indicated that the paleocurrent direction of the ripples had been roughly perpendicular to the cross-laminations, moving in a direction outward from this section of the left bank. The homogeneity of the facies suggests that deposition of the facies had been a continuous (or nearly continuous) process. Any extended halt to the depositional process would be reflected possibly by a change in sediment grade, or vegetation layer. Contact with the underlying facies 4B was not distinct, as the sedimentary structures of both facies were very faint.

The homogeneity of the sediment makes interpretation difficult, as it was not possible to conclusively establish if the sediment is fluvial or aeolian in origin. The possibility of an aeolian origin to the facies is significant as sand dunes are present in nearby Camp Borden (see chapter two concerning the origin of the sand dunes). The graphic mean and inclusive graphic standard deviation (Folk and Ward, 1957) of a sample of the facies (Fig. 25), was compared to a plot of river and dune sediments from Friedman (1961). This comparison was inconclusive as the sample fell in a transitional zone of the graph; however, the plot was proximal to the fluvial field on the graph. The presence of fragmented mollusk shells observed in facies also does not conclusively establish a fluvial origin, as they could have been contained in sediment that had been subsequently reworked by winds.

Facies 4B. Facies 4B was thought to have been derived from the lateral accretion of a river channel. Evidence of this was that facies 4B was composed of epsilon cross-bedding slightly dipped in an upstream direction (Fig. 24), which is indicative of channel migration (Allen, 1963). An apparent erosion surface between the facies and the underlying facies 5B, appears to indicate that possible scouring by a migrating channel may have occurred. Although partically destroyed by the presence of facies 2B, the pinching out of the facies at trench five would represent the original location or the maximum downstream migration of the channel. The upstream dip of the epsilon cross-bedding indicates that accretion then occurred in an upstream direction relative to the Nottawasaga River. Nothing is known of the upstream margin of the facies, as it becomes obscured in an extensively slumped and vegetated portion of the bank.

Given the proximity of the Pine River just upstream, it would seem that the rhythmites were derived from upstream migration of the tributary, a process that appears to be continuing today (see chapter four). If this facies was related to the migration of the tributary, then the channels of the Pine and Nottawasaga rivers were at a higher level than today.

A layer of marl was observed within trenches six, seven, and eight. This layer of marl, like that observed in section A, represents the occurrence of a low energy depositional environment. It was also thought to have formed during the period of the Nipissing Great Lakes when the study site was submerged beneath Lake Edenvale. The presence of the rhythmites overlying the marl indicates that an increase in the deposition environment has occurred.

Facies 5B. As with facies 5A, this facies was attributed to representing part of the sedimentation that occurred in the area following the recession of glacial Lake Algonquin. Facies 5B appeared as a wide variety of sedimentary structures, ranging from structureless sediment, tabular cross-laminations, large-scale troughs, and climbing ripples (Fig. 24). General paleocurrent direction was roughly perpendicular to the bank, in an easterly direction.

CHAPTER SIX

DISCUSSION AND CONCLUSIONS

In determining how representative the flow diagram (Fig. 11) was of the current in the river, the two components which form a flow vector, speed and direction, must be assessed separately from the profiles sampled (Figs. 12 to 16, and Fig. 19). Flow direction was found to have a low degree of fluctuation at each point of measurement throughout the study reach, although direction did tend to vary slightly closer to the channel bed. The one exception to this trend occurred at the confluence where turbulence was obviously quite high. Based on the profiles sampled, the flow direction can be assessed as being very well represented by the vector mean throughout the study reach. Generally, flow speed was found to be fairly well represented by the vector mean except in areas of extreme turbulence, for instance, at the confluence and along the bed in very rapidly flowing water. Turbulent waters, as explained, can result in erratic measurements of flow speed, which may be represented poorly by any calculation of a mean. Providing these areas of weakness are recognized, the vector mean was a good representation of the flow speeds measured in the river. The net assessment is that the flow diagram was felt to be a very good representation of the flow, so long as one recognizes very turbulent areas of the river where the limitations of the current meter were significant (or potentially so).

In most of the profiles measured in the study, vectors increased gradually or were uniformly distributed above the bed. The velocity profiles in these cross-sections did not logarithmically increase with greater height above the bed. In these instances, the logarithmic distributions would be assumed to occur at a depth below ten cm. as this was the minimum depth measured in the river.

In this study, the connection between the erosional and depositional pattern, and associated cross-channel geometry that are normally attributed to the existence of a helicoidal flow cell at a river meander, was confirmed. Confirmation occurred in the bends at the mouth of Pine River, and in the Nottawasaga River where a helicoidal flow pattern was observed within the measured vector distribution. At these locations, single and double cell (of potentially significant size) helicoidal flow patterns were observed in the Nottawasaga and Pine Rivers respectively, suggesting that perhaps both models of helicoidal flow may be partially correct at river bends.

Helicoidal flow was also present along the portion of the confluence directly affected by the waters entering from Pine River before significant mixing (with waters of the main channel) had occurred. In this more complex situation, the presence of helicoidal flow as apparent from the flow vectors in Fig. 10, was reflected by the formation of a large bar immediately downstream of the Pine River mouth. The asymmetry of the Nottawasaga channel upstream of the confluence suggests helicoidal flow probably influenced the observed channel morphology, although none existed during the period of flow measurement. Over the pool, helicoidal flow could be observed in the flow diagram, but the morphology of this portion of the study reach was thought to have arisen from a different (and unknown) mechanism. Here the flow speeds were not thought to be sufficient to transport sediment, hence deposition in the pool may have been occurring. Thus, it would seem the presence of a helicoidal flow pattern does not ensure the formation of the characteristic erosional and depositional pattern and asymmetrical channel, unless flow speeds are intense enough to allow scouring of the bed and the transport of sediment.

Paleocurrent evidence from exposed bars and observations of the river banks have indicated that large-scale reverse circulations along both the concave and convex sides of a meander appear capable of causing bank erosion. These observations are in marked contrast to reports of reverse circulations being areas of deposition. Intuitively, it would seem that the ability of a reverse circulation to cause scouring probably depends upon the flow magnitudes and the particle sizes of the bank sediment. Erosion occurs if magnitudes of the reverse circulation are sufficiently high; conversely deposition results from weak flows. An interesting question is what happens to the sediments that have been eroded by the reverse circulation.

From the observation of erosional and depositional patterns, it is possible to hypothesize near-future trends along the study reach. Barring some unforeseen influence by man or nature that alters the observed processes, the mouth of Pine River should continue its upstream migration so long as the flow enters the confluence from a similarly oriented meander. In the upstream section of the study reach, the combination of accretion of the left bank and erosion along the opposite bank will probably result in the migration of the confluence eastward, causing continued development to the inward curvature of the right bank. Around the bend in the Nottawasaga River, the channel will probably continue to migrate outward through erosion of the left bank and accretion of the point bar. The presence of the reverse circulation along the right bank immediately downstream of the point should prevent significant downstream migration of the meander. It is not known exactly how the area being eroded by the reverse circulation along the left bank will change with time. Yet, a similar pattern of erosion should continue to occur in the affected area of the bank, so long as the large-scale reverse circulation exists at high discharge levels. The presence of the log jam along the concave bank in the downstream meander may continue to cause accretion to occur along that bank. This accretion may extend into the study reach causing continued deposition along the area of bank occupied by the second side bar.

Further areas of study can be identified from this research. The measurement of current and sediment transport patterns at 'spring' discharge levels would provide a better understanding of the processes that have had an obvious function in the formation of the observed channel morphology, but were inactive during the period encompassed by this study. Paleocurrent measurements of ripple marks on exposed bars, while providing some information on high discharge flow patterns, are of obviously limited value as they can only cover a portion of the channel. Considerable caution must be exercised before any such study should be undertaken as turbulence may potentially cause stability problems with a small moored boat (like the one utilized in this study).

Reverse circulations are clearly an area of flow that needs to be studied in more detail, as they have been shown to be capable of eroding banks thereby effecting channel migration. The possible effects of a log jam in the deposition of sediment upon the concave bank of the bend immediately downstream of the study reach has been alluded to in the text. The long-term observation of this section of the river would show how the river reacts to such an obstruction, information that would be potentially valuable to any bank-shoring projects planned by man.

In conclusion, this study has shown that very detailed measurements of flow around a river bend are feasible and can yield high rewards for geomorphologists. Continued detailed studies of river bends will produce a better understanding of bend processes and controls. Ultimately, the more details that are accumulated on river meandering, the more precise fluvial models will be, as a model can only be as good as the assumptions and variables on which it is constructed.

REFERENCES

Allen J.R.L. 1963. "The Classification of Cross-Stratified Units with Notes on Their Origin." Sedimentology. V.2. p. 93-114.

_______. 1973. "A Classification of Climbing Ripple Cross-Laminations." J. Geol. Soc. Lond., v.129, p.537-541.

Bagnold R.A. 1960. "Some Aspects of the Shape of River Meanders" Prof. Paper U.S. Geol. Surv., 282-E 135-144.

Bathurst J.C., Thorne C.R. and Hey R.D. 1977. "Direct Measurements of Secondary Currents in River Bends." Nature, V. 269, p.504-506.

Beckinsale R.P. 1969. "River Regimes." in Water, Earth and Man, (ed. by R.J. Chorley), London: Methuen and Co. Ltd. p.455-471.

Blackburn J.A. Vik S. Saunderson H. and Stone M. 1984. "Data Logger Based on a Portable Computer." Rev. Sci. Instrum., V.55, p.1862-1863.

Bridge J.S. and Jarvis J. 1976. "Flow and Sedimentary Processes in the Meandering River South Esk, Glen Clova, Scotland." Earth Surf. Proc., V.1, p.301-336.

_______. 1977. "Velocity Profiles and Bed Shear Stress over Various Bed Configurations in a River Bend." Earth Surf. Proc., V.2, p.281-294.

_______. 1982. "The Dynamics of a River Bend: a Study in Flow and Sedimentary Processes." Sedimentolog., V.29. p.499-541.

Callander R.A. 1978. "River Meanders." Ann. Rev. Fluid. Mech., V.10, p.129-158.

Carey W.C. and Keller M.D. 1957. "Systematic Changes in the Beds of Alluvial Rivers." J. Hydraul. Div. Am. Soc. Civ. Engrs. V.83. Paper 1331. 14p.

Carson M.A. and Lapointe M.F. 1983. "The Inherent Asymmetry of River Meander Planforms." J. Geol., V.91, p.41-55.

Chapman L.J. and Putnam D.F. 1966. The Physiography of Southern Ontario. (Toronto: University of Toronto Press). 386p.

Collinson J.D. 1970. "Bedforms of the Tana River." Geogr. Annalr., V.52A, p.31-56.

Craig J. 1977. Simcoe County: The Recent Past. (Corporation of the County of Simcoe). 306p.

Curray J.R. 1956. "The Analysis of Two-Dimensional Orientation Data." J. Geol., V.64, p.117-131.

Davies D.K. 1966. "Sedimentary Structures and Sub-facies of a Mississippi River Point Bar." J. Geol., V.74, p.234-239.

Deane R.E. 1950. "Pleistocene Geology of the Lake Simcoe District, Ontario." Geol. Surv. Can., Memoir 256, 108p.

Dietrich W.E. Smith J.D. and Dunne T., 1979. "Flow and Sediment Transport in a Sand Bedded Meander." J. Geol., V.87, p.305-315.

Einstein H.A. and Harder J.A. 1954. "Velocity Distributions and the Boundary Layer at Channel Bends." Trans. Am. Geophys. Un., V.35, p.114-120.

Fitzgerald W.D. 1982. Post-Glacial History of The Minesing Basin, Ontario. University of Waterloo. Unpublished M.Sc. Thesis 89p

Folk R.L. and Ward W.C. 1957. "Brazos River Bar: A Study in the Significance of Grain Size Parameters." J. Sedim. Petrol., V.27, p.3-26.

Friedmann G.M. 1961. "Distinction Between Dune, Beach and River Sands from their Textural Characteristics." J. Sedim. Petrol., V.31, p.514-529.

Goldthwait J.W. 1910. "An Instrumental Survey of the Shoreline of Extinct Lakes Algonquin and Nipissing in Southwestern Ontario." Geol. Surv. Can. Memoir 10. 57p.

Harris R.C. Roulston P. and DeFreitas C. 1975. "The Settlement of Mono Township." Can. Geogr., V.19, p.1-17.

Hey R.D. and Thorne C.R., 1975. "Secondary Flows In River Channels." Area, V.7, p.191-195.

Hickin E.J. 1978. "Mean Flow Structure in Meanders of the Squamish River, British Columbia." Can. J. Earth Sci., V.15, p.1833-1849.

_______. 1979. "Concave-Bank Benches on the Squamish River, British Columbia, Canada." Can. J. Earth Sci., V.16, p.200-203.

_______. 1984. "Vegetation and River Channel Dynamics." Can. Geogr., V.28, p.111-126.

Hough J.L. 1963. "The Prehistoric Great Lakes of North America." Am. Scient., V.51, p.84-109.

Hunter A.F. 1908. A History of Simcoe: Vol 1, Its Public Affairs. (Barrie:The Historical Commitee of Simcoe County). 335p.

Jackson R.G. 1975. "Velocity-Bedform-Texture Patterns of Meander Bend in the Lower Wabash River of Illinois and Indiana." Bull. Geol. Soc. Am., V.86, p.1511-1522.

_______. 1976. "Large Scale Ripples of the Lower Wabash River." Sedimentology, V.23, p.593-623.

Jopling A.V. and Walker R.G. 1968. "Morphology and Origin of Ripple-Drift Laminations, with Examples from the Pleistocene of Massachusetts." J. Sedim. Petrol., V.38, p.971-984.

Karrow P.F. Anderson T.W. Clarke A.H. Delorme L.D. and Sreenivasa M.R. 1975. "Stratigraphy, Paleontology and Age of Lake Algonquin Sediments in Southwestern Ontario, Canada." Quat. Res., V.5, p.49-87.

Lane E.W. and Borland W.M. 1954. "River-Bed Scour during Floods." J. Hydraul. Div. Am. Soc. Civ. Engrs. V. 119, p.1069-1080.

Leeder M.R. and Bridges P.H. 1975. "Flow Separation in Meander Bends." Nature. V. 253. p.338-339.

Leopold L.B. and Wolman M.G. 1960. "River Meanders." Bull. Geol. Soc. Am.. V.71, p.769-794.

Leverett F. and Taylor F.B. 1915. "The Pleistocene of Indiana and Michigan and the Great Lakes." U.S. Geol. Surv. Monograph 53, 529p.

Lewis C.F.M. 1969. "Late Quaternary History of Lake Levels In the Huron and Erie Basins." Proc. 12th Conf. Great Lake Research. Int. Assoc. Great Lakes Res. p.250-270.

Martini I.P. 1974. "Wasaga Beach: a Quaternary Classic Landscape Its Geological History and Biological Carrying Capacity." in. Quaternary Environments: Proceedings of a Symposium. (ed. by W.C. Mahaney), York University Geographic Monographs No.5. p.61-77.

Milne J.A. 1982. "Bed-Material Size and the Riffle-Pool Sequence." Sedimentology. V.29. p.267-278.

Mosley M.P. 1976. "An Experimental Study of Channel Confluences." J. Geol.. V.84. p.535-562.

Nanson G.C. and Page K. 1983. "Lateral Accretion of Fine-Grained Concave Benches on Meandering Rivers." Spec. Publs. Int. Ass. Sediment.. V.6. p.133-143.

Niller N. and Stravrakis N. 1982. "Reversed Circulation over a Point Bar on the Great Fish River." Trans. Geol. Soc. S. Afr.. V. 85. p.215-219.

Page K. and Nanson G.C. 1982. "Concave-Bank Benches and Associated Floodplain Formation." Earth Surf. Proc.. V.7. p.529-543.

Paterson G.C. 1961. The County of Simcoe, (Education Commitee Simcoe Council), 75p.

Pollin S. 1974. "Land, Lumber and Transportation in Wasaga Beach: a Historical Report on Wasaga Beach in the Nineteenth Century." Min. Nat. Resour., Huronia Dist., Wasaga Beach. 61p.

Porter C.J.B.L. 1973. "An Inventory of the Historical Resources of Wasaga Beach: The Nottawasaga River, a Route to the North -west1785-1830." Min. Nat. Resour., Huronia Dist., Wasaga Beach. 146p.

Prest V.K. 1970. "Quaternary Geology of Canada." in Geology and Economic Minerals of Canada, Geol. Soc. Can., ~~Econ.~~ Geol. Ser. 1 (5th ed.), p.676-764.

Richards K.S. 1976. "Channel Width and the Riffle-Pool Sequence." Bull. Geol. Soc. Am., V.87, p.883-890.

______. 1976b. "The Morphology of Riffle-Pool Sequences." Earth Surf. Proc., V.1, p.71-88.

______. 1978. "Channel Geometry in the Riffle-Pool Sequence." Geogr. Annalr., V.60A. p.23-27.

Sanders J.E. 1960. "Origin of Convoluted Laminae." Geol. Mag., V.97, p.410-421.

Saunderson H.C. 1975. "A Comparison of Empirical and Theoretical Frequency Distributions for Two-Dimensional Paleocurrent Data from the Brampton Esker and Associated Deposits." Geogr. Annalr., V.57A, p.189-200.

Shen H.W. and Komura S. 1968. "Meandering Techniques in Straight Alluvial Channels." J. Hydraul. Div. Am. Soc. Civ. Engrs, V.94, p.997-1016.

Stanley G.M. 1936. "Lower Algonquin Beaches of Penetanguishene Peninsula." Bull. Geol. Soc. Am., V.47, p.1933-1960.

_______. 1937. "Lower Algonquin Beaches of Cape Rich, Georgian Bay." Bull. Geol. Soc. Am., V.48, p.1665-1686.

_______. 1938. "Impounded Early Algonquin Beaches at Sucker Creek, Grey County, Ontario." Papers of the Michigan Acad., V.23, p.477-495.

Taylor F.B. 1908. "Field Work on the Pleistocene Deposits of Southwestern Ontario." Geol. Surv. Can. Summary Report, p.103-111.

Taylor G. Crook K.A.W. and Woodyer K.D. 1971. "Upstream -Dipping Foreset Cross-Stratification: Origin and Implications for Paleoslope Analysis." J. Sedim. Petrol., V.41, p.578-581.

Ten Haaf E. 1956. "Significance of Convolute Laminations." Geol. Mijnb., V.18, p.188-194.

Terlecky P.M. 1974. "The Origin of a Late Pleistocene and Holocene Marl Deposit." J. Sedim. Petrol., V.44, p. 456-465.

Thomson J. 1876. "On the Origin of Windings of Rivers in Alluvial Plains, with remarks on the Flow of Water round Bends in Pipes." Proc. Roy. Soc. Lond., V.25, p.5-8.

Thorne C.R. and Hey R.D. 1979. "Direct Measurement of Secondary Currents at a River Inflexion Point." Nature, V.280, p.226-228.

Toebes G.H. and Sooky A.A. 1967. "Hydraulics of Meandering Rivers with Floodplains." J. Waterways Harb. Div. Am. Soc. Civ. Engrs., V.93, p.213-236.

Wilson I.G. 1973. "Equilibrium Cross-section of Meandering and Braided Rivers." Nature, V.241, p.393-394.

Woodyer K.D. 1975. "Concave-Bank Benches on Barmon River, N.S.W." Austral. Geogr., V.1, p.36-40.

Yalin M.S. 1977. Mechanics of Sediment Transport. (2nd Edit.), (Toronto: Pergamon press), 298p.

APPENDIX A

The vector means calculated from each set of sixty-four current measurements obtained over the study reach, are listed in the succeeding tables.

Key

Profile eg. A1;156-D=25

A1 - Indicates that the measurements represented by the vector mean were obtained along cross-section 'A', profile one (see Fig. 11 for location)

156 - Azimuth of lubber line of boat

D=25 - Depth from water surface that measurements were recorded

Azimuth - Direction of vector mean relative to True North

Speed - Speed component of vector mean

X - 'X' component of vector mean

Y - 'Y' component of vector mean

PROFILE	AZIMUTH	SPEED (CM/S)	-X-	-Y
A1;156-0=5	325.00	16.92	9.70	-13.86
A1;156-0=25	323.00	16.72	10.06	-13.35
A1;156-0=45	323.00	17.13	10.31	-13.68
A1;156-0=65	323.00	14.72	8.86	-11.76
A2;142-0=5	318.00	16.97	11.36	-12.61
A2;142-0=25	320.00	17.85	11.47	-13.67
A2;142-0=45	321.00	18.26	11.49	-14.19
A2;142-0=65	321.00	17.03	10.72	-13.23
A2;142-0=85	319.00	17.28	11.34	-13.04
A2;142-0=105	320.00	19.11	12.28	-14.64
A2;142-0=125	321.00	16.67	10.49	-12.96
A2;142-0=145	317.00	14.55	9.92	-10.64
A3;142-0=5	319.00	18.43	12.09	-13.91
A3;142-0=25	321.00	19.17	12.06	-14.90
A3;142-0=45	322.00	18.25	11.24	-14.38
A3;142-0=65	319.00	19.20	12.60	-14.49
A3;142-0=85	324.00	17.42	10.24	-14.09
A3;142-0=105	319.00	17.79	11.67	-13.43
A3;142-0=125	322.00	16.44	10.12	-12.95
A3;142-0=145	322.00	17.61	10.84	-13.88
A3;142-0=165	320.00	15.70	10.09	-12.03
A4;150-0=5	327.00	18.09	9.85	-15.17
A4;150-0=25	324.00	17.25	10.14	-13.96
A4;150-0=45	327.00	18.48	10.06	-15.50
A4;150-0=65	327.00	18.16	9.89	-15.23
A4;150-0=85	326.00	17.80	9.95	-14.76
A4;150-0=105	329.00	16.70	8.60	-14.31
A4;150-0=125	331.00	15.07	7.31	-13.18
A5;160-0=5	329.00	17.81	9.47	-15.27
A5;160-0=25	330.00	18.71	9.36	-16.20
A5;160-0=45	333.00	16.69	7.58	-14.87
A5;160-0=65	335.00	16.12	6.81	-14.61
A5;160-0=85	337.00	10.76	4.20	-9.90
A6;135-0=5	337.00	15.82	6.18	-14.56
A6;135-0=25	342.00	15.45	4.77	-14.69
A7;146-0=5	313.00	11.57	8.06	-7.89
A7;146-0=25	324.00	11.07	6.51	-8.96
B1;253-0=5	48.00	44.90	-33.37	-30.04
B1;253-0=25	48.00	47.71	-35.06	-31.92
B1;253-0=45	54.00	53.32	-43.10	-31.34
B1;253-0=65	52.00	44.69	-35.22	-27.51
B2;252-0=5	49.00	59.46	-44.88	-39.01
B2;252-0=25	47.00	54.49	-39.85	-37.16
B2;252-0=40	37.00	47.85	-28.80	-38.21
B3;235-0=5	28.00	24.70	-11.60	-21.81

PROFILE	AZIMUTH	SPEED (CM/S)	-X-	-Y
C1;147-0=5	318.00	24.88	16.65	-18.49
C1;147-0=25	321.00	24.60	15.48	-19.12
C1;147-0=45	319.00	25.04	16.43	-18.90
C1;147-0=65	319.00	24.25	15.91	-18.30
C1;147-0=85	320.00	23.63	15.19	-18.10
C1;147-0=105	320.00	23.96	15.40	-18.35
C1;147-0=125	328.00	24.39	12.92	-20.68
C1;147-0=145	325.00	22.08	12.66	-18.09
C2;150-0=5	327.00	25.97	14.14	-21.78
C2;150-0=25	327.00	26.67	14.53	-22.37
C2;150-0=45	327.00	27.45	14.95	-23.02
C2;150-0=65	326.00	25.53	14.28	-21.17
C2;150-0=85	328.00	26.20	13.88	-22.22
C2;150-0=105	328.00	26.52	14.05	-22.49
C2;150-0=125	330.00	24.65	12.33	-21.35
C2;150-0=145	332.00	23.75	11.15	-20.97
C3;150-0=5	346.00	41.40	10.02	-40.17
C3;150-0=25	351.00	44.15	6.91	-43.61
C3;150-0=45	349.00	41.10	7.84	-40.34
C3;150-0=65	343.00	37.61	11.00	-35.97
C3;150-0=85	336.00	35.78	14.55	-32.69
C3;150-0=105	333.00	38.55	17.50	-34.35
C3;150-0=125	330.00	37.27	18.64	-32.28
C3;150-0=145	334.00	35.74	15.67	-32.12
C3;150-0=165	329.00	33.96	17.49	-29.11
C3;150-0=185	322.00	28.79	17.72	-22.69
C5;142-0=5	259.00	8.02	7.87	1.53
C4;143-0=5	20.00	12.22	-4.18	-11.48
C4;143-0=25	349.00	19.75	3.77	-19.39
C4;143-0=45	340.00	28.34	9.69	-26.63
C4;143-0=65	329.00	32.89	16.94	-28.19
C4;143-0=85	316.00	43.56	29.15	-32.37
C4;143-0=95	321.00	43.19	27.18	-33.56

D1;136-0=5	317.00	33.64	22.94	-24.60
D1;136-0=25	320.00	34.73	22.32	-26.60
D1;136-0=45	320.00	33.94	21.82	-26.00
D1;136-0=65	319.00	35.37	23.20	-26.69
D1;136-0=85	321.00	34.40	21.65	-26.73
D1;136-0=105	318.00	32.46	21.72	-24.12
D1;136NO DEPTH??	319.00	33.21	21.79	-25.06
D1;136-0=125	318.00	30.50	20.41	-22.67
D1;136-0=135	316.00	24.44	16.98	-17.58
D2;149-0=5	329.00	47.69	24.56	-40.86
D2;149-0=25	326.00	40.68	22.75	-33.73
D2;149-0=45	326.00	41.20	23.04	-34.16
D2;149-0=65	326.00	44.24	24.74	-36.68
D2;149-0=85	323.00	42.84	25.78	-34.21
D2;149-0=105	327.00	42.58	23.19	-35.71
D2;149-0=125	327.00	40.35	21.98	-33.84
D2;149-0=145	323.00	35.91	21.61	-28.68
D3;138-0=5	330.00	41.81	20.91	-36.21
D3;138-0=25	334.00	44.22	19.38	-39.74
D3;138-0=45	328.00	44.78	23.73	-37.98
D3;138-0=65	321.00	44.93	28.28	-34.92
D3;138-0=85	321.00	46.65	29.36	-36.25
D3;138-0=105	321.00	43.17	27.17	-33.55
D4;148-0=5	318.00	40.23	26.92	-29.90
D4;148-0=25	319.00	40.14	26.33	-30.29
D4;148-0=45	321.00	39.60	24.92	-30.77

PROFILE	AZIMUTH	SPEED (CM/S)	-X-	-Y
E1;154-0=5	312.00	39.96	29.70	-26.74
E1;154-0=25	312.00	31.98	23.77	-21.40
E1;154-0=45	309.00	16.41	12.75	-10.33
F1;154-0=65	316.00	11.38	7.91	-8.19
E2;162-0=5	315.00	64.91	45.90	-45.90
E2;162-0=25	314.00	60.51	43.53	-42.03
E2;162-0=45	317.00	50.97	34.76	-37.28
E2;162-0=65	321.00	48.68	30.60	-37.83
E3;148-0=5	315.00	65.50	46.32	-46.32
E3;148-0=25	316.00	62.34	43.31	-44.84
E3;148-0=45	317.00	53.19	36.28	-38.90
E4;154-0=5	314.00	63.36	45.58	-44.01
E4;154-0=25	309.00	59.45	46.20	-37.41
E4;154-0=45	314.00	47.32	34.04	-32.87
E5;149-0=5	311.00	58.64	44.26	-38.47
E5;149-0=25	310.00	50.60	38.76	-32.52
E5;149-0=45	312.00	43.74	32.51	-29.27
E6;152-0=5	313.00	46.04	33.67	-31.40
E6;152-0=25	309.00	37.74	29.33	-23.75
E7;152-0=5	312.00	33.86	25.16	-22.66
E7;152-0=25	317.00	29.62	20.20	-21.66
E7;152-0=45	326.00	25.70	14.37	-21.31
F1;178-0=5	38.00	2.52	-1.55	-1.99
F1;178-0=15	345.00	3.29	.85	-3.18
F2;164-0=5	341.00	13.48	4.39	-12.75
F2;164-0=25	351.00	14.79	2.31	-14.61
F2;164-0=45	353.00	13.53	1.65	-13.43
F3;180-0=5	348.00	27.69	5.76	-27.08
F3;180-0=25	350.00	30.23	5.25	-29.77
F3;180-0=45	354.00	28.73	3.00	-28.57
F4;171-0=5	338.00	40.47	15.16	-37.52
F4;171-0=25	338.00	38.18	14.30	-35.40
F4;171-0=45	340.00	34.22	11.70	-32.16
F4;171-0=65	342.00	33.20	10.26	-31.58
F4;171-0=85	344.00	29.57	8.15	-28.42
F5;164-0=5	338.00	40.68	15.24	-37.72
F5;164-0=25	340.00	38.30	13.10	-35.99
F5;164-0=45	342.00	38.80	11.99	-36.90
F5;164-0=65	343.00	37.16	10.86	-35.54
F5;164-0=85	349.00	38.23	7.29	-37.53
F5;164-0=105	355.00	33.39	2.91	-33.26
F5;164-0=125	358.00	28.34	.99	-28.32
F6;172-0=5	338.00	43.84	16.42	-40.65
F6;172-0=25	337.00	42.73	16.70	-39.33
F6;172-0=45	340.00	41.93	14.34	-39.40
F6;172-0=65	343.00	35.82	10.47	-34.25
F6;172-0=85	344.00	33.10	9.12	-31.82
F6;172-0=105	348.00	29.20	6.07	-28.56
F6;172-0=125	354.00	26.03	2.72	-25.89
F7;173-0=5	337.00	41.78	16.32	-38.46
F7;173-0=25	339.00	38.47	13.79	-35.91
F7;173-0=45	341.00	33.86	11.02	-32.02
F7;173-0=65	342.00	31.70	9.80	-30.15
F7;173-0=85	344.00	31.17	8.59	-29.96
F7;173-0=105	346.00	27.70	6.70	-26.88
F7;173-0=120	352.00	23.61	3.29	-23.38
F8;163-0=5	341.00	21.23	6.91	-20.07
F8;163-0=25	342.00	24.04	7.43	-22.86
F8;163-0=45	342.00	23.96	7.40	-22.79

PROFILE	AZIMUTH	SPEED (CM/S)	-X-	-Y
G1;181-0=5	352.00	20.79	2.89	-20.59
G1;181-0=25	355.00	19.68	1.72	-19.61
G1;181-0=40	353.00	16.77	2.04	-16.64
G2;180-0=5	358.00	29.81	1.04	-29.79
G2;180-0=25	359.00	30.01	.52	-30.01
G2;180-0=45	5.00	28.71	-2.50	-28.60
G3;179-0=5	351.00	36.86	5.77	-36.41
G3;179-0=25	353.00	36.59	4.46	-36.32
G3;179-0=45	355.00	35.53	3.10	-35.39
G3;179-0=65	355.00	34.44	3.00	-34.31
G3;179-0=85	358.00	30.83	1.08	-30.81
G4;173-0=5	350.00	39.30	6.82	-38.70
G4;173-0=25	351.00	37.70	5.90	-37.24
G4;173-0=45	353.00	36.78	[illegible]	-36.51
G4;173-0=65	355.00	35.46	3.09	-35.33
G4;173-0=85	2.00	35.97	-1.26	-35.95
G4;173-0=105	6.00	32.89	-3.44	-32.71
G4;173-0=115	7.00	31.39	-3.83	-31.16
G5;183-0=5	349.00	40.35	7.70	-39.61
G5;183-0=25	350.00	40.45	7.02	-39.84
G5;183-0=45	351.00	39.33	6.15	-38.85
G5;183-0=65	353.00	40.83	4.98	-40.53
G5;183-0=85	356.00	37.23	2.60	-37.14
G5;183-0=105	358.00	35.24	1.23	-35.22
G5;183-0=125	2.00	31.69	-1.11	-31.67
G5;183-0=[illegible]5	8.00	30.02	-4.18	-29.73
G6;191-0=5	356.00	25.67	1.79	-25.61
G6;191-0=25	352.00	35.01	4.87	-34.67
G6;191-0=45	352.00	37.56	5.23	-37.19
G6;191-0=65	352.00	32.19	4.48	-31.88
G6;191-0=85	349.00	30.36	5.79	-29.80
G6;191-0=105	348.00	24.88	5.17	-24.34
H1;186-0=23	5.00	21.74	-1.89	-21.66
H1;186-0=5	1.00	24.16	-.42	-24.16
H2;186-0=65	7.00	29.02	-3.54	-28.80
H2;186-0=33	6.00	32.40	-3.39	-32.22
H2;186-0=5	7.00	32.06	-3.91	-31.82
H3;215-0=5	4.00	39.62	-2.76	-39.52
H3;215-0=25	6.00	37.74	-3.94	-37.53
H3;215-0=45	7.00	37.35	-4.55	-37.07
H3;215-0=65	9.00	36.12	-5.65	-35.68
H3;215-0=80	8.00	32.06	-4.46	-31.75
H4;207-0=5	4.00	44.57	-3.11	-44.46
H4;207-0=25	8.00	40.25	-5.60	-39.86
H4;207-0=45	9.00	38.77	-6.06	-38.29
H4;207-0=65	10.00	37.72	-6.55	-37.15
H4;207-0=85	11.00	35.98	-6.87	-35.32
H4;207-0=100	11.00	27.23	-5.20	-26.73
H5;194-0=5	2.00	45.26	-1.58	-45.23
H5;194-0=25	4.00	42.72	-2.98	-42.62
H5;194-0=45	4.00	41.94	-2.93	-41.84
H5;194-0=65	7.00	39.53	-4.82	-39.24
H5;194-0=85	6.00	39.56	-4.14	-39.34
H5;194-0=105	8.00	38.17	-5.31	-37.80
H5;194-0=125	11.00	34.09	-6.50	-33.46
H5;194-0=145	13.00	32.48	-7.31	-31.65
H6;201-0=5	11.00	47.92	-9.14	-47.04
H6;201-0=25	9.00	44.26	-6.92	-43.72
H6;201-0=45	10.00	44.48	-7.72	-43.80
H6;201-0=65	10.00	45.25	-7.86	-44.56
H6;201-0=85	10.00	43.81	-7.61	-43.14
H6;201-0=105	16.00	40.07	-11.04	-38.52

PROFILE	AZIMUTH	SPEED (CM/S)	-X-	-Y
I1;207-0=25	13.00	25.95	-5.84	-25.28
I1;207-0=5	16.00	30.48	-8.40	-29.30
I2;202-0=50	21.00	31.31	-11.22	-29.23
I2;202-0=30	20.00	36.57	-12.51	-34.36
I2;202-0=10	17.00	37.86	-11.07	-36.21
I3;209-0=90	25.00	27.43	-11.59	-24.86
I3;209-0=70	22.00	33.33	-12.48	-30.88
I3;209-0=50	18.00	37.64	-11.63	-35.80
I3;209-0=30	16.00	40.12	-11.06	-38.57
I3;209-0=10	16.00	41.02	-11.31	-39.43
I4;211-0=145	32.00	36.59	-19.39	-31.03
I4;211-0=125	30.00	38.49	-19.24	-33.33
I4;211-0=105	26.00	38.42	-16.84	-34.53
I4;211-0=85	24.00	41.71	-16.96	-38.10
I4;211-0=65	20.00	42.65	-14.59	-40.08
I4;211-0=45	18.00	43.55	-13.46	-41.42
I4;211-0=25	19.00	42.81	-13.94	-40.48
I5;216-0=157	28.00	41.60	-19.53	-36.73
I5;216-0=137	25.00	47.46	-20.06	-43.01
I5;216-0=117	25.00	46.55	-19.67	-42.18
I5;216-0=97	23.00	46.92	-18.33	-43.19
I5;216-0=77	26.00	46.25	-20.27	-41.57
I5;216-0=57	25.00	46.05	-19.46	-41.74
I5;216-0=37	25.00	46.19	-19.52	-41.86
I5;216-0=22	29.00	47.66	-23.11	-41.68
I6;204-0=25	20.00	27.26	-9.32	-25.62
I6;204-0=5	24.00	21.35	-8.68	-19.50
J1;212-0=27	4.00	16.57	-1.16	-16.53
J1;212-0=7	15.00	25.55	-6.61	-24.68
J2;213-0=35	25.00	34.44	-14.55	-31.21
J2;213-0=15	25.00	40.43	-17.09	-36.64
J3;214-0=105	32.00	28.87	-15.30	-24.48
J3;214-0=85	28.00	35.27	-16.56	-31.14
J3;214-0=65	29.00	39.09	-18.95	-34.19
J3;214-0=45	26.00	40.95	-17.95	-36.84
J3;214-0=25	23.00	43.68	-17.07	-40.21
J3;214-0=7	21.00	47.71	-17.10	-44.54
J4;228-0=140	36.00	38.34	-22.54	-31.02
J4;228-0=120	37.00	42.96	-25.85	-34.31
J4;228-0=100	34.00	44.03	-24.62	-36.50
J4;228-0=80	30.00	43.40	-21.70	-37.59
J4;228-0=60	28.00	43.22	-20.29	-38.16
J4;228-0=40	28.00	44.39	-20.84	-39.19
J4;228-0=20	26.00	44.59	-19.55	-40.08
J5;230-0=160	36.00	37.96	-22.31	-30.71
J5;230-0=140	36.00	42.39	-24.92	-34.29
J5;230-0=120	31.00	45.99	-23.69	-39.42
J5;230-0=100	32.00	46.17	-24.47	-39.15
J5;230-0=80	30.00	45.80	-22.90	-39.66
J5;230-0=60	30.00	44.81	-22.40	-38.81
J5;230-0=40	31.00	45.88	-23.63	-39.33
J6;216-0=45	45.00	10.23	-7.23	-7.23
J6;216-0=25	34.00	17.02	-9.52	-14.11
J6;216-0=5	32.00	16.65	-8.82	-14.12

PROFILE	AZIMUTH	SPEED (CM/S)	-X-	-Y
K1;237-D=45	310.00	5.97	4.57	-3.84
K1;237-D=35	212.00	10.99	5.82	9.32
K1;237-D=25	218.00	10.44	6.43	8.23
K1;237-D=15	226.00	11.08	7.97	7.70
K1;237-D=5	246.00	10.59	9.67	4.31
K2;244-D=100	33.00	7.64	-4.16	-6.41
K2;244-D=90	324.00	4.39	2.58	-3.55
K2;244-D=80	84.00	7.42	-7.38	-.78
K2;244-D=70	54.00	4.55	-3.68	-2.67
K2;244-D=60	90.00	6.75	-6.75	.00
K2;244-D=50	93.00	1.09	-1.09	.06
K2;244-D=40	49.00	1.19	-.90	-.78
K2;244-D=30	228.00	3.36	2.50	2.25
K2;244-D=20	262.00	6.67	6.61	.93
K2;244-D=10	68.00	7.33	-6.80	-2.75
K3;213-D=173	82.00	36.05	-35.70	-5.02
K3;213-D=163	78.00	36.50	-35.70	-7.59
K3;213-D=143	66.00	31.11	-28.42	-12.65
K3;213-D=123	77.00	35.19	-34.29	-7.92
K3;213-D=103	56.00	29.24	-24.24	-16.35
K3;213-D=83	49.00	28.54	-21.54	-18.72
K3;213-D=63	49.00	27.75	-20.94	-18.21
K3;213-D=43	46.00	29.50	-21.22	-20.49
K3;213-D=23	39.00	29.25	-18.41	-22.73
K3;213-D=13	46.00	22.22	-15.98	-15.44
K4;229-D=273	73.00	46.26	-44.24	-13.53
K4;229-D=263	66.00	47.43	-43.33	-19.29
K4;229-D=253	59.00	45.26	-38.80	-23.31
K4;229-D=233	62.00	47.03	-41.53	-22.08
K4;229-D=213	55.00	44.50	-36.45	-25.52
K4;229-D=193	51.00	43.08	-33.48	-27.11
K4;229-D=173	47.00	40.56	-29.66	-27.66
K4;229-D=133	45.00	42.21	-29.85	-29.85
K4;229-D=113	44.00	41.77	-29.02	-30.05
K4;229-D=83	36.00	42.14	-24.77	-34.09
K4;229-D=5*	32.00	42.97	-22.77	-36.44
K5;232-DEPTH=170	50.00	20.94	-16.04	-13.46
K5;232-D=160	51.00	23.34	-18.14	-14.69
K5;232-D=150	51.00	27.50	-21.37	-17.31
K5;232-D=130	51.00	36.17	-28.11	-22.76
K5;232-D=110	50.00	43.47	-33.30	-27.94
K5;232-D=90	48.00	44.63	-33.17	-29.86
K5;232-D=60	46.00	46.43	-33.40	-32.25
K5;232-D=30	42.00	45.50	-30.45	-33.81
K5;232-D=5	38.00	45.02	-27.72	-35.48
K6;252-D=75	41.00	22.00	-14.43	-16.60
K6;252-D=65	33.00	23.76	-12.94	-19.93
K6;252-D=55	34.00	23.20	-12.97	-19.23
K6;252-D=35	38.00	25.26	-15.55	-19.91
K6;252-D=5	44.00	13.60	-9.45	-9.78

PROFILE	AZIMUTH	SPEED (CM/S)	-X-	-Y
L1;258-D=50	227.00	5.33	3.90	3.64
L1;258-D=40	231.00	6.63	5.15	4.17
L1;258-D=30	244.00	10.31	9.27	4.52
L1;258-D=20	235.00	6.23	5.10	3.57
L1;258-D=10	221.00	7.03	4.61	5.31
L2;236-D=160	58.00	11.75	-9.96	-6.23
L2;236-D=140	83.00	20.83	-20.67	-2.54
L2;236-D=120	78.00	23.25	-22.74	-4.83
L2;236-D=100	74.00	8.17	-7.85	-2.25
L2;236-D=80	70.00	15.64	-14.70	-5.37
L2;236-D=60	69.00	16.89	-15.77	-6.05
L2;236-D=40	83.00	18.17	-18.03	-2.21
L2;236-D=20	100.00	12.38	-12.19	2.15
L2;236-D=5	88.00	11.37	-11.36	-.40
L4;244-D=245	55.00	7.56	-6.19	-4.34
L4;244-D=225	71.00	22.07	-20.87	-7.19
L4;244-D=205	66.00	22.70	-20.74	-9.23
L4;244-D=185	67.00	22.85	-21.03	-8.93
L4;244-D=165	64.00	22.74	-20.44	-9.97
L4;244-D=145	67.00	24.41	-22.47	-9.54
L4;244-D=125	63.00	30.12	-26.84	-13.67
L4;244-D=105	59.00	33.20	-28.46	-17.10
L4;244-D=85	60.00	34.17	-29.59	-17.09
L4;244-D=65	53.00	28.82	-23.02	-17.34
L4;244-D=45	55.00	26.66	-21.84	-15.29
L4;244-D=25	53.00	26.06	-20.81	-15.68
L4;244-D=5	45.00	21.99	-15.55	-15.55
L3;235-D=233	66.00	26.39	-24.11	-10.73
L3;235-D=213	67.00	25.65	-23.61	-10.02
L3;235-D=193	66.00	25.75	-23.52	-10.47
L3;235-D=173	58.00	30.37	-25.76	-16.09
L3;235-D=153	60.00	33.53	-29.04	-16.77
L3;235-D=133	55.00	32.50	-26.62	-18.64
L3;235-D=113	49.00	32.49	-24.52	-21.32
L3;235-D=93	48.00	28.79	-21.40	-19.26
L3;235-D=73	40.00	28.85	-18.54	-22.10
L3;235-D=53	40.00	22.35	-14.37	-17.12
L3;235-D=33	36.00	19.15	-11.26	-15.49
L3;235-D=13	34.00	20.72	-11.59	-17.18
L5;255-D=260	72.00	17.73	-16.86	-5.48
L5;255-D=240	72.00	21.04	-20.01	-6.50
L5;255-D=220	65.00	23.25	-21.07	-9.83
L5;255-D=200	61.00	29.45	-25.76	-14.28
L5;255-D=180	61.00	31.11	-27.21	-15.08
L5;255-D=160	57.00	33.41	-28.02	-18.20
L5;255-D=140	55.00	38.00	-31.13	-21.80
L5;255-D=120	51.00	37.85	-29.41	-23.82
L5;255-D=100	49.00	40.61	-30.65	-26.64
L5;255-D=80	47.00	41.77	-30.55	-28.49
L5;255-D=60	45.00	41.74	-29.51	-29.51
L5;255-D=40	43.00	41.59	-28.36	-30.42
L6;276-D=76	251.00	6.37	6.02	2.07
L6;276-D=56	43.00	2.82	-1.92	-2.06
L6;276-D=36	249.00	12.57	11.74	4.50
L6;276-D=16	240.00	11.88	10.29	5.94
L6;276-D=5	254.00	11.45	11.01	3.16

PROFILE	AZIMUTH	SPEED (CM/S)	-X-	-Y
M1;266-D=5	100.00	8.58	-8.45	1.49
M1;266-D=25	95.00	11.77	-11.73	1.03
M1;266-D=45	85.00	8.30	-8.27	-.72
M1;266-D=60	78.00	6.12	-5.99	-1.27
M2;270-D=5	101.00	14.60	-14.33	2.79
M2;270-D=25	89.00	13.89	-13.89	-.24
M2;270-D=45	90.00	10.71	-10.71	.00
M2;270-D=65	94.00	12.01	-11.98	.84
M2;270-D=85	94.00	13.26	-13.23	.92
M2;270-D=105	97.00	12.71	-12.62	1.55
M2;270-D=125	101.00	14.37	-14.11	2.74
M2;270-D=145	88.00	13.59	-13.58	-.47
M2;270-D=165	89.00	11.55	-11.55	-.20
M3;272-D=5	94.00	13.05	-13.02	.91
M3;272-D=25	66.00	13.21	-12.07	-5.37
M3;272-D=45	67.00	11.39	-10.48	-4.45
M3;272-D=65	78.00	10.56	-10.33	-2.20
M3;272-D=85	74.00	12.86	-12.36	-3.54
M3;272-D=105	80.00	12.95	-12.75	-2.25
M3;272-D=125	92.00	9.59	-9.58	.33
M3;272-D=145	93.00	8.90	-8.93	.47
M3;272-D=165	87.00	9.92	[illegible]	-.52
M3;272-D=185	110.00	10.76	-10.11	3.68
M3;272-D=205	108.00	6.96	-6.62	2.15
M3;272-D=225	90.00	9.48	-9.48	.00
M3;272-D=245	112.00	12.91	-11.97	4.84
M3;272-D=265	107.00	9.68	-9.26	2.83
M3;272-D=285	108.00	13.20	-12.55	4.08
M3;272-D=305	115.00	15.91	-14.42	6.72
M3;272-D=325	114.00	11.20	-10.23	4.56
M3;272-D=340	127.00	11.81	-9.43	7.11
M4;283-D=5	55.00	14.72	-12.06	-8.44
M4;283-D=25	106.00	15.66	-15.05	4.32
M4;283-D=45	69.00	12.70	-11.86	-4.[illegible]
M4;283-D=65	72.00	11.47	-10.91	-3.54
M4;283-D=85	95.00	12.13	-12.08	1.06
M4;283-D=105	88.00	11.19	-11.18	-.39
M4;283-D=125	92.00	13.32	-13.31	.46
M4;283-D=145	81.00	9.60	-9.48	-1.50
M4;283-D=165	90.00	9.17	-9.17	.00
M4;283-D=185	95.00	10.79	-10.75	.94
M4;283-D=205	94.00	8.95	-8.93	.62
M4;283-D=225	103.00	14.45	-14.08	3.25
M4;283-D=245	110.00	9.65	-9.07	3.30
M4;283-D=265	97.00	10.46	-10.38	1.27
M4;283-D=285	101.00	11.12	-10.92	2.12
M4;283-D=305	110.00	12.31	-11.57	4.21
M4;283-D=325	123.00	11.89	-9.97	6.48
M4;283-D=345	116.00	9.91	-8.91	4.34
M4;283-D=365	109.00	9.82	-9.28	3.20
M4;283-D=385	120.00	11.96	-10.36	5.98
M4;283-D=405	106.00	9.09	-8.74	2.51
M4;283-D=425	143.00	8.68	-5.22	6.93
M4;283-D=445	148.00	11.31	-5.99	9.59

M5;278-0=5	115.00	17.52	-15.88	7.40
M5;278-0=25	114.00	14.91	-13.62	6.06
M5;278-0=45	103.00	7.60	-7.41	[illegible]
M5;278-0=65	113.00	11.91	-10.96	4.65
M5;278-0=85	106.00	10.95	-10.53	3.02
M5;278-0=105	109.00	13.43	-12.70	4.37
M5;278-0=125	107.00	11.22	-10.73	3.28
M5;278-0=145	121.00	15.14	-12.98	7.80
M5;278-0=165	104.00	7.22	-7.01	1.75
M5;278-0=185	124.00	9.69	-8.03	5.42
M5;278-0=225*	112.00	8.86	-8.21	3.32
M5;278-0=245	122.00	11.50	-9.75	6.09
M5;278-0=265	115.00	11.74	-10.64	4.96
M5;278-0=285	127.00	7.85	-6.27	[illegible]
M5;278-0=305	125.00	12.68	-10.39	7.27
M5;278-0=325	121.00	7.53	-6.45	3.88
M5;278-0=345	126.00	10.66	-8.62	6.27
M5;278-0=365	147.00	4.61	-2.51	3.87
M5;278-0=385	125.00	6.08	-4.98	3.49
M5;278-0=405	121.00	10.13	-8.68	5.22
M5;278-0=425	144.00	5.64	-3.32	4.56
M6;260-0=5	118.00	22.26	-19.65	10.45
M6;260-0=25	122.00	19.21	-16.29	10.18
M6;260-0=45	121.00	17.64	-15.12	9.09
M6;260-0=65	120.00	18.63	-16.13	9.31
M6;260-0=85	120.00	19.03	-16.48	9.51
M6;260-0=105	116.00	18.35	-16.49	8.14
M6;260-0=125	113.00	17.22	-15.85	6.73
M6;260-0=145	117.00	15.07	-13.43	6.84
M6;260-0=165	118.00	15.21	-13.43	7.14
M6;260-0=185	118.00	15.70	-13.86	7.37
M6;260-0=205	129.00	12.25	-9.52	7.71
M6;260-0=225	176.00	5.56	-.39	5.55
M6;260-0=245	228.00	9.52	7.07	6.37
M6;260-0=5	118.00	22.26	-19.65	10.45
M6;260-0=25	122.00	19.21	-16.29	10.18
M6;260-0=45	121.00	17.64	-15.12	9.09
M6;260-0=65	120.00	18.63	-16.13	9.31
M6;260-0=85	120.00	19.03	-16.48	9.51
M6;260-0=105	116.00	18.35	-16.49	8.14
M6;260-0=125	113.00	17.22	-15.85	6.73
M6;260-0=145	117.00	15.07	-13.43	6.84
M6;260-0=165	118.00	15.21	-13.43	7.14
M6;260-0=185	118.00	15.70	-13.86	7.37
M6;260-0=205	129.00	12.25	-9.52	7.71
M6;260-0=225	176.00	5.56	-.39	5.55
M6;260-0=245	228.00	9.52	7.07	6.37
M7;281-0=5	113.00	9.10	[illegible]	3.56
M7;281-0=25	112.00	9.68	[illegible]	3.65
M7;281-0=45	120.00	6.26	-5.42	3.13

PROFILE	AZIMUTH	SPEED (CM/S)	-X-	-Y
N1;256-0=5	72.00	18.88	-17.96	-5.83
N1;256-0=20	73.00	17.47	-16.71	-5.11
N2;268-0=5	78.00	22.10	-21.62	-4.59
N2;268-0=25	80.00	20.78	-20.46	-3.61
N2;268-0=45	78.00	19.90	-19.47	-4.14
N2;268-0=6[illegible]	74.00	19.29	-18.54	-5.32
N3;275-0=5	81.00	20.91	-20.65	-3.27
N3;275-0=25	79.00	19.70	-19.34	-3.76
N3;275-0=45	82.00	21.14	-20.93	-2.94
N3;275-0=65	83.00	20.92	-20.76	-2.55
N3;275-0=85	82.00	19.73	-19.54	-2.75
N3;275-0=105	80.00	19.26	-18.97	-3.34
N3;275-0=125	82.00	19.47	-19.28	-2.71
N3;275-0=145	78.00	19.78	-19.35	-4.11
N3;275-0=165	80.00	17.50	-17.23	-3.04
N4;263-0=5	64.00	19.17	-17.23	-8.40
N4;263-0=25	62.00	19.80	-17.08	-9.30
N4;263-0=45	66.00	18.86	-17.23	-7.67
N4;263-0=65	69.00	20.93	-19.54	-7.50
N4;263-0=85	68.00	17.21	-15.96	-6.45
N4;263-0=105	71.00	18.61	-17.60	-6.06
N4;263-0=125	71.00	18.43	-17.43	-6.00
N4;263-0=145	77.00	18.78	-18.30	-4.22
N4;263-0=165	82.00	19.63	-19.44	-2.73
N4;263-0=185	79.00	19.53	-19.17	-3.73
N4;263-0=205	81.00	20.71	-20.46	-3.24
N4;263-0=225	82.00	19.54	-19.35	-2.72
N4;263-0=245	79.00	18.33	-17.99	-3.50
N4;263-0=265	81.00	18.11	-17.89	-2.83
N5;257-0=5	66.00	20.84	-19.04	-8.48
N5;257-0=25	73.00	20.94	-20.03	-6.12
N5;257-0=45	71.00	21.17	-20.02	-6.89
N5;257-0=65	65.00	18.96	-17.18	-8.01
N5;257-0=85	70.00	19.74	-18.55	-6.75
N5;257-0=105	73.00	21.78	-20.83	-6.37
N5;257-0=125	71.00	18.95	-17.92	-6.17
N5;257-0=145	73.00	20.74	-19.83	-6.06
N5;257-0=165	74.00	20.15	-19.37	-5.55
N5;257-0=185	73.00	19.84	-18.97	-5.80
N5;257-0=205	69.00	20.94	-19.55	-7.50
N5;257-0=225	72.00	21.45	-20.40	-6.63
N5;257-0=245	71.00	17.76	-16.79	-5.78
N5;257-0=265	74.00	17.36	-16.69	-4.79
N5;257-0=285	63.00	18.17	-16.19	-8.25
N6;259-0=5	76.00	22.13	-21.47	-5.35
N6;259-0=25	71.00	21.94	-20.74	-7.14
N6;259-0=45	72.00	21.64	-20.58	-6.69
N6;259-0=65	71.00	20.91	-19.77	-6.81
N6;259-0=85	74.00	20.26	-19.48	-5.58
N6;259-0=105	73.00	19.39	-18.54	-5.67
N6;259-0=125	73.00	19.80	-18.93	-5.79
N6;259-0=145	72.00	21.25	-20.21	-6.57
N6;259-0=165	73.00	18.45	-17.64	-5.39
N6;259-0=185	73.00	19.77	-18.91	-5.78
N6;259-0=205	73.00	18.21	-17.41	-5.32
N6;259-0=225	66.00	18.11	-16.54	-7.37
N6;259-0=245	67.00	16.23	-14.94	-6.34
N6;259-0=260	65.00	11.08	-9.87	-5.03
N7;275-0=5	249.00	1.10	1.03	.39
N7;275-0=25	241.00	3.14	2.75	1.52
N7;275-0=45	244.00	2.42	2.18	1.06
N7;275-0=65	206.00	2.20	.96	-1.98

APPENDIX B

In Appendix B are circular histograms of current ripple paleocurrent measurements obtained at various sites along the river bank. The current histograms labelled A to H correspond to the sample sites on the point and side bars along the right bank (Fig. 21). The ripple troughs observed in facies 4A and 3B are represented by the circular histograms I and J. Circular histograms K and L represent the current ripples observed in the basal unit of trenches eleven and twelve.

Key

N=50 - Indicates the sample consisted of fifty current ripples

V MN=40.6 - The vector mean of the samples equals 40.6 degrees

V MG=90.8% - The vector magnitude of the sample was 90.8%

A N=50, V MN=38.0, V MC=91.1%

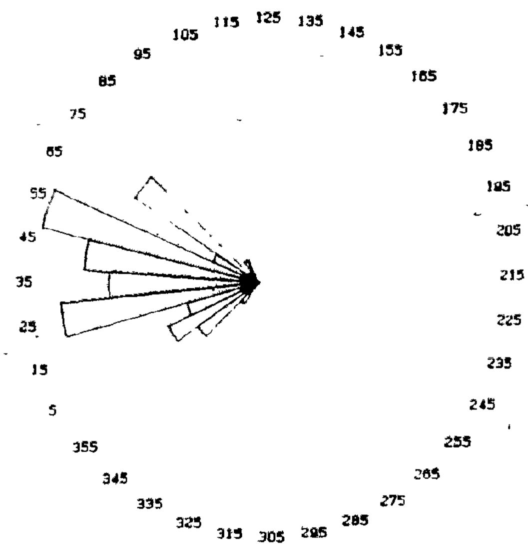

B N=50, V MN=34.6, V MN=40.7%

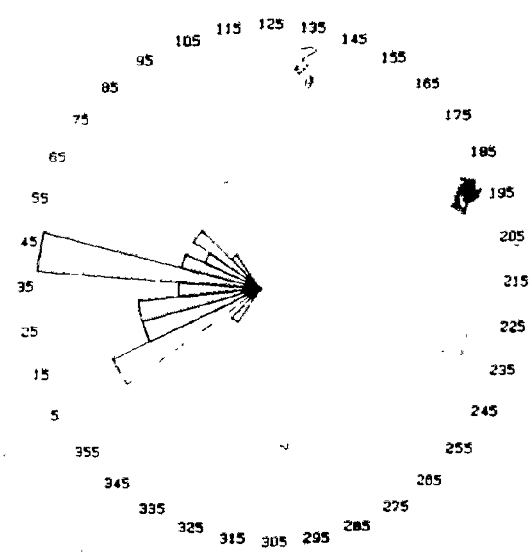

C

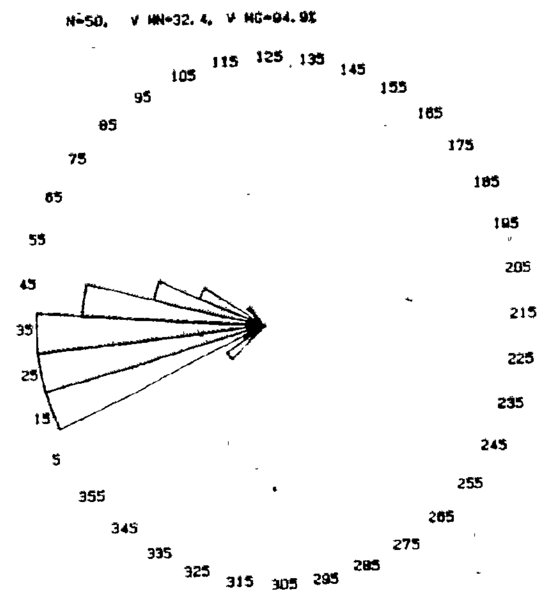
N=50, V MN=32.4, V MG=94.9%
115 125 135 145 155 165 175 185 195 205 215 225 235 245 255 265 275 285 295 305 315 325 335 345 355 5 15 25 35 45 55 65 75 85 95 105

D

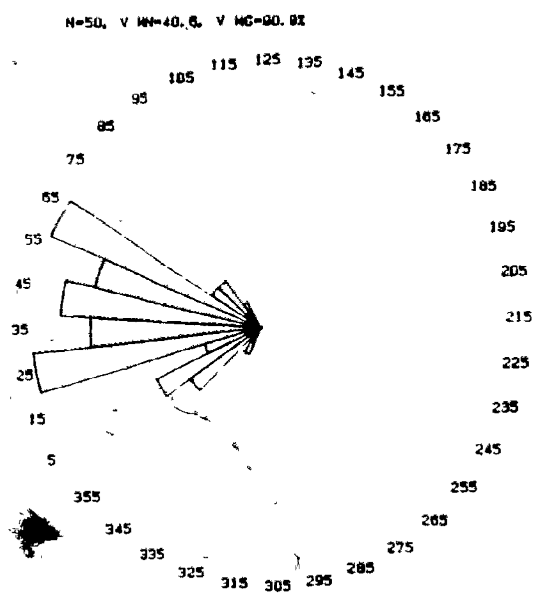
N=50, V MN=40.6, V MG=90.9%
115 125 135 145 155 165 175 185 195 205 215 225 235 245 255 265 275 285 295 305 315 325 335 345 355 5 15 25 35 45 55 65 75 85 95 105

E

N=50. V MN=18.4. V MG=95.1%

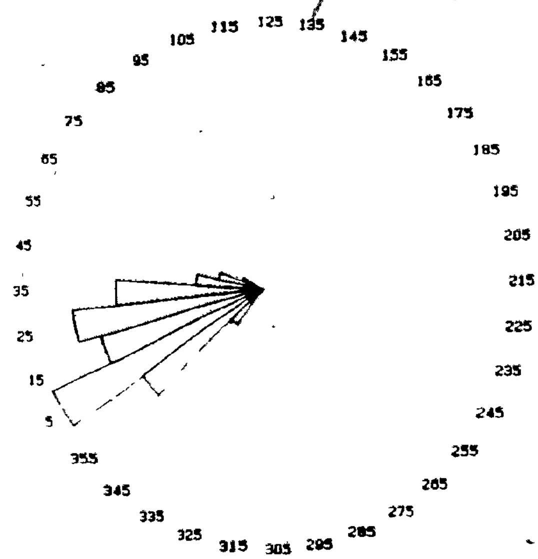

F

N=50. V MN=4.3. V MG=95.5%

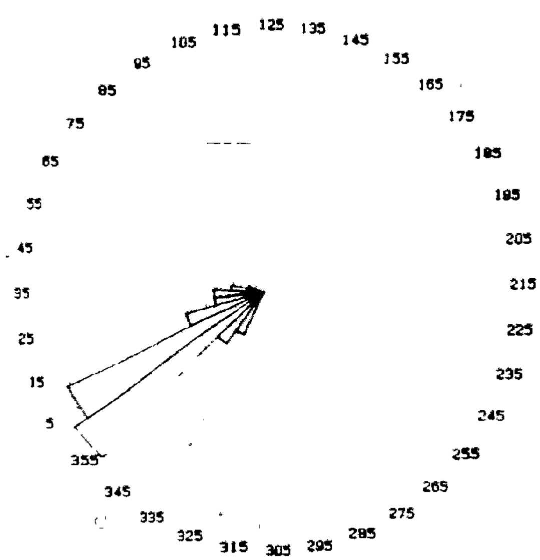

G

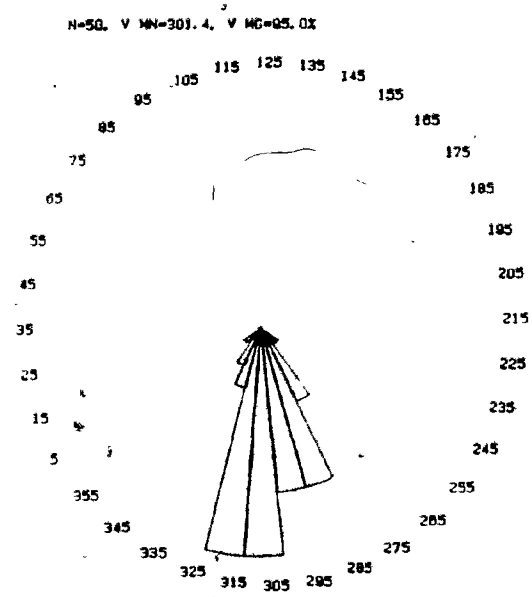
N=50, V MN=301.4, V MG=95.0%
5
15
25
35
45
55
65
75
85
95
105
115
125
135
145
155
165
175
185
195
205
215
225
235
245
255
265
275
285
295
305
315
325
335
345
355

H

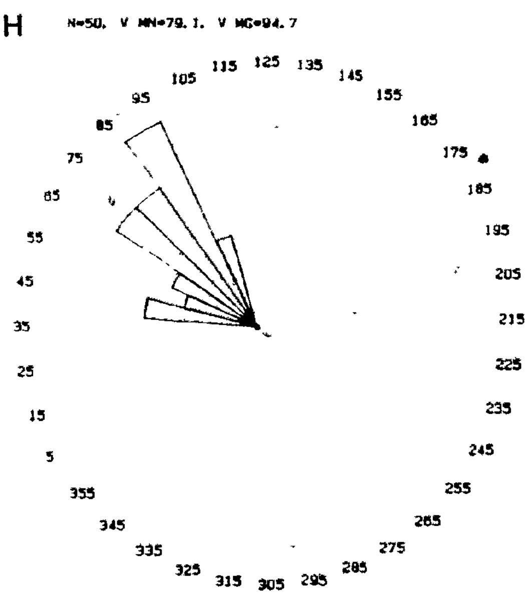
N=50, V MN=79.1, V MG=94.7
5
15
25
35
45
55
65
75
85
95
105
115
125
135
145
155
165
175
185
195
205
215
225
235
245
255
265
275
285
295
305
315
325
335
345
355

I N=50. V MN=92.9. V MC=98.1%

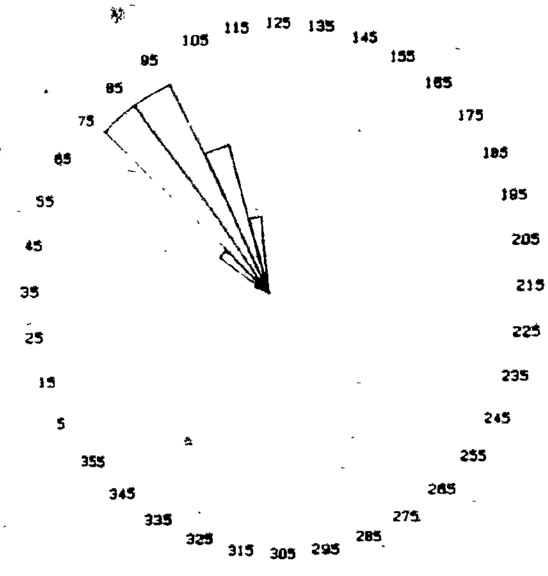

J N=50. V MN=346.6. V MC=94.4%

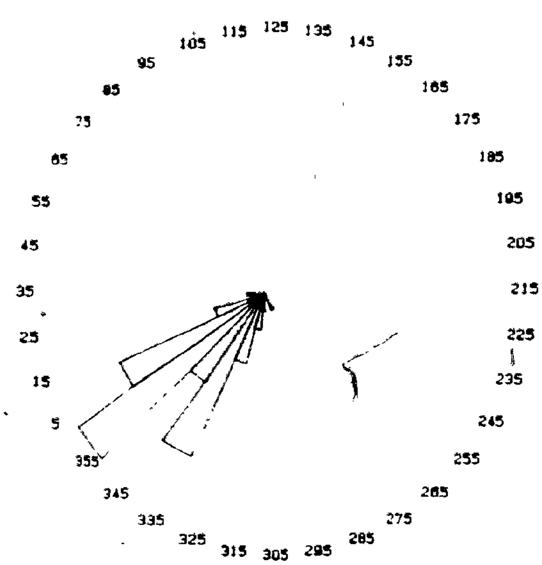

K N=50, V.M.=308.4, V MG=91.6%

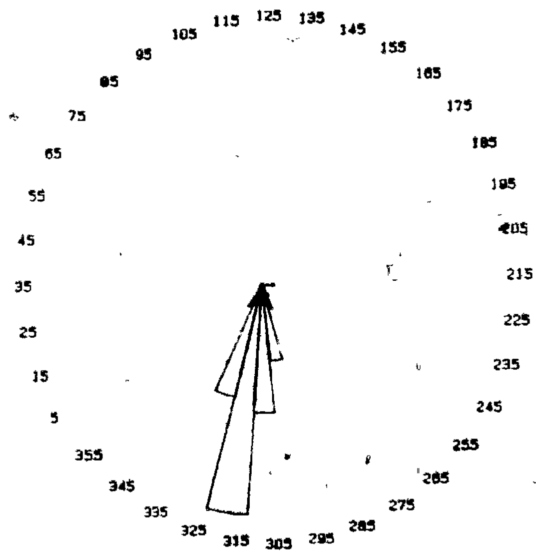

L N=50, V MN=325.6, V MG=97.6%

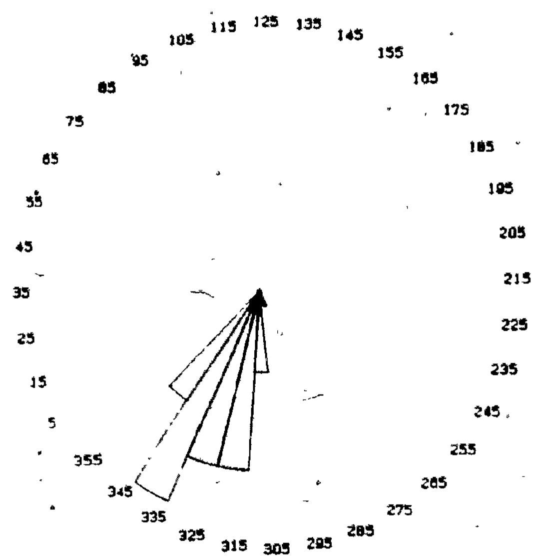

1 of

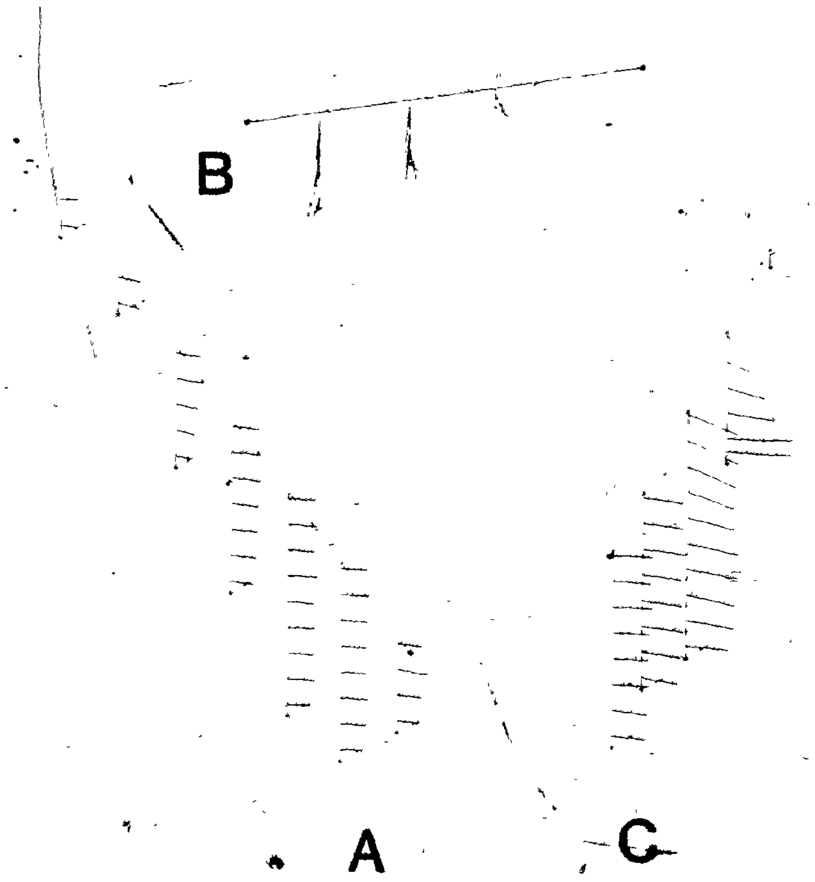

MAP of the STUDY REACH show

of the CROSS-SECTIONS and PR

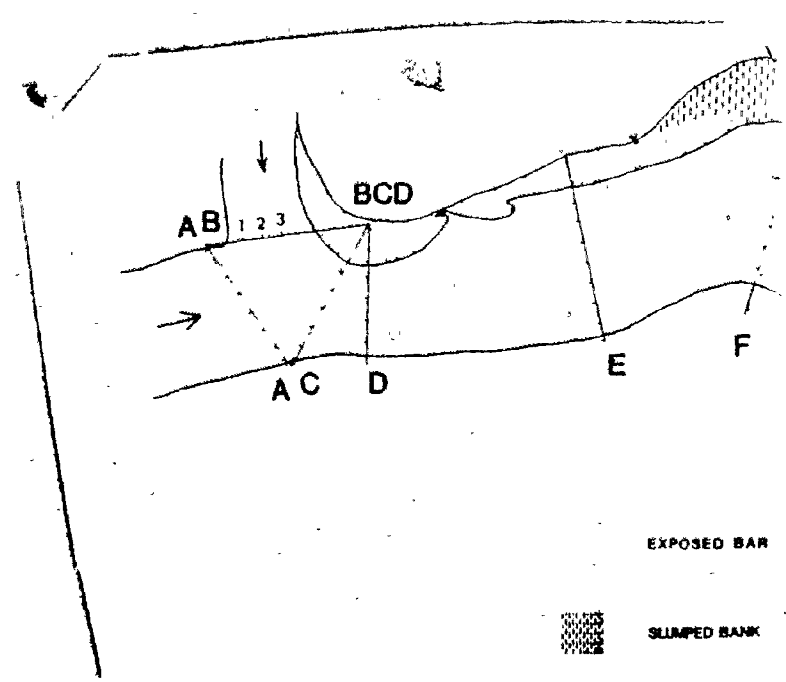

2oF

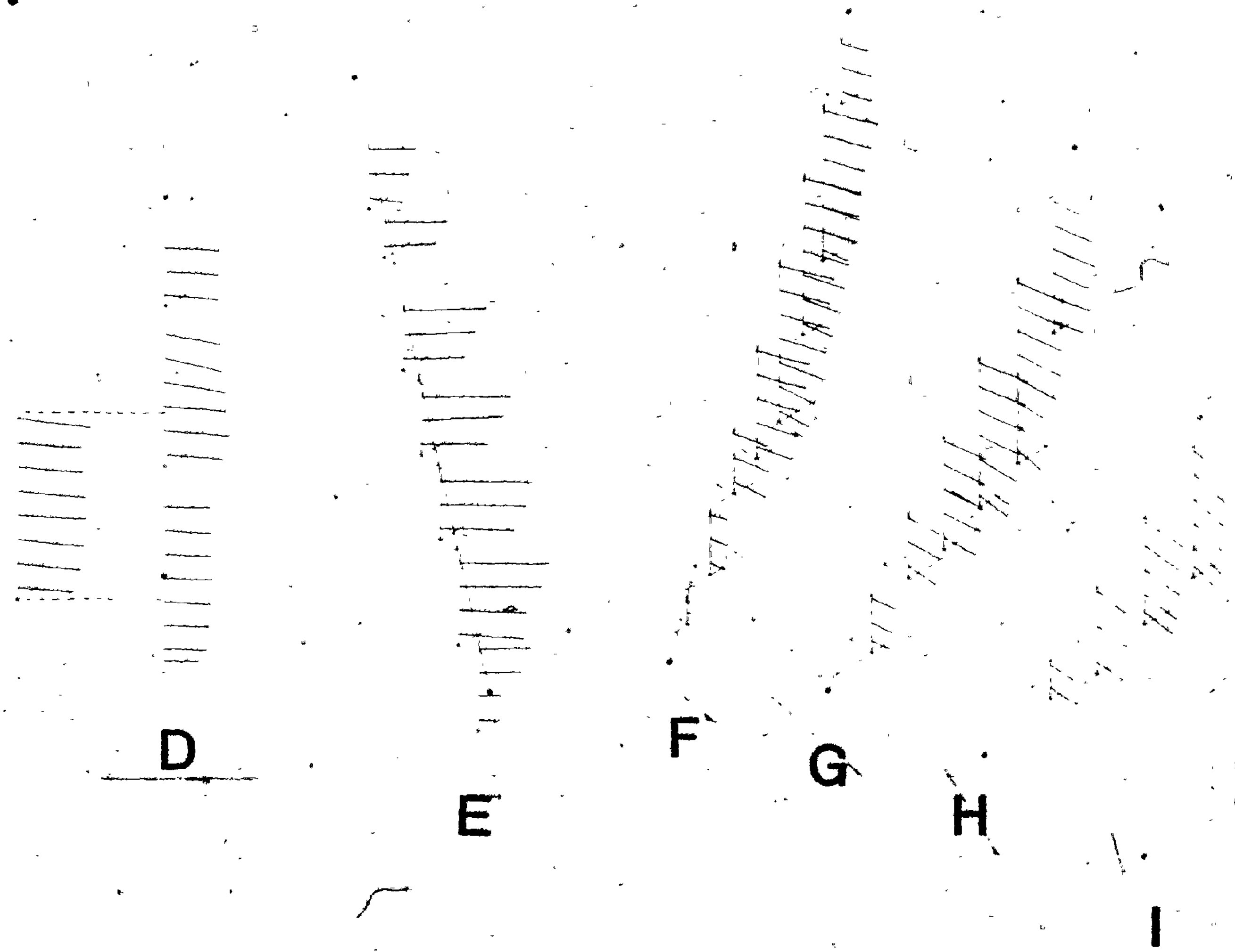

...howing the LOCATION

...d PROFILES

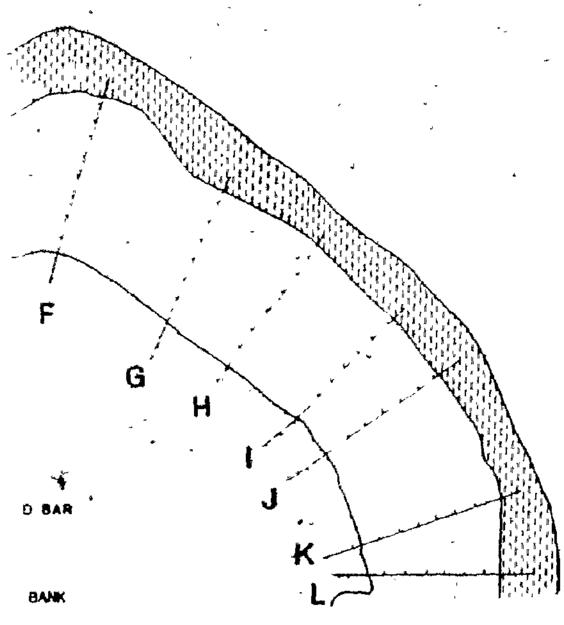

Vector Interpretation Key

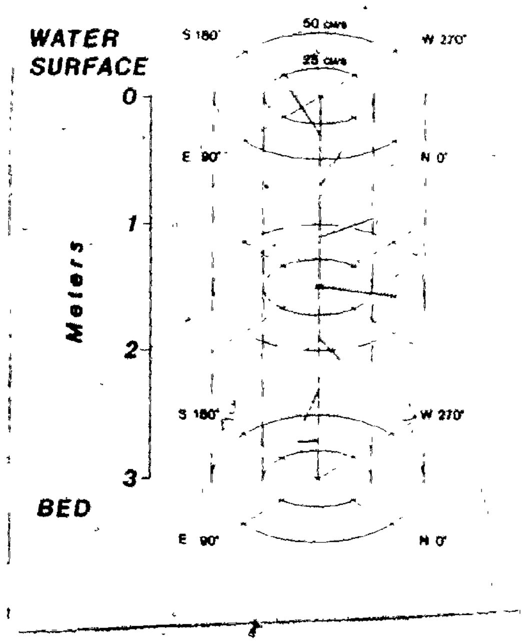

M

3oF

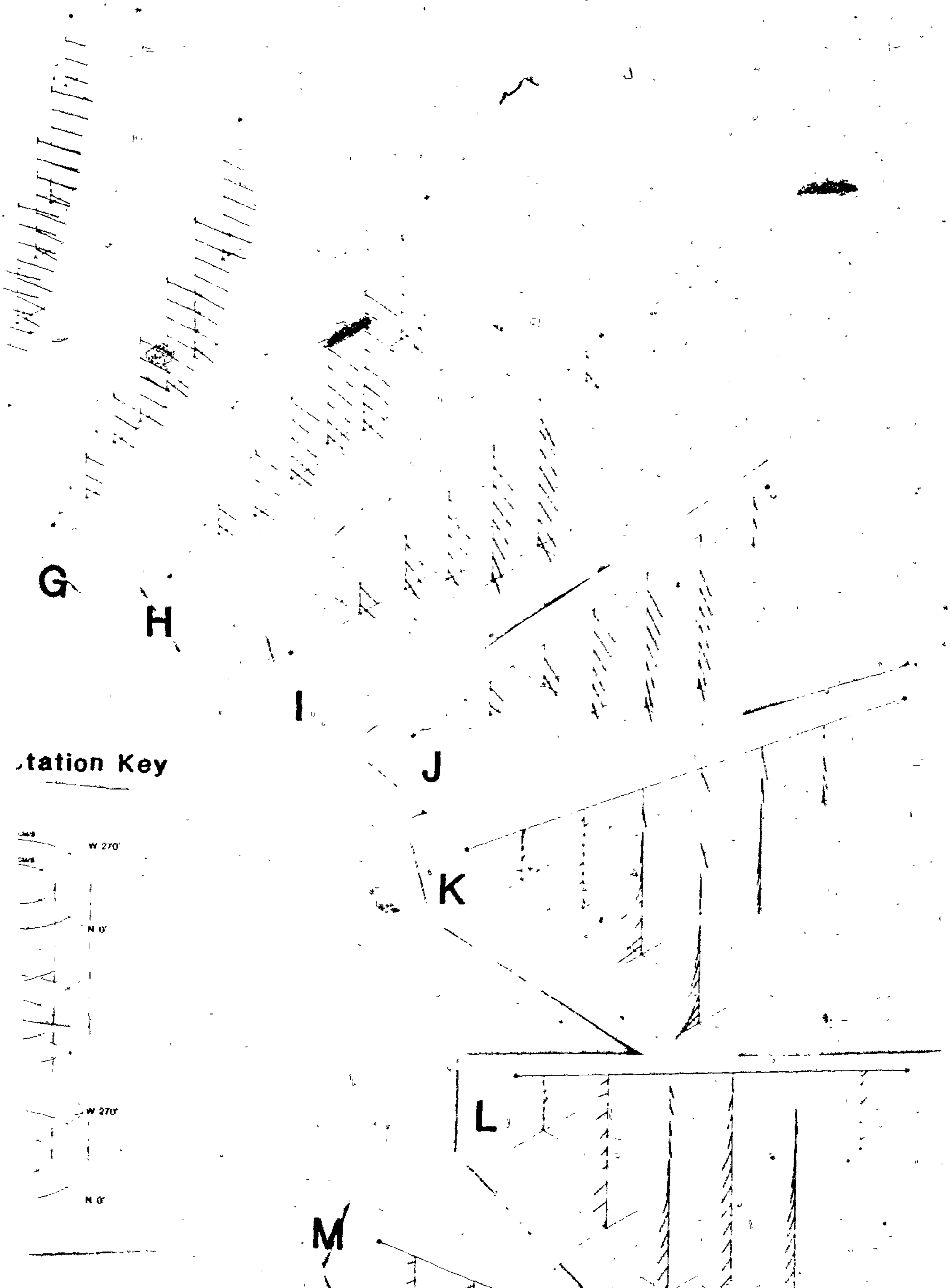

MAP of the STUDY REACH show

of the CROSS-SECTIONS and PF

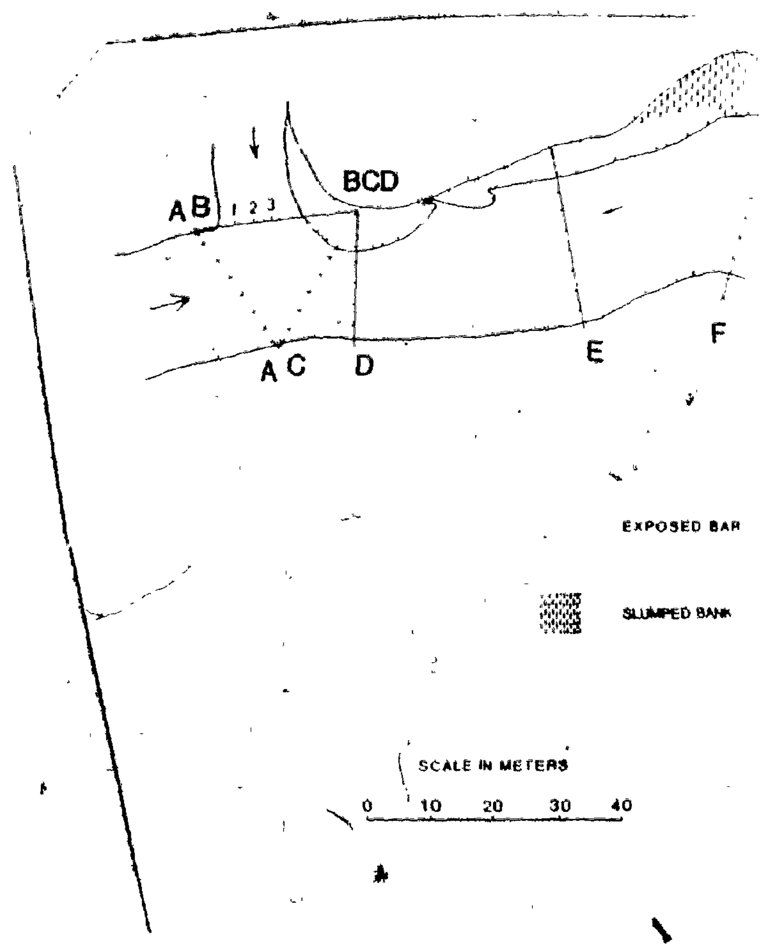

Fig. 11 Diagram showing the vector means measured al the vertical profiles for each of the fourteen cross-sections. The marks on the cross-sections in the refe map represent the location of the profiles. The syst of numerical designations applied to the individual pr at each cross-section is exemplified by 'B' and 'M'. alignment of the individual cross-sections correspond their respective orientation on the reference map.

ing the LOCATION

ROFILES

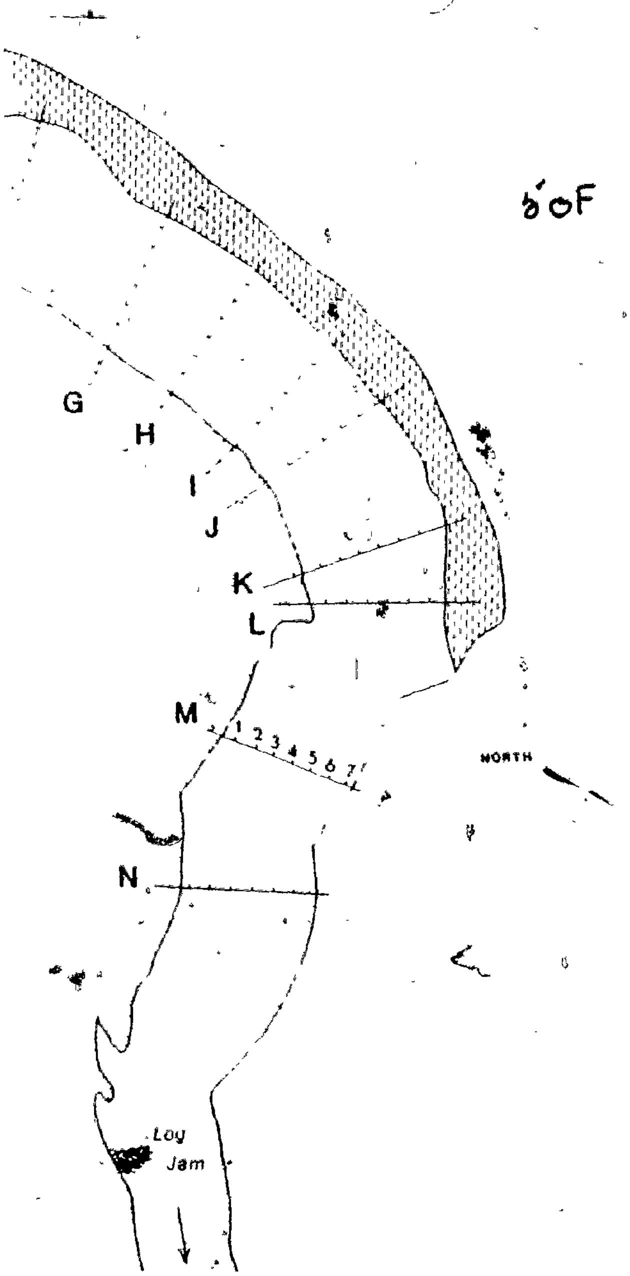

long
-
erence
stem
rofiles
The
to

Vector Interpretation Key

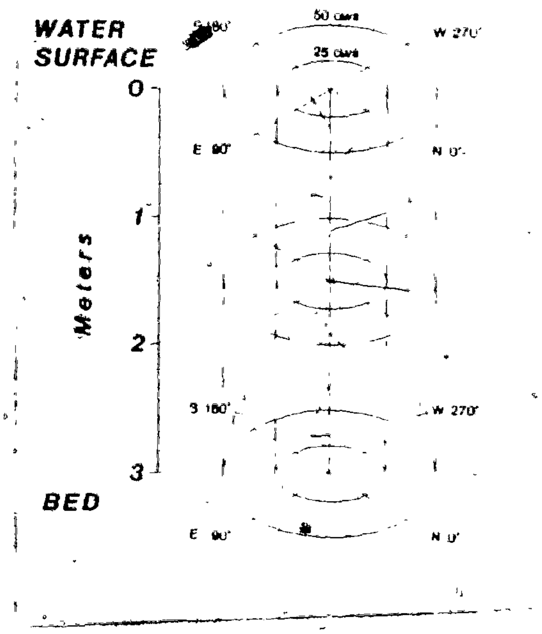

Cross-Sectional Scale

Scale in Meters

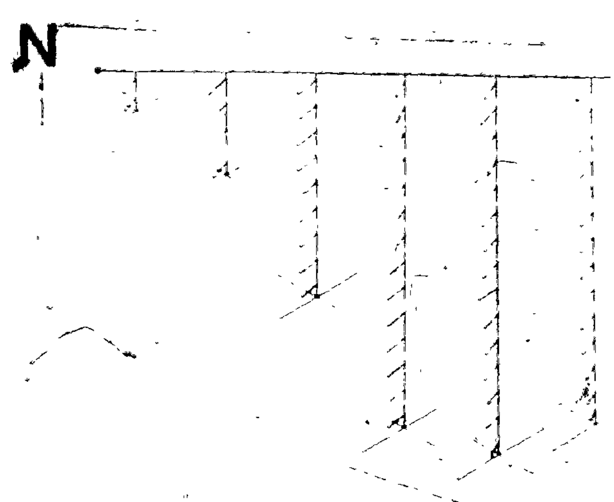

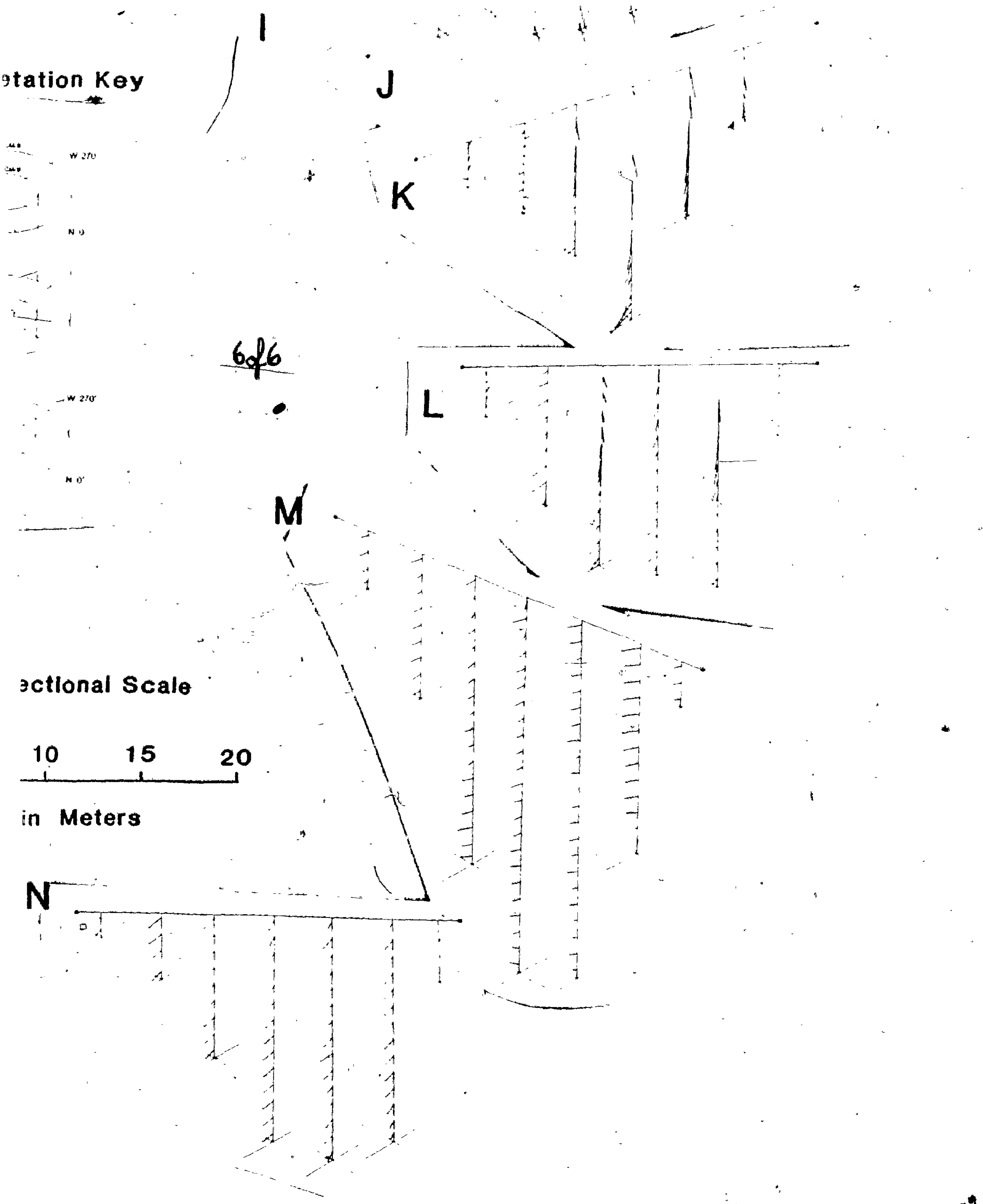
I
J
K
L
M
N
etation Key
W 270
N 0
W 270'
N 0'
6of6
ectional Scale
10
15
20
in Meters